Hybrid Differential Evolution and Enhanced Particle Swarm Optimization Technique for Design of Phased Antenna Arrays

By

Mohamed Thulaij Alsharaa

A Thesis submitted in partial fulfillment of the requirement of the degree of

MASTER OF SCIENCE

Department of Electrical and Electronics Engineering
University of Bahrain
Bahrain

Supervised by:

Dr. Mohab A. Mangoud

Department of Electrical and Electronics Engineering
University of Bahrain
Bahrain

Dr. Hassan M. Elragal

Department of Electrical and Electronics Engineering
University of Bahrain
Bahrain

2011

DECLARATION

I declare that this work is the result of my own investigation and that it has not already been accepted in substance of any degree, nor is it being currently submitted for any degree.

Signed:..... Date:...2-11-2011...

The thesis defence committee considers the thesis titled:

"Hybrid Differential Evolution and Enhanced Particle Swarm Optimization Technique for Design of Phased Antenna Arrays"

Submitted by Mohamed Thulaij Alsharaa to the Department of Electrical and Electronics Engineering satisfactory and acceptable for the Master of Science degree in Electrical Engineering.

Thesis defence committee:

Prof. Peter Excell

Dr. Raida Al-Alawi

Dr. Mohab Mangoud

Dr. Hassan Elragal

ACKNOWLEDGMENTS

I would like to express my gratitude to Allah (God) for providing me the blessings to complete this work. I also would like to ask him that this work would be a useful tool to help in improving the engineering community in my country Bahrain.

Thanks to everyone who helped me in completing this work. I submit my highest appreciation to my thesis supervisor, Dr. Mohab Mangoud, who helped in every step of the way. Dr. Mohab suggested the topic and provided the platform and most of the references to complete the thesis. I also would like to express my thanks to Dr. Hassan Elragal, my thesis co-supervisor, who helped me in the thesis programs and never hesitate to provide relentless support and motivation at all times.

Finally, I certainly would like to thank my parents, my wife and my daughters "Eilaf and Fatima" for their endless advises, support, patience and for encouraging me to further pursue my doctoral studies in the future.

Abstract

In the last decades of the twentieth century, the use of the evolutionary algorithms has been widely spread in the field of phased antenna arrays design. These algorithms such as genetic algorithms (GA), simulated annealing (SA), particle-swarm optimization (PSO) and differential evolution (DE) have been successfully used in the pattern synthesis applications.

This thesis introduces methods of designing reconfigurable phased arrays using a novel hybrid Differential Evolution (DE) and Enhanced Particle Swarm Optimization (EPSO) technique. The proposed technique combines DE and enhanced version of standard PSO with improved mechanism that updates velocity and global best solutions. In the hybrid algorithm, DE and EPSO are executed in parallel with frequent information sharing to enhance the newly generated population.

To demonstrate the effectiveness of the proposed algorithm over each separate algorithm, many examples were simulated using MATLAB program. The first application was multiple null steering for linear and circular antenna arrays using DE, EPSO and the newly proposed hybrid DE/EPSO. Nulls are controlled using position control method by perturbing the position values of the selected arrays' elements that affect forming the specified nulls locations in the radiation pattern. Also, the numbers of selected elements are optimized to have a minimum number of mobilized elements.

On the Second application, the hybrid algorithm is used in designing different configurations of concentric circular arrays (CCA) and concentric hexagonal arrays (CHA) with low sidelobe level (SLL) in the azimuth plane of the radiation pattern. Comparisons of different configurations having the same number of elements: two-ring, three-ring and four-ring are presented. The outer rings of these configurations are rotated with optimized angles to minimize SLL. Both amplitude and phase (complex excitations) are set or optimized in an adequate way using the hybrid technique to achieve the design of the configuration with minimum SLL. Also, the effect of adding a central element to these configurations is studied Amplitude dynamic range ratio and directivity are also studied for each configuration.

On the third application, the hybrid algorithm is used in designing time modulated linear and planar arrays. The amplitude excitations of time modulated array only require a low dynamic range ratios or even a uniform distribution while designing low/ultra-low sidelobe patterns, which are much easier for hardware implementation. The inherent drawback of time modulated arrays is that there are many sideband signals spaced at multiples of the modulation frequency, which implies that part of the radiated or received power is shifted to the sidebands. The hybrid algorithm is used to optimize the switch-on times of the arrays elements in order to minimize the SLL and the sideband level (SBL) that accompanied the radiation pattern of the time modulated antenna arrays.

All results obtained using the hybrid methods are compared with the results of individual DE and EPSO methods. Simulation results show the refined global search ability and effectiveness of the proposed algorithm over each separate algorithm.

4.8.1 Objective Function Formulation of the Design Problem. 51
4.8.2 Analysis and numerical results 53
4.8.3 Conclusion of Rotating the Outer Ring(s) of UCCA and UCHA 54
4.9 Second optimization problem: Optimizing Complex weights in hexagonal, Concentric Circular and Concentric Hexagonal Antenna Arrays 56
4.9.2 Analysis and numerical results. 58
4.9.2.1 CA and HA case 58
4.9.2.2 Two-ring case 58
4.9.2.3 Three-ring case 61
4.9.2.4 Four-ring case 67
4.9.3 Conclusion of Optimizing Complex weights in hexagonal, Concentric Circular and Concentric Hexagonal Antenna Arrays 67
4.10 Conclusion 71

Chapter 5: Sidelobe Suppression in Time Modulated Unequally Element Spaced Linear and Planar Arrays Using Hybrid DE/EPSO 72
5.1 Introduction 72
5.2 Sidelobe Suppression in Unequally Spaced Linear Arrays through Time Modulation 73
5.2.1 Objective Function Formulation of the Design Problem 74
5.2.2 Analysis and numerical results 78
5.2.3 Conclusion of unequally spaced TMLA 81
5.3 Sidelobe Suppression in Planar Arrays through Time Modulation and Complex Weights Optimization 81
5.3.1 Objective Function Formulation of the Design Problem. 83
5.3.2 Analysis and Numerical Results 84
5.3.3 Conclusion of TMCCA and TMCHA 89
5.4 Conclusion 89

Chapter 6: Conclusions and Future Work 90
6.1 Conclusions 90
6.2 Future work 93

List of Tables

Table 2.1 SLL of unequally spaced 16-elements linear array using DE, EPSO and hybrid EPSO/DE algorithms versus the results in reference [27]..... 20

Table 3.1 Comparison between position perturbation types and optimization algorithms for linear array and 2 nulls case..... 29

Table 3.2 Comparison between position perturbation types and optimization algorithms for linear array and 5 nulls case..... 30

Table 3.3 Values of the position vector for arbitrary perturbation of linear array using hybrid DE/EPSO..... 31

Table 3.4 Comparison between position perturbation types and optimization algorithms for circular array and 2 nulls case..... 35

Table 3.5 Comparison between position perturbation types and optimization algorithms for circular array and 5 nulls case..... 37

Table 3.6 Values of the position vector for arbitrary perturbation of circular array using hybrid DE/EPSO..... 38

Table 4.1 The SLL and Beam width for both 36 elements Geometries..... 44

Table 4.2 The configurations details: number of elements and the dimensions of each ring for UCCA and UCHA..... 47

Table 4.3 The Beam Width and SLL of different configurations of UCCA and UCHA..... 50

Table 4.4 The values of rotated angles in each ring and SLL of all configurations of UCCA and UCHA without affecting the main lobe beam width..... 54

Table 4.5 Comparison between optimized Hexagonal array and optimized circular array Ref. [35] in SLL, BW and directivity..... 59

Table 4.6 Comparison between Config.2-2 {12, 24} CCAA and CHAA with and w/o central element in SLL, δBW , directivity and I_{max}/I_{min}..... 60

Table 4.7 Comparison between Config.3.2 {6,12 ,18} CCAA and CHAA with and without central element in SLL, BW and Directivity..... 64

Table 4.8 Comparison between Config.4.1 {6, 6, 12, 12} CCAA and CHAA with and without central element in SLL, BW and Directivity..... 68

Table 5.1 A comparison of 32-Elements TMLA features SLL, BW, Directivity and SBLs, using the three algorithms versus the results in reference [3].....79

Table 5.2 A comparison of 36-elements TMCHA and TMCCA features SLL, SBL, BW, Gain and I_{max}/I_{min} using the three algorithms with the results in reference [65].....85

List of Figures

Fig. 2.1 Schematic of the full evolution cycle of Differential Evolution (courtesy: [24])..... 9

Fig. 2.2 Particle Swarm Optimization as modeled by a swarm of bees searching for flowers (courtesy: [26])..... 12

Fig. 2.3 Flowchart of the PSO algorithm..... 12

Fig. 2.4 Flowchart of the Hybrid DE/EPSO algorithm..... 16

Fig. 2.5 Linear array geometry..... 18

Fig. 2.6 The radiation pattern of the unequally spaced linear array optimized with the three algorithms versus the results in [27]..... 21

Fig. 2.7 Convergence curves for the three algorithms used to design unequally spaced linear array..... 21

Fig.3.1 Geometry of the linear array, depicted the 3 different position perturbation: axial, elevation and arbitrary perturbation..... 25

Fig. 3.2 The initial and the three algorithms perturbed pattern for linear array with imposed nulls at 105° and 110°..... 29

Fig. 3.3 Convergence curves for the three algorithms used to design perturbed linear array..... 30

Fig. 3.4 The initial and the three algorithms perturbed pattern for linear array with imposed nulls at 18°, 32°, 123°, 130° and 138°..... 31

Fig. 3.5 Geometry of circular array with illustration of the different types of elements position perturbation..... 32

Fig. 3.6 The initial and the three algorithms perturbed pattern for circular array with imposed nulls at 54°, 110°..... 36

Fig.3.7 Convergence curves for the three algorithms used to design perturbed circular array (2 null - arbitrary perturbation case)..... 36

Fig. 3.8 The initial and the three algorithms perturbed pattern for circular array with imposed nulls at 54°, 73°, 94°, 110° and 152°..... 37

Fig 4.1 Geometry of Circular Array with 36 elements..... 43

Fig 4.2 Geometry of Hexagonal Array with 36 elements.....43
Fig. 4.3 Radiation pattern of uniform Hexagonal and Circular Arrays with 36 elements and 0.25λ inter-element spacing at θ=90°. 44

Fig.4.4 Geometries of UCCA and UCHA for different configurations: (a) two-rings, (b) three-rings, and (c) four-rings.....48

Fig.4.5 The radiation pattern of Config.3.2 {6, 12, 18} UCHA and UCCA at θ=90°.....50

Fig. 4.6 The geometries with rotated outer rings with respect to the inner ring x-axis, for the: (a)UCCA and (b)UCHA.....52

Fig.4.7 The radiation pattern of rotated Config.4.1 {6, 6, 12, 12} UCHA using the three optimization algorithms, versus unrotated geometry pattern at θ=90°.....55

Fig.4.8 The radiation pattern of Rotated Config.3.2 {6, 12, 18} UCHA using the three optimization algorithms, versus unrotated geometry pattern at θ=90°.....55

Fig. 4.9 The radiation pattern of the hexagonal array optimized using the three algorithms, versus the reference pattern of the circular array.....59

Fig.4.10 Optimized amplitude and phase values of hexagonal array elements using Hybrid EPSO/DE algorithm.....60

Fig4.11 The radiation pattern of optimized Config.2.2{12, 24} CCAA without central element using the 3 optimization algorithms compared to chebyshev-like pattern.....62

Fig4.12 The radiation pattern of optimized Config.2.2 {12, 24} CCAA with central element using the 3 optimization algorithms compared to chebyshev-like pattern.....62

Fig.4.13 Optimized Amplitude and Phase of Config.2.2 {12, 24} CCAA elements, without central element using Hybrid EPSO/DE algorithm.....63

Fig.4.14 Optimized Amplitude and Phase of Config.2.2 {12, 24} CCAA elements, with central element using Hybrid EPSO/DE algorithm.....63

Fig.4.14 Optimized Amplitude and Phase of Config.2.2 {12, 24} CCAA elements, with central element using Hybrid EPSO/DE algorithm.....63

Fig4.15 The radiation pattern of optimized Config.3.2 {6, 12, 18} CHAA without central element using the 3 optimization algorithms compared to chebyshev-like pattern.....65

Fig4.16 The radiation pattern of optimized Config.3.2 {6, 12, 18} CHAA with central element using the 3 optimization algorithms compared to chebyshev-like pattern.....65

Fig.4.17 Optimized Amplitude and Phase of Config.3.2 {6, 12, 18} CHAA elements without central element using Hybrid EPSO/DE algorithm.....66

Fig.4.18 Optimized Amplitude and Phase of Config.3.2 {6, 12, 18} CHAA elements with central element using Hybrid EPSO/DE algorithm.....66

Fig.4.19 The radiation pattern of Config.4.1 {6, 6, 12, 12} CHAA without central element using the 3 optimization algorithms compared to chebyshev-like pattern.....69

Fig.4.20 The radiation pattern of optimized Config.4.1 {6, 6, 12, 12} CHAA with central element using the 3 optimization algorithms compared to chebyshev-like pattern.....69

Fig.4.21 Optimized Amplitude and Phase of Config.4.1 CHAA elements w/o central element using Hybrid EPSO/DE algorithm.....70

Fig.4.22 Optimized Amplitude and Phase of Config.4.1 CHAA elements with central element using Hybrid EPSO/DE algorithm.....70

Fig.5.1 Geometry of the Time Modulated Linear Array TMLA.....76

Fig.5.2 Scheme of the time switching function.....76

Fig.5.3 Normalized power patterns at the carrier frequency f_0 and the related to the sideband radiations (f_0+f_p, f_0+2f_p) optimized with hybrid EPSO/DE algorithms.....79

Fig.5.4 Switch-on time's sequence of 32-Elements TMLA synthesized using hybrid EPSO/DE algorithms for Fig. 5.3.....80

Fig.5.5 Element's location in λ of 32-Elements TMLA synthesized using hybrid EPSO/DE algorithms.....80

Fig. 5.6 The 3-D space and frequency response of the time modulated linear array in correspondence with the pulse sequence and element's location in Fig.5.4 and Fig.5.5 respectively.....81

Fig. 5.7 shows the radiation pattern of optimized TMCHA at f_0, f_0+f_p, f_0+2f_p and f_0+3f_p using hybrid EPSO/DE algorithm.....86

Fig.5.8 The optimized Amplitude and Phase of TMCHA elements using hybrid EPSO/DE algorithm of Fig.5.7.....86

Fig.5.9 The optimized Switch-on times sequence of TMCHA elements using hybrid EPSO/DE algorithm of Fig.5.7.....87

Fig. 5.10 The 3-D space and frequency response of TMCHA using hybrid EPSO/DE algorithm.....87

Fig. 5.11 shows the radiation pattern of optimized TMCHA in polar coordinates at (a) f_0, (b)f_0+f_p, (c)f_0+2f_p and (d) f_0+3f_p using hybrid EPSO/DE algorithm at $\theta=0°$.....88

Chapter 1

Introduction

The rapid growth in the wireless communication systems gave the antenna designers the motivation to develop new design tools that improve these systems performance. Most of these systems contain an antenna array combined with a suitable signal processor [1-2], i.e., the antenna elements are working in conformity to control array element phasing, which is processed through appropriate hardware. In these systems, the designers pay a special attention to the performance of antenna array over a specific steering range. Most of the antenna array design problems concentrate on finding weights that shape the radiation pattern to meet the designer's requirement for that desirable pattern like maximum gain, minimum sidelobe level, etc. However, the objective function of the design problem is modeled as an optimization problem. The design of antenna arrays has a nonlinear and non-convex reliance of array elements parameters [3]. Therefore, different types of techniques were presented to solve the nonlinear problems of the antenna array designs as it will be illustrated in the forthcoming sections.

1.1 Overview of Phased Antenna Array Research

Antennas with a certain radiation pattern may be arranged in an array (line, circle, plane, etc.) to yield a different radiation pattern. The most popular antenna arrays are as follow:

Linear array - antenna elements arranged along a straight line.

Circular array - antenna elements arranged around a circular ring.

Hexagonal array - antenna elements arranged in a hexagon shape.

Planar array - antenna elements arranged over some planar surface (example - rectangular array).

Conformal array - antenna elements arranged to conform to some non-planar surface (such as an aircraft skin).

Many analytical and numerical techniques have been used over the past years for the pattern synthesis of antenna arrays. These techniques have several limitations like time consumption and some complexity constraints. Evolutionary algorithms can overcome these limitations by searching the design space and find the best solutions.

Researchers have been investigating evolutionary algorithms for antenna design and optimization since early 1990s [3-10], and the field has grown rapidly in last decades as computer speed has increased and electromagnetic simulators have became more sophisticated. Evolutionary algorithms automate trial and error engineering substituting automated search through millions of potential solutions for sophisticated search by engineers through a much smaller number of designs. For evolutionary design, the engineer chooses the evolutionary technique, parameters and the basic form of the antenna, e.g., linear and circular antenna arrays. Evolutionary algorithms then search for optimal configurations in the space defined by the engineer.

In the antenna array designs, there are many topics of interest like imposing nulls in certain directions. Sidelobe level reduction also considered one of the most important topics of the antenna array designs, as well as the main lobe beam steering. Many controlling parameters can be used to accomplish these designs. Amplitude and phase excitations of the array elements could be used as control keys, as well as the inter-element distances between array elements.

1.2 Evolutionary Algorithms for Antenna Design Applications

In recent years, evolutionary algorithms have shown great results in finding practical solutions in multi dimension design problems. Evolutionary algorithms such as genetic algorithms (GAs), simulated annealing (SA), particle swarm optimizers (PSO) and differential evolution (DE) have

been widely used in pattern synthesis applications [6]. Many researches used different types of these algorithms in antenna design.

In [7] the authors presented how to optimally thin an array using genetic algorithms. The genetic algorithm determines which elements are turned off in an array to find the lowest sidelobe level. The arrays are thinned to obtain sidelobe levels of less than -20 dB. In [8] genetic algorithm optimization was applied to adjust the subarray separation to reduce the sidelobe of the antenna beam pattern of satellite reflector antenna. Simulation results show that the sidelobe of the low profile phased array antenna is suppressed to a low radiation level.

In [9] simulated annealing SA is applied to the synthesis of arrays in order to reduce the peaks of side lobes by optimizing the elements' inter-element distance and weight coefficients. While in [10] the simulated annealing was used to optimize the length and space between elements of Yagi-Uda antennas to achieve excellent gain and impedance properties.

Particle swarm optimization algorithm PSO and differential evolution algorithm DE are a novel optimization tools, because they are easy to implement with a small number of controlling parameters compared to GA and SA. Poor convergence and trapping in local minima of the GA, and the need to set the initial parameter that satisfy the constraints, for each variable of SA and long computation time forced many researchers to use DE and PSO in their antenna array designs.

Particle swarm optimization algorithm was used in [11] to design non-uniform circular antenna arrays with optimum side lobe level (SLL) reduction. PSO was used to determine an optimized set of complex weights and antenna element separations that provide a radiation pattern with lowest side lobe level with the constraint of a fixed major lobe beamwidth. The results show that the design of non-uniform circular antenna arrays using PSO method provides a side lobe level reduction better than that obtained using GA. In [12] the authors used a modified type of PSO to design three-ring concentric circular antenna arrays (CCAA) without and with central element feeding. Each design was optimizing complex weights and radii to get low SLL.

The interest has been focused on differential evolution (DE) algorithm in [13] as optimization tool to synthesize radiation pattern in conformal antenna arrays in the presence of platform. DE was applied to optimize the amplitude weights of elements to reduce the sidelobe with the desired phase weights found by the scan angle and array geometry. In [14] an adaptive differential evolution (DE) algorithm has been used to optimize the distance between the elements of the linear array to synthesize a radiation pattern with minimum SLL and null placement control.

1.3 Contributions of This Work

The thesis contributions could be classified into two parts. The first part is developing a novel evolutionary optimization technique which is the hybrid differential evolution and enhanced particle swarm optimization (Hybrid DE/EPSO). The second part is applying the novel hybrid DE/EPSO to the designs of phased antenna arrays. The first design problem was null steering by position perturbation of selected elements to the linear and circular arrays. By this nulling method, up to five deep nulls imposed simultaneously in the initial radiation pattern with minimum number of perturbed elements and acceptable increase in the side lobe level (SLL).

The second design problem was redesigning of a circular array with fixed number of elements into different concentric hexagonal and concentric circular configurations arrays. Many advantages were achieved by the rearrangement of the circular array elements like the reduction in the SLL, increasing in the directivity and increasing in the inter-element distance which has a direct impact in mitigating the mutual coupling effect between elements. Finally the third design problem presented the time modulated arrays to achieve ultra low SLL for both linear and planar arrays. The use of the time as control parameter in the unequally spaced linear array, yields to obtain better SLL than using the excitation phase as a control parameter for the same array. For the planar array, the time modulated concentric hexagonal array achieved better gain and almost same SLL of the time modulated circular array using same number of elements.

1.4 Outline of Thesis

In this thesis, the objective is to develop an enhanced optimization algorithm, and then apply it as a tool for antenna array design.

In chapter 2, a hybrid algorithm containing differential evolution and enhanced particle swarm optimization algorithms is developed. This novel algorithm enhanced the ability to find the global solution of a given objective problem. This algorithm is used in the rest of the thesis for different applications of phased antenna arrays design as follow.

In chapter 3, hybrid DE/EPSO algorithm used in multi-null steering in both linear and circular array, using the position perturbation method of minimum selected elements of the array. By this method the algorithm could impose up to five nulls in the radiation pattern. This is obtained with preserving certain sidelobe level of the initial chebyshev pattern.

In chapter 4, hybrid DE/EPSO is used in designing different configurations of concentric circular and concentric hexagonal arrays, having the same number of element with different number of rings, to achieve the lowest sidelobe level radiation pattern. The algorithm is used to optimize the complex weight (amplitude and phase) of the elements current, to minimize the sidelobe level of the concentric configuration arrays in the azimuth plane.

In chapter 5, the hybrid algorithm is used to optimize switch-on times and inter-element distances of unequally spaced linear array to minimize the sidelobe level, with minimum sideband level of the harmonic frequencies. For the concentric circular and concentric hexagonal arrays the hybrid algorithm used to optimize both of complex weights and the switch-on times of the array elements, to achieve ultra low sidelobe level of the radiation pattern with minimum sideband radiation in the harmonics and sufficient directivity in the main lobe of the center frequency pattern.

Chapter 6 concludes the thesis and suggests some of topic which could be useful for the future work in the phased antenna array design using the optimization algorithm.

Chapter 2

Hybrid Differential Evolution / Enhanced Particle Swarm Optimization Algorithm

2.1 Introduction

Recently evolutionary algorithms have been widely used as a robust technique to design phased antenna arrays [15]. Evolutionary algorithms such as genetic algorithms (GAs), simulated annealing (SA), particle-swarm optimizers (PSO) and differential evolution (DE) have been broadly used in pattern synthesis applications [6]. Several methods for improving global optimization performance are previously proposed. These methods can be classified into three categories. First, performing the same optimization scheme successively with different initializations. Although this method increases the chance of finding the optimum solution, it has high computational cost. Second, improving the optimization algorithm itself by introducing a modified version with enhanced searching capability [16]. Finally, is to introduce hybrid techniques of different evolutionary algorithms with collaborative usage of population.

A hybrid technique that includes the essence and merits of GA and gradient-descent methods was introduced in [17]. The idea is to embed a gradient-descent algorithm into the evolution concept of the GA in order to provide a structured random search. Later on, improved genetic algorithm - extremism disturbed simple particle swarm optimization (IGA-EDSPSO) hybrid technique has been presented in [18]. The algorithm is executed such that best solutions are exchanged between improved version of GA and a simplified version of PSO in an iterative way.

Other robust hybrid methods applying combination of more than two different meta-heuristic optimizers have been developed in [19]. Recently, the idea of hybridization DE and PSO has

been emerged to inherit advantages of both techniques [20-22]. In [20] a combination of DE and PSO has been presented in sequential procedures. In [21] the mutation operation of DE is embedded in the PSO algorithm to improve its diversity exploration. The mutation operators are activated if velocity value of PSO is near to zero or violated from the boundaries. Another hybrid version of differential evolution named as HDE is introduced in [22]. HDE starts with the classical DE algorithm and then switch to PSO when the DE procedure starts to slow down.

In this chapter, a hybrid DE and enhanced version of PSO (EPSO) is proposed to increase the search space. The main idea is to execute the two techniques simultaneously. The evolved generations are obtained by merging and interchanging individuals produced from both techniques. The proposed evolutionary algorithm is developed and then applied for optimizing different antenna array configurations. In the forthcoming sections the differential evolution, the classical particle swarm, the enhanced particle swarm and the hybrid version of DE/EPSO will be presented, to have an idea about their performance in searching the global minimum solution for any given objective function.

2.2 Differential Evolution (DE)

Differential Evolution (DE) [23] is a parallel direct search meta-heuristic approach for global optimization. The initial vector population is chosen randomly. Each population vector is set as a target vector. Mutation operation is performed by adding the weighted difference between two population vectors to a third one. The parameters of mutated vector are then mixed with the parameters of the target vector, to produce the so-called trial vector. Parameter mixing is often referred to as "crossover". If the trial vector yields a lower cost function value than the target vector, then the trial vector replaces the target vector in the following generation. Each population vector has to serve once as the target vector so that competitions happened in one generation. The DE algorithm is summarized schematically in Figure 2.1. Stepwise, it is defined as:

Step 1. Initialize N-dimensional population vectors with P individuals, all randomly chosen from lower and upper bound interval $[lb, ub]$.

Step 2. For each target vector $x^i(k)$ for individual i at time k, where $i \in \{1, 2,...,P\}$, select another 3 random individuals (x^{r1}, x^{r2} and x^{r3}) from the population. r_1, r_2 and r_3 are random integers with mutually different indices $\in \{1, 2,..,P\}$. One of these selected individuals (x^{r1}) will serve as the base vector, and the other two (x^r and x^{r3}) will produce the differentiation vector ($x^{r2} - x^{r3}$).

Step 3. Create a mutant vector $x_{mut}(k+1) = x^{r1} + F \cdot (x^{r2} - x^{r3})$, where F is a constant of differentiation that is a randomly selected real number from the [0, 2] set.

Step 4. Crossover is introduced between target vector $x^i(k)$ and mutant vector $x_{mut}(k+1)$ in order to increase the diversity of the perturbed vector and create a trial vector as:

$$x^{i,j}{}_{trial}(k+1) = \begin{cases} x^{i,j}{}_{mut}(k+1) & \text{if } rand(j) \le C_r \\ x^{i,j}(k) & \text{otherwise} \end{cases} \qquad (2.1)$$

where $x^{i,j}(k)$ is the j^{th} element in the $x^i(k)$ target vector, $rand(j)$ is a random number taken from the interval [0, 1], $j \in \{1, 2, \ldots, N\}$ and C_r is preset crossover probability.

Step 5. When all the target vectors $x^i(k)$, $i \in \{1, 2, \ldots, P\}$, have been processed this way, evaluate the objective function with the new trail vectors. If the objective function value of any trial vector is less than that of the corresponding target vector, replace the target vector with the new trial vector.

Step 6. Repeat from step 2 until convergence criterion is met.

Where lb and ub are also N-dimensional vectors. Thus, DE has only 2 control parameters, the constant of differentiation F, and the probability of crossover Cr.

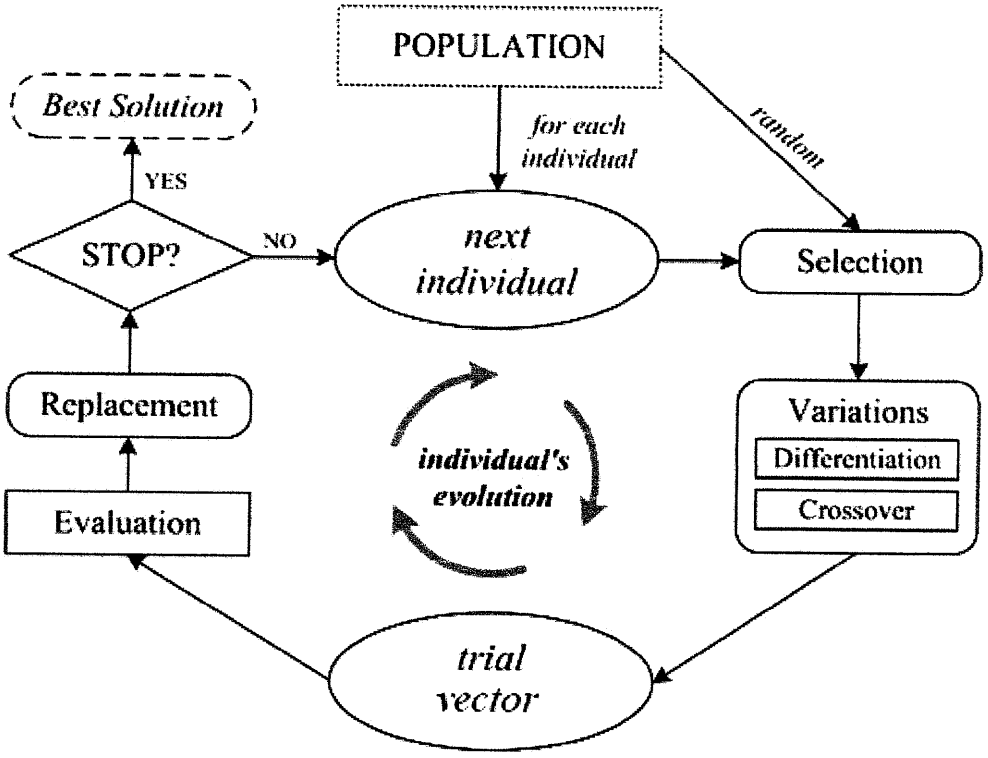


Fig. 2.1 Schematic of the full evolution cycle of Differential Evolution. (courtesy: [24])

2.3 Classical Particle Swarm Optimization (PSO)

Particle Swarm Optimization is a swarm intelligence method for global optimization [25]. For classical PSO, consider an optimization problem that requires the optimization of a certain objective function which consists of N variables. A group or swarm of particles is defined, where each particle is designated a random position in the N-dimensional problem space so that each particle position represents a potential solution to the optimization problem. Each of these particle positions is aimed to achieve a cost based on how it enhances the problem solution. These particles then swim through the problem space subject to set of update rules to new positions, which are subsequently gained.

As the particles navigate the problem space, each particle remembers its own personal best position that it has ever found, called its local best and each particle also knows the best position found by any particle in the swarm, called the global best. On consecutive iterations, particles are pulled toward these best solutions. Overshoot and undershoot accompanied with random adjustment discover areas through the problem space, finally reach the best solution.

This process can be visualized as a swarm of bees in a field [26] as it shown in fig.2.2. Their goal is to find the location with the highest density of flowers. Without any knowledge of the field in advance, the bees start in random locations with random velocities looking for flowers. Each bee can recall the locations where it found the most flowers density, and with swarm communication it knows the locations where the other bees found the flowers. Divided between going back to the location where it had personally discover the most flowers, or finding the location by others to have the most flowers, the infirm bee navigate in both directions changing its trajectory to fly somewhere between the two location. In its trajectory, a bee might find a place with a higher flowers density than it had found before. Then it will drift to this new location as well as the location of the higher flowers density found by the whole swarm. Sometimes, one bee may fly over a place with higher flowers density than had been discovered by any bee in the swarm. The whole swarm would then be directed to that location in additional to their own personal discovery. In this way, the bees sweep the field. Always, they are checking the field they fly over against previously discovered locations of highest density hoping to find the highest density of flowers. Finally, the bees' flight leads them to the only place in the field

with the highest flowers density. When the whole swarm of the bees could not desperately find any location of higher flower densities, they are eventually drawn back to the highest flower density.

The following steps are accomplished on each particle individually (see Fig. 2.3):

Step 1. The positions, $x^i(k)$ and velocities, $v^i(k)$ of the initial population of particles are randomly generated for the i^{th} particle at time k. Where i is the current particle number in the swarm, $i \in \{1, 2, \ldots, P\}$ and P is the swarm size.

Step 2. According to fitness function values for each particle, locate particle with the local best position value $p^i(k)$ over the current swarm, and also update the global best position $p^g(k)$ for the current and all the previous swarm moves.

Step 3. Update the velocities, according to

$$v^i(k+1) = w.v^i(k) + c_1.r_1.(p^i(k) - x^i(k)) + c_2.r_2.(p^g(k) - x^i(k)) \qquad (2.2)$$

where, r_1 and r_2 are uniformly distributed random variables in [0, 1], w is an inertia factor, c_1 is a self confidence factor, c_2 is a swarm confidence factor.

Step 4. Update the position of each particle i, by the procedure

$$x^i(k+1) = v^i(k+1) + x^i(k) \qquad (2.3)$$

Step 5. If any $x^i(k+1)$ exceeds the boundaries set by lb or ub, the particle will "bounce" back from the boundary, and thus always be inside the allowed search space.

Step 6. Repeat from step 2 until convergence is attained.

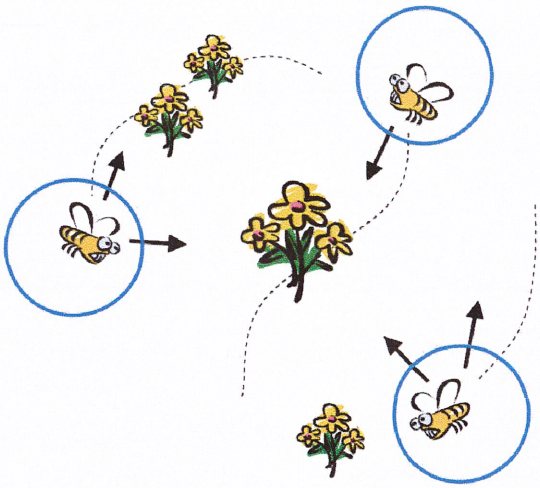


Fig. 2.2 Particle Swarm Optimization as modeled by a swarm of bees searching for flowers (courtesy: Robinson [26]).

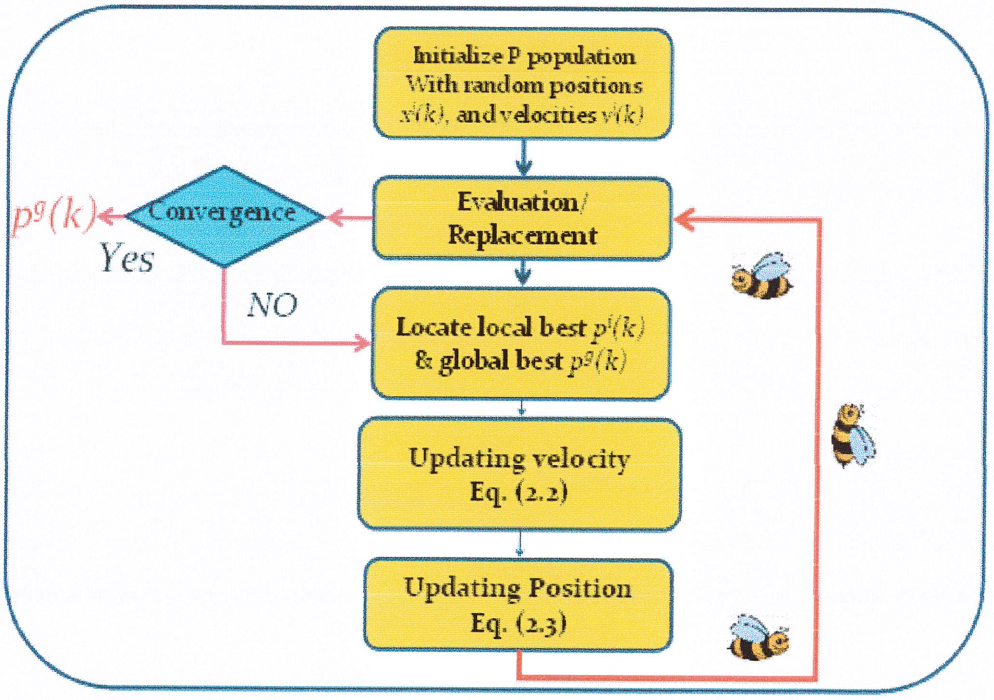


Fig. 2.3 Flowchart of the PSO algorithm

2.4 Enhanced Particle Swarm Optimization (EPSO)

Enhanced Practical Swarm Optimization (EPSO) algorithm [16] is similar to classical PSO with improved global search ability. This is achieved by introducing an updating formula for global best particle position and adding two new terms in the velocity updating formula of classical PSO. EPSO algorithm can be summarized in steps as follows:

Step 1. The positions, $x^i(k)$ and velocities, $v^i(k)$ of the initial population of particles are randomly generated for the i^{th} particle at time k. Where i is the current particle number in the swarm, $i \in \{1, 2, \ldots, P\}$ and P is the swarm size.

Step 2. According to fitness function values for each particle, locate particle with the best position value $p^i(k)$ over the current swarm, and also update the global best position $p^g(k)$ for the current and all the previous swarm moves

Step 3. Update the position of the global best particle with zero velocity according to the following equation:

$$p^g(k+1) = [1 + \lambda . U]\, p^g(k) \tag{2.4}$$

where U is a Gaussian random number with zero mean and unit variance, λ is a convergence acceleration parameter.

Step 4. Update velocities of all particles at time $k+1$ as follows:

$$\begin{aligned} v^i(k+1) = w.v^i(k) + c_1.r_1.(p^i(k) - x^i(k)) + c_2.r_2.(p^g(k) - x^i(k)) \\ + c_3.r_3.(p^i_{fdr}(k) - x^i(k)) + c_4.r_4.(p^g_{fdr}(k) - x^i(k)) \end{aligned} \tag{2.5}$$

where, r_1, r_2, r_3 and r_4 are uniformly distributed random variables in [0, 1], w is an inertia factor, c_1 is a self confidence factor, c_2 is a swarm confidence factor, c_3 and c_4 are acceleration constants, $p^i_{fdr}(k)$ and $p^g_{fdr}(k)$ are local and global candidate positions

that are selected by locating the individual with minimum fitness to distance ratio (FDR) over all particles in the swarm

The local and global *FDR* for each particle at time k is defined as:

$$FDR^i_{local} = \frac{fitness(p^g(k)) - fitness(x^i(k))}{dist(p^i(k), x^i(k))} \tag{2.6}$$

$$FDR^i_{global} = \frac{fitness(p^g(k)) - fitness(x^i(k))}{dist(p^g(k), x^i(k))} \tag{2.7}$$

where *fitness(.)* is the cost function to be minimized and $dist(p^g(k), x^i(k))$ is a measure related to the distance between the particle global best position and all other particles on the swarm defined as:

$$dist(p^z(k), x^i(k)) = \left| \sum_{j=1}^{N} \sqrt{p^{z,j}(k)^2 - x^{i,j}(k)^2} \right| \tag{2.8}$$

where $p^z(k)$ is either the local best $p^i(k)$ or global best $p^g(k)$ position vectors, $p^{z,j}(k)$ is the j^{th} component of the $p^z(k)$ vector. $x^{i,j}(k)$ is the j^{th} components of the i^{th} particle position vector $x^i(k)$ that is represented as $x^i(k) = (x^{i,1}, x^{i,2}, ..., x^{i,N})$ in the N-dimensional search space (particle size).

Step 5. The position of each particle is updated using its velocity vector at time $k+1$ as:

$$x^i(k+1) = x^i(k) + v^i(k+1) \tag{2.9}$$

Step 6. Repeat from step 2 until convergence criterion is met.

2.5 Hybrid DE/EPSO Algorithm

In the introduction of this chapter, some of hybrid techniques combining two algorithms were introduced. In this section, the hybrid technique of the two robust meta-heuristic global optimizers DE and EPSO is presented. The hybridization purpose is to include the essence and merits of both techniques. Generally, a Hybrid DE/EPSO procedure is aimed to give a fairly accurate optimum solution by increasing the solution space. For each generated population from both optimizers that are simultaneously executed, a new generation is produced to form DE/EPSO population. By interchanging individuals between the two parallel optimizers, better solutions could be achieved.

Also, it decreases the chance of trapping in local minima. The proposed hybridization works as follows (see Fig. 2.4):

Step 1. Initialize N-dimensional population of vectors with P individuals and apply DE to create a new generation.

Step 2. Initialize another N-dimensional population of vectors with P individuals and apply EPSO to create new generation.

Step 3. Merge the two new generations ($2P$ individuals) and locate the individual with the minimum fitness function value (*best individual*).

Step 4. Randomly select P individuals from the merged generation and insure that the selected individuals contain the *best individual* located in step 3. If not, sort the selected individuals according to their fitness function values and replace the individual with the highest fitness function value by the *best individual*.

Step 5. Apply EPSO to the generation that contains the *best individual* which is produced in step 4. This is to ensure that the EPSO will perform properly since the global best solution is needed in the updating equations.

Step 6. Apply DE to the remaining P individuals from the merged $2P$ population of step 3.

Step 7. Go to step 3 until a convergence criterion is met.

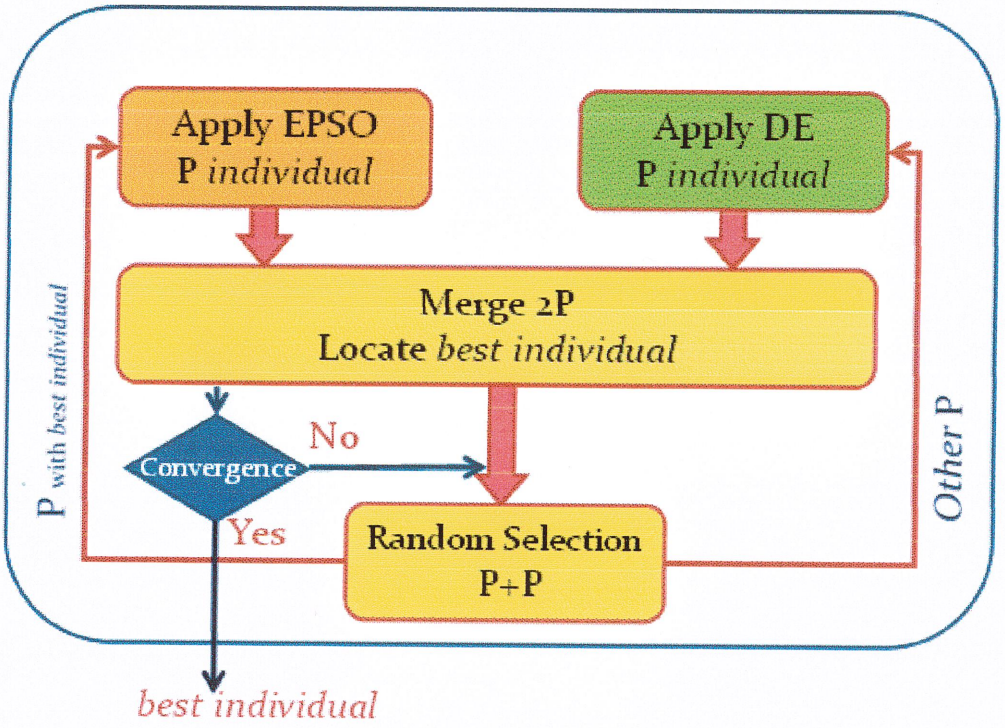


Fig. 2.4 Flowchart of the Hybrid DE/EPSO algorithm.

2.6 Optimization Example

The proposed hybrid EPSO/DE algorithm has been developed, and in this section it is desired to test the robustness of this hybrid algorithm. So, to show the capability of the proposed hybrid EPSO/DE algorithm, an evaluation example was conducted using three algorithms (DE, EPSO and hybrid EPSO/DE). This example is found in [27] (Wysota et al), and its objective is to minimize the sidelobe level (SLL) of the radiation pattern by element displacement of 16-elements linear array.

2.6.1 Design of unequally spaced linear array.

Consider a linear array placed along x-axis as shown in Fig.2.5. The Linear array consists of an even number of isotropic elements distributed symmetrically with respect to the y-axis. The array factor *(AF)* can be written as:

$$AF(\theta) = 2\sum_{n=1}^{M} a_n . \cos[kx_n \cos\theta] \qquad (2.10)$$

Where a_n is the amplitude excitation of the n^{th} element, $k=2\pi/\lambda$, λ is the wavelength, x_n is the position of the n^{th} element measured from the origin along x axis and θ angle in x-y plane. Assuming a vector $\boldsymbol{d} = [d_1, d_2, \ldots d_M]$ of spacing where d_n is a spacing between adjacent elements, then x_n can be described by follow:

$$x_n = \sum_{i=1}^{n} d_i \qquad (2.11)$$

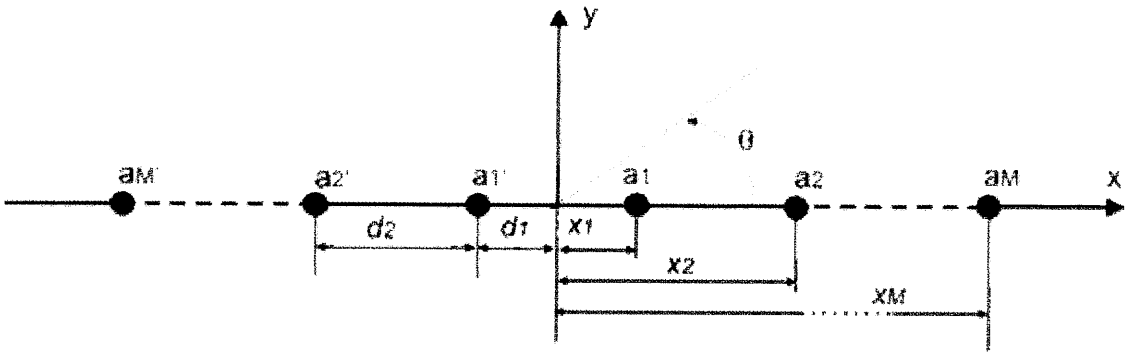


Fig. 2.5 Linear array geometry (courtesy: Wysota et al [27]).

2.6.2 Objective function formulation

The objective of this example is minimizing SLL of the linear array which could be achieved by optimizing the following fitness function [27]:

$$f = SLL = \max_{\theta \in c} \{20.\log|\mathrm{AF}(\theta)|\} \qquad (2.12)$$

Where c represents SLL region.

2.6.3 Numerical Results and Discussion

In this section numerical result of 16-elements non-uniform array of isotropic elements is considered. The array is assumed to be uniformly excited (*i.e.* $a_n=1$ where $n=1, 2, ..M$) and symmetric about x-axis, therefore the dimension of the problem is a half number of array elements. So there are eight elements locations to be optimized. The element spacing d_n is allowed to vary from 0.25λ to 2λ except d_1, which varying from 0.125λ to1λ.

All simulation examples in this thesis were performed using MATLAB® software version R2009b and all the used algorithms (DE, EPSO and Hybrid DE/EPSO) are M-files written in MATLAB® codes. The DE algorithm uses the following parameters: population size = 20, number of generations = 300000, constant of differentiation F in range of [0, 2] and probability of crossover $C_r = 0.9$. Meanwhile, EPSO algorithm uses the following parameters: swarm size = 20, number of generations = 300000, inertia weight factor $w = 0.5$, acceleration constants $c_1 = c_2 = 2$, $c_3 = 0.5$, $c_4 = 0.55$. These values of the algorithms parameters are applied to all optimization problems in the forthcoming chapters.

The DE, EPSO and the Hybrid EPSO/DE algorithms were applied to optimize the fitness function. Each algorithm was implemented to find the elements location of the linear array with lowest SLL. Table 2.1 presents the resulted SLL optimized using the three different algorithms and the SLL optimized in [27] using Hybrid Particle Swarm Optimization (HPSO), which is combination of standard PSO and gradients technique. It is obvious that the Hybrid EPSO/DE algorithm case gives the lowest SLL (-26 dB). Which is better than the SLL (-25.3 dB) that presented in [27]. Fig. 2.6 depicts the radiation pattern of the unequally spaced linear array optimized with the different algorithms including the results in [27].

Fig. 2.7 plots the convergence curves for the three algorithms used to design unequally spaced linear array. It is clear in this figure that the Hybrid EPSO/DE curve is converging better than DE and EPSO.

Table 2.1 SLL of unequally spaced 16-elements linear array using DE,EPSO and hybrid EPSO/DE algorithms versus the results in reference [27].

Algorithm	SLL[dB]	Inter-Element distance d
HPSO Ref. [27]	**-25.3**	[0.1270 λ 0.2500λ 0.2880λ 0.2950λ 0.2510λ 0.4240λ 0.3810λ 0.6340λ]
DE	**-19.5**	[0.1350 λ 0.2600λ 0.2800λ 0.3000λ 0.2220λ 0.4568λ 0.3508λ 0.6768λ]
EPSO	**-23**	[0.1220 λ 0.2350λ 0.2920λ 0.2970λ 0.2120λ 0.4555λ 0.3400λ 0.6478λ]
Hybrid EPSO/DE	**-26**	[0.1250 λ 0.2389λ 0.2915λ 0.2989λ 0.2033λ 0.4554λ 0.3400λ 0.6481λ]

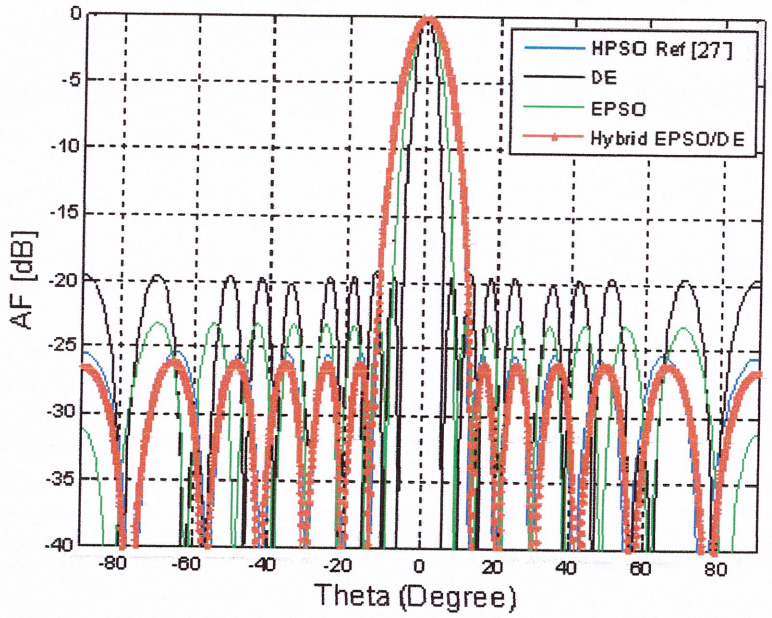


Fig. 2.6 The radiation pattern of the unequally spaced linear array optimized with the three algorithms versus the results in(Wysota et al [27]).

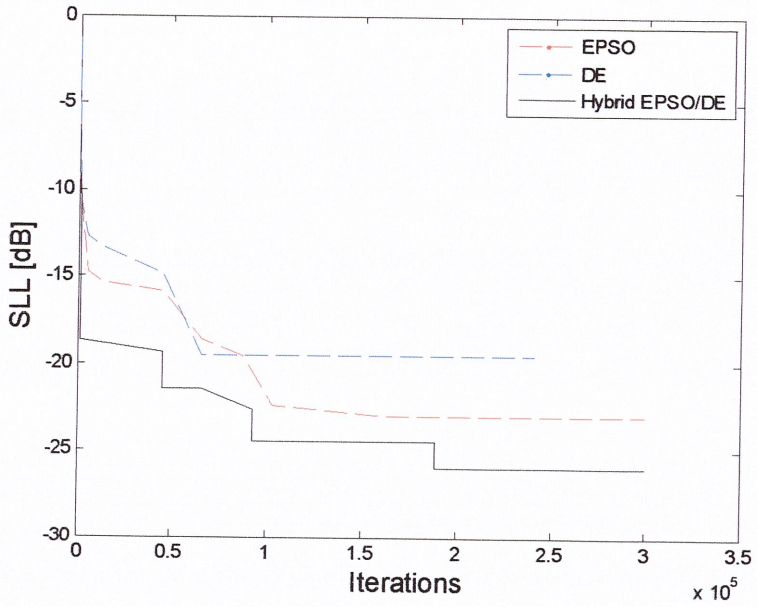


Fig. 2.7 Convergence curves for the three algorithms used to design unequally spaced linear array.

2.7 Conclusion

In this chapter, a novel hybrid global optimization algorithm DE/EPSO combining differential evolution (DE) and enhanced particle swarm optimization (EPSO) has been introduced. The hybrid DE/EPSO procedure gave a fairly accurate optimum solution by increasing the solution space. The Hybrid algorithm proved that it decreases the chance of trapping in local minima which enhanced the optimization performance.

The proposed technique has been applied for SLL minimization by optimizing the elements locations of 16-element linear array as a verifying example. Simulation results using MATLAB® show that the hybrid DE/EPSO outperforms the classical DE, EPSO and HPSO [27] in obtaining the desired pattern. It can be concluded that the hybrid DE/EPSO is an effective algorithm with improved accuracy, and it could be a promising tool to be applied for the design of reconfigurable antenna arrays, which is the objective of the following chapters.

Chapter 3

Null Steering by Position Perturbation of Selected Elements in Linear and Circular Antenna Arrays

3.1 Introduction

The intensive use of electromagnetic waves in our environment result in undesired radiation sources which interfere with some communication systems radiations. This interference decreases the signal-to-noise ratio and eventually degrades the performance of these systems. This illustrates the necessity of giving a significant attention for the study of array pattern nulling techniques. These techniques are aimed to suppress any radiation from specific direction in the radiation pattern of the antenna array. The source of the undesired radiation could be generated intentionally as in the case of the jammers, which used as one of the electronic warfare methods in the military field. The technique of null steering including controlling the excitation amplitude only, the excitation phase only, the complex weights (the amplitude and phase) and the inter-element distance only have been illustrated well in previous studies [28-32].

Null steering using complex weights as control parameter is the most efficient method since it has greater degree of freedom for the solution space [28]. In this chapter, it will be focused on the position perturbation of linear and circular antenna arrays to form pattern nulling. This technique needs servomotor for each element to make elements mobilized. This technique set the phase shifters to be used only for steering the main beam toward the desired direction determined by the designer. However, when the number of mobilized elements in the array increases, the complexity of the array implementation will be higher. Also, the process will require longer computational time to find the new position for the perturbed array's elements. So it is desired to reduce the number of mobilized elements by perturbing only the position of selected elements

depending on their contribution in the null forming. The selection process is introduced in [29] by eliminating the elements with less contribution to control the nulls in the antenna pattern. However, the solution is obtained using a semi-analytical technique.

It is desired to form deep nulls in the radiation pattern with minimum number of perturbed elements, these elements were chosen according to their contribution in forming nulls. To accomplish this, the elements positions are optimized in three different directions using a numerical iterative procedure with powerful and efficient evolutionary algorithm. Both EPSO and DE techniques are previously used for null steering by optimizing the amplitudes, phases or positions of antenna array elements [16, 30]. The proposed hybrid EPSO/DE that is introduced in chapter 2 is applied to both linear and circular antenna arrays in this chapter. This hybrid technique iteratively selects the best solution obtained from the two optimization algorithms.

The rest of this chapter is organized as follows: Section 3.2 describes the null steering using position perturbation for:

A. Linear antenna arrays

B. Circular antenna arrays.

Finally, some conclusion remarks are noted in Section 3.3.

3.2 Null steering using position perturbation.

3.2.1 Linear array Case.

For a phased symmetrically placed $2N$ elements along x-axis with equal inter-element spacing of d_0, the array factor can be written as:

$$AF(\theta) = 2\sum_{n=1}^{N} a_n . \cos[d_n (u - u_s)] \qquad (3.1)$$

where a_n is the n^{th} excitation amplitude, d_n is the n^{th} element position from array's center, $d_n = d_0 (n-0.5)$. $u = k \sin(\theta)$ where θ is angle measured from the broadside direction. $u_s = k \sin(\theta_s)$ is

main beam steering angle and $k=2\pi/\lambda$ is the wave number. The geometry of the linear array is shown in fig. 3.1.

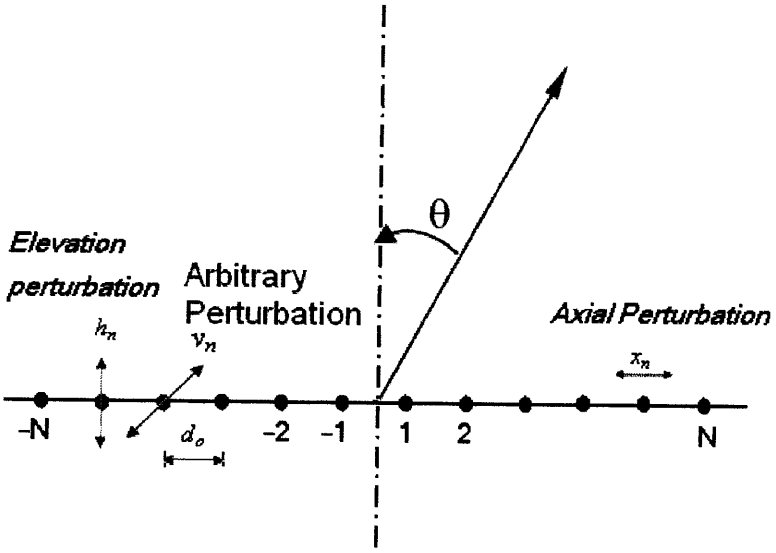


Fig. 3.1 Geometry of the linear array, depicted the 3 different position perturbation: axial, elevation and arbitrary perturbation.

The perturbed patterns corresponding to the element positional perturbations can be written as [31]:

For axial perturbation:

$$AF(\theta) = 2\sum_{n=1}^{N} a_n \cdot \cos\left[d_n\,(u-u_s) + x_n(u-u_s)\right] \tag{3.2}$$

For elevation perturbation:

$$AF(\theta) = 2\sum_{n=1}^{N} a_n \cdot \cos\left[d_n\,(u-u_s) + h_n(k\cos\theta - u_s)\right] \tag{3.3}$$

For arbitrary perturbation:

$$AF(\theta) = 2\sum_{n=1}^{N} a_n \cos\left[d_n\,(u-u_s) + v_n(k\cos(\beta_n - \theta) - u_s)\right] \tag{3.4}$$

Each element is subjected to positional perturbations of either x_n along the array axis or h_n normal to the array axis or $v_n = |v_n| e^{j\beta n}$ along the both directions where:

$$|v_n| = (h_n^2 + x_n^2)^{1/2} \tag{3.5}$$

$$\beta_n = \tan^{-1}(h_n / x_n) \tag{3.6}$$

Owing to the array symmetry, the perturbation vector v, can be defined for only half of the elements number as $v = [v_1, v_2, \ldots, v_N]$.

3.2.1.1 Objective function formulation

For null steering techniques it is always desired to get the prescribed null with very slight change in the main beam width and minimum increase in the maximum side lobe level (MSL). This is attained by solving minimax of the optimization problem that is subject to two constrains. The problem can be described as:

$$\begin{aligned} &\min_{dn} \in C \left\{ \max_{\theta_1, \theta_2 .., \theta_m} |AF(a_n, \theta, d_n)| \right\} \\ &\text{Subject to} \quad MSL \le SLL_p \ \& \ \delta BW \le \varepsilon \end{aligned} \tag{3.7}$$

Where $AF(a_n, \theta, d_n)$ is the array factor of the linear antenna array. $\theta_1, \theta_2, \ldots \theta_m$ are elevation angles of the desired null locations, m is the total number of nulls, C is the set of all vectors and d_n is the element's position to be optimized. MSL is the maximum side lobe level in the perturbed pattern. SLL_p is prescribed value of side lobe level. δBW and ε are the change and maximum allowed change in the main beam width respectively.

This problem is optimized using the developed EPSO/DE technique and the fitness function that is needed to be optimized can be written as:

$$f = \sum_{\theta=-90^0}^{\theta=90^0} |AF_i(\theta) - w_{null}(\theta).AF_i(\theta)| + \alpha(\theta) \tag{3.8}$$

where $AF_i(\theta)$ is the initial Chebyshev pattern, w_{null} is weight function define the desired nulls place. $\alpha(\theta)$ is factor to control *MSL*. In this section, the linear array is assumed to have $2N$ symmetric elements. This means that the numbers of elements to be optimized are N elements. The problem is then extended to iteratively minimize number of mobilized elements as follows:

Step 1: Optimize the position vector v for N elements noting that the array has symmetric configuration.

Step 2: Eliminate two elements with lowest $|v_n|$ by setting them to zero.

Step 3: Optimize v for N-2 elements and record the resultant v and corresponding (f) value.

Step 4: Eliminate one more element with the lowest $|v_n|$.

Step 5: Optimize v and record the resultant v and the corresponding (f) value.

Step 6: Go to *Step 4* if there is no significant decreasing change (approximately 20%) between current and previous iterations. Otherwise retrieve previous iteration and stop eliminating elements.

3.2.1.2 Numerical results and Analysis

The main goal of this optimization problem is to achieve nulls depth less than -100dB with minimum number of position perturbed elements for different configurations for uniform spacing linear antenna arrays. An initial design with Chebyshev linear array is considered for the optimization process. The array consist of 20-element, 0.5λ inter-element spacing and MSL =-35 dB and main beam direction toward the broadside is used as initial pattern. The used parameters in fitness function were chosen as:

$$w_{null}(\theta) = \begin{cases} 0 & if\ \theta = \theta_i \\ 1 & otherwise \end{cases} \tag{3.9}$$

where $i=1, 2..., m$ *and* m is total nulls number.

$$\alpha(\theta) = \begin{cases} MSL & if\ MSL > SLL_p \\ 0 & otherwise \end{cases} \tag{3.10}$$

$\varepsilon = 1°$ that is the maximum allowable change in beamwidth. The boundaries for parameters x_n, h_n in axial and elevation are {-0.08, 0.08}, and for $|v_n|$ is {0,0.08}, for β_n is {-π , π} in arbitrary, parameters x_n , h_n and $|v_n|$ are given in λ. A comparison is performed between the three configurations axial, elevation and arbitrary using the three algorithms DE, EPSO, Hybrid EPSO/DE for each configuration on certain null locations. These locations are chosen to be two maxima of the side lobes in the Chebyshev pattern, this comparison is shown in Table 3.1. Figure 3.2 shows the array factor pattern with nulls placed at angles 105° and 110°. It is obvious from Table 3.1 that arbitrary configuration has the minimum number of position perturbed elements (6 elements only, better peak SSL and satisfying null depth) to form the nulls compared with axial and elevation configurations. Also it is found that the proposed algorithm Hybrid EPSO/DE has the maximum null depth and peak side lobe better than using each algorithm separately. The same problem is optimized using a semi analytical method in [29], the solution is found to be 12 perturbed elements with MSL of -28dB and null depth value about -80dB. In comparing, the results obtained using our developed optimization method are found to has less number of minimum elements perturbed, and less MSL and deeper null value, besides achieving the nulls in asymmetric locations by applying elevation and arbitrary perturbation.

Figure 3.3 shows the convergence curve for the three optimization techniques that are used to achieve the imposed two nulls by arbitrary perturbing the elements of the considered linear antenna array. As shown EPSO, DE and hybrid DE/EPSO achieve convergence after 3000, 6000 and 8000 iterations respectively, that are equivalent to 150, 300 and 400 generations. The figure also indicates that the proposed hybrid DE/EPSO has the minimum value of fitness function. It should be noted here that the fitness function is a weighted sum function of the null depth, SLL change and the number of perturbed elements.

Another example is demonstrated with five nulls imposed at 18°, 32°, 123°, 130° and 138° simultaneously as shown in Figure 3.4 with 10 perturbed elements only. From Table 3.2, the arbitrary configuration optimized by the hybrid algorithm proved to be the best solution with only ten perturbed elements and -212 dB null depth. The second best solution is found to be the axial perturbation which is better than the elevation perturbation that has a higher MSL. Table 3.3 shows the values and locations of the perturbed elements of the 20 element linear antenna array for arbitrary perturbation for the two and five nulls cases using Hybrid algorithm.

Table 3.1. Comparison between position perturbation types and optimization algorithms for linear array and 2 nulls case

Null	Perturbation	Algorithm	No. of Perturbed Elements	SLL [dB]	Null Depth [dB]
105°, 110°	Axial	DE	10	-30	86
		EPS	10	-30.5	-42.2
		HYBRID	10	-30.5	-127
	Elevation	DE	10	-30	-335
		EPSO	14	-30	-239
		HYBRID	8	-30	-296
	Arbitrary	DE	6	-29	-80.5
		EPSO	6	-30.5	-125
		HYBRID	6	-32	-225

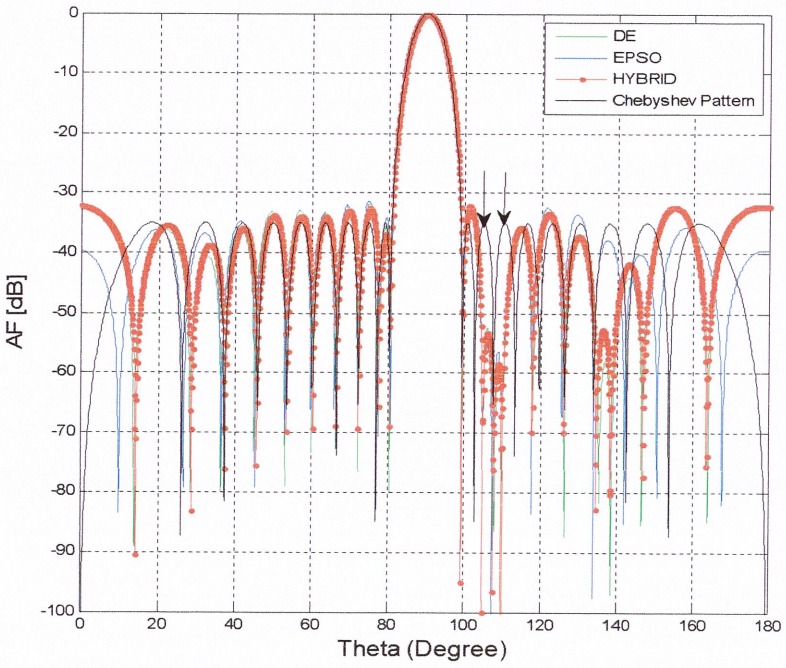


Figure 3.2 The initial and the three algorithms perturbed pattern for linear array with imposed nulls at 105° and 110°.

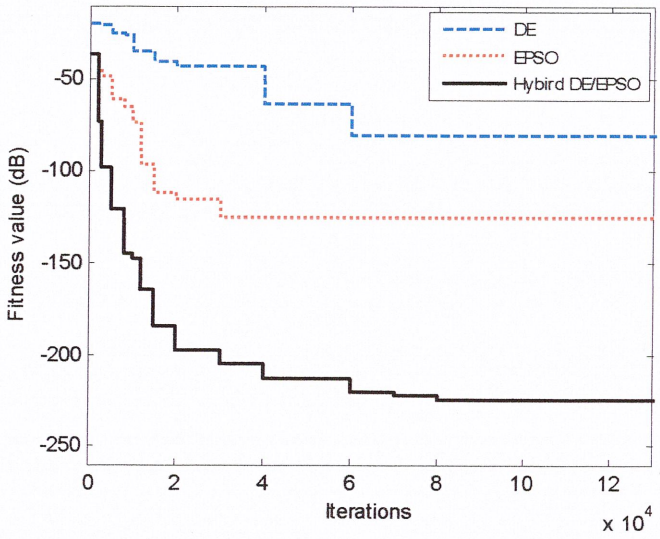


Fig. 3.3 Convergence curves for the three algorithms used to design perturbed linear array

Table 3.2. Comparison between position perturbation types and optimization algorithms for linear array and 5 nulls case

Null	Perturbation	Algorithm	No. of Perturbed Elements	SLL [dB]	Null Depth [dB]
18°, 32°, 123°, 130°, 138°	Axial	DE	16	-31	-43.2
		EPSO	16	-31	-47.2
		HYBRID	16	-31	-48.7
	Elevation	DE	16	-31	-36.6
		EPSO	16	-31	-41.8
		HYBRID	16	-31	-41.8
	Arbitrary	DE	16	-31.1	-39.3
		EPSO	12	-31.2	-212
		HYBRID	10	-31.1	-212

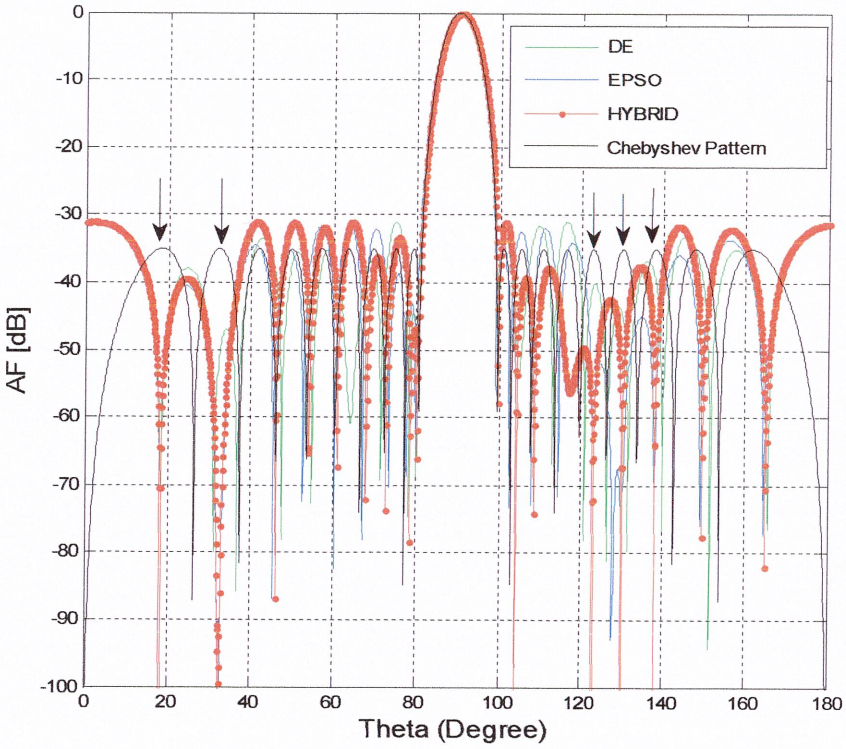


Figure 3.4 The initial and the three algorithms perturbed pattern for linear array with imposed nulls at 18°, 32°, 123°, 130° and 138°

Table 3.3 Values of the position vector for arbitrary perturbation of linear array using hybrid DE/EPSO

Element Location	**Nulls 105°, 110°**		**Nulls 18°, 32°, 123°, 130° , 138°**	
	v_n	β_n	v_n	β_n
±1	0	0	0	0
±2	0	0	0	0
±3	0	0	0	0
±4	0	0	0.0137	2.9216
±5	0	0	0	0
±6	0		0.0261	2.7572
±7	0.0332	4.1457	0	0
±8	0	0	0.0292	2.5362
±9	00181	3.3935	0.0659	3.269
±10	0.0678	0.9771	0. 646	1.3362

3.2.2 Circular Array Case

Recently, the circular array has gained an increased popularity in researches more than linear array due its wide steering capability in the azimuth. In some communication systems it is desirable to suppress the noise generated either intentionally by certain jammers or unintentionally by other undesired communication systems. So many techniques were developed to form nulls in the array pattern toward the directions of the interference which are called the null steering techniques.

Similarly to linear array in previous section, in this section, it will be focused on the position perturbation of circular antenna array to form nulls in the radiation pattern.

Consider a circular antenna array as shown in Fig. 3.5. The array consists of $2N$ isotropic elements equally spaced by d_0 around the circumference of a circle of radius r on the $x-y$ plane.

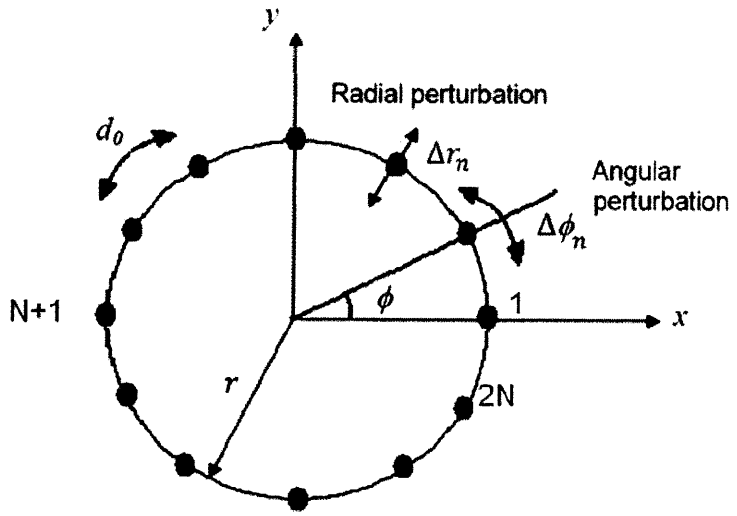


Fig. 3.5 Geometry of circular array with illustration of the different types of elements position perturbation

So the radiation pattern of this array can be described by its array factor which is given by [34] as:

$$AF(\phi) = \sum_{n=1}^{2N} I_n \, e^{j k r[\cos(\phi-\phi_n)-\cos(\phi_0-\phi_n))} \tag{3.11}$$

where I_n is the amplitude excitation of the n^{th} element, $r = (2Nd_o) / 2\pi$, k is the wave number, ϕ_n is the angular position of the n^{th} element on the x-y plane where $\phi_n = 2\pi\,(n-1/2N)$ for $n \in \{1, 2, \ldots, 2N\}$, ϕ_0 is the direction of the main beam. Each element in the array is subjected to one of three types of perturbation. Radial perturbation (Δr_n) along the radius r, angular perturbation ($\Delta\phi_n$) along the circumference of the circle or arbitrary perturbation that can be represented in by ($\Delta r_n e^{j\Delta\phi_n}$). The arbitrary perturbation can also be presented by the displacement vector v with respect to elements initial positions, where $v_n = |v_n| e^{j\beta_n}$, β_n in the range between $\{-\pi, \pi\}$. Noting that the array has even number $2N$ with equal inter-elements spacing d_o and $\phi_{n+N} = \phi_n + \pi$ then the overall position vector v can be reduced to N dimensions vector as $v = [\, v_1, v_2, .., v_N \,]$. The array factor patterns in this case can be written as:

$$AF(\phi, v) = 2\sum_{n=1}^{N} I_n \cos\{k(r+|v_n|)[\cos(\phi-(\phi+\beta_n))-\cos(\phi_0-(\phi_n+\beta_n))]\} \tag{3.12}$$

3.2.2.1 Objective function formulation

As in linear array, to get nulling pattern in a certain radiation pattern, one or more of its properties will be changed like main beam width BW (directivity), sidelobe level SLL and peak sidelobes location. In this section it will be focused to get the desired null depth with very slight change in the main beam width and acceptable increase in the side lobe level SLL. This is attained by solving minimax of the optimization problem that is subject to two constrains. The objective function can be described as:

$$F(v) = a\sum_{m=1}^{M} |AF(\phi_m, v)|^2 + b\sum_i \frac{1}{\Delta\phi_i} \int_{\phi_{1i}}^{\phi_{2i}} |AF(\phi, v)| d\phi \tag{3.13}$$

where AF (ϕ_m , v) is the array factor for circular phased array. v is the perturbation position vector that needs to be optimized, ϕ_m is the angle of the prescribed null locations, M is the total number of nulls, [ϕ_{1i} , ϕ_{2i}] are the i^{th} spatial region boundaries of the array pattern excluding the main beam in which average peak *SLL* need to be constrained, $\Delta\phi_i = \phi_{1i} - \phi_{2i}$, a and b are weighting coefficient. In (3.13), the first term represents the fitness function that need to be optimized for nulls control purpose, while the second term is used for constraining the average *SLL*. The null steering technique is developed by optimizing (3.13) for a given prescribed nulls to obtain the array geometry. The problem is then extended to iteratively minimize number of mobilized elements in accordance with the procedure of the linear array case which is described earlier.

3.2.2.2 Analysis and numerical results

Similarly to linear array case, the goal of this section is to achieve nulls depth in the radiation pattern as deep as -100dB with minimum number of position perturbed elements for different configurations of the position perturbation for uniform spacing circular antenna arrays. A circular array with 36-element and 0.25λ inter-element arc spacing is used. To get Chebyshev-like for a circular array, the amplitude and phase excitation values in [35] are used which result in pattern with SLL= -31.4dB. The optimized parameter in each configuration is: for radial and arbitrary Δr_n in range of {-0.1, 0.1}, for angular and arbitrary $\Delta\phi_n$ in range of {-2.5, 2.5}, where Δr_n in λ and $\Delta\phi_n$ in degrees.

A comparison is accomplished between the three configurations angular, radial and arbitrary using the three algorithms DE, EPSO, HYBRID EPSO/DE for each configuration on certain null locations. These locations are chosen to be two maxima of the sidelobes in the Chebyshev-like pattern at angles 54° and 110° as shown in figure 3.6, the comparison is shown in Table 3.4 which verified that the arbitrary configuration is the best of null forming (-332 dB) with 18 elements perturbed (half number of array), then the radial (-324 dB) with 18 elements perturbed, then the angular configuration, all with MSL not more than -30 dB. Figure 3.6 shows the array factor pattern with nulls placed at angles 54° and 110° optimized with the three different

algorithms. While Fig. 3.7 presents the convergence curves for imposing two nulls using arbitrary perturbation of circular array.

Another comparison is demonstrated with five nulls imposed at 54°, 73°, 94°, 110° and 152° simultaneously as shown in Table 3.5, which proved that the arbitrary configuration with hybrid algorithm is the best with -177 dB nulls formed by 22 elements perturbed as we can see in Table 3.5. The second best solution is the radial perturbation with 26 elements perturbed and -223 dB null depth, all with MSL not more than -27 dB. Figure 3.8 shows the array factor pattern with nulls placed at 54°, 73°, 94°, 110° and 152°.Table 3.6 shows the values and locations of the perturbed elements of the 36 element circular antenna array for arbitrary perturbation for the two and five nulls cases using Hybrid algorithm.

Table 3.4. Comparison between position perturbation types and optimization algorithms for circular array and 2 nulls case

Angle	Perturb. type	Algorithm	No. perturbed Element	SLL [dB]	Null depth [dB]
54°, 110°	Angular	DE	36	-30	-33.3
		EPSO	36	-30	-34.9
		HYBRID	36	-30	-34.4
	Radial	DE	28	-30	-166.5
		EPSO	28	-30	-208
		HYBRID	18	-30	-324.9
	Arbitrary	DE	36	-30	-34
		EPSO	18	-30	-221.7
		HYBRID	18	-30	-332.5

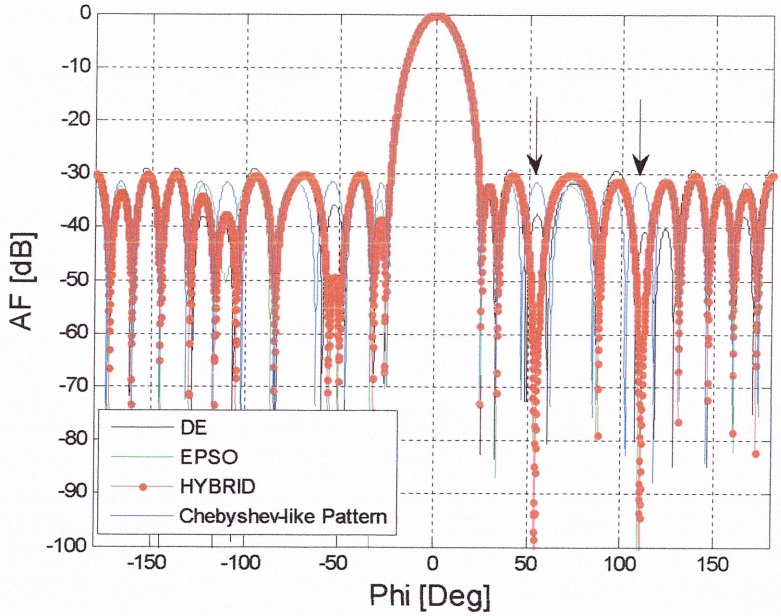


Figure 3.6 The initial and the three algorithms perturbed pattern for circular array with imposed nulls at 54°, 110°

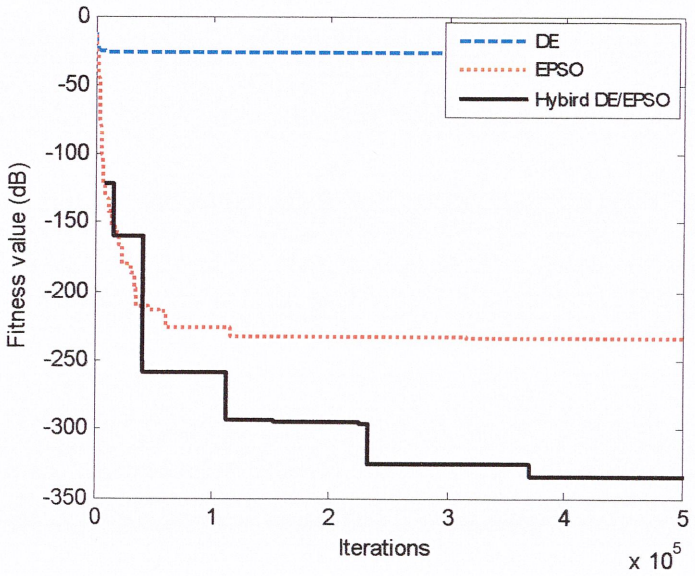


Fig.3.7 Convergence curves for the three algorithms used to design perturbed circular array (2 null - arbitrary perturbation case

Table 3.5. Comparison between position perturbation types and optimization algorithms for circular array and 5 nulls case

Angle	Perturb. type	Algorithm	No. perturbed Element	SLL [dB]	Null depth [dB]
54°,73°, 94°, 110°, 152°	Angular	DE	36	-27	-32.3
		EPSO	36	-27	-34.5
		HYBRID	36	-27	-34.3
	Radial	DE	36	-27	-39.5
		EPSO	26	-27	-222
		HYBRID	26	-27	-223.4
	Arbitrary	DE	24	-27	-212.2
		EPSO	24	-27	-201.7
		HYBRID	22	-27	-177.9

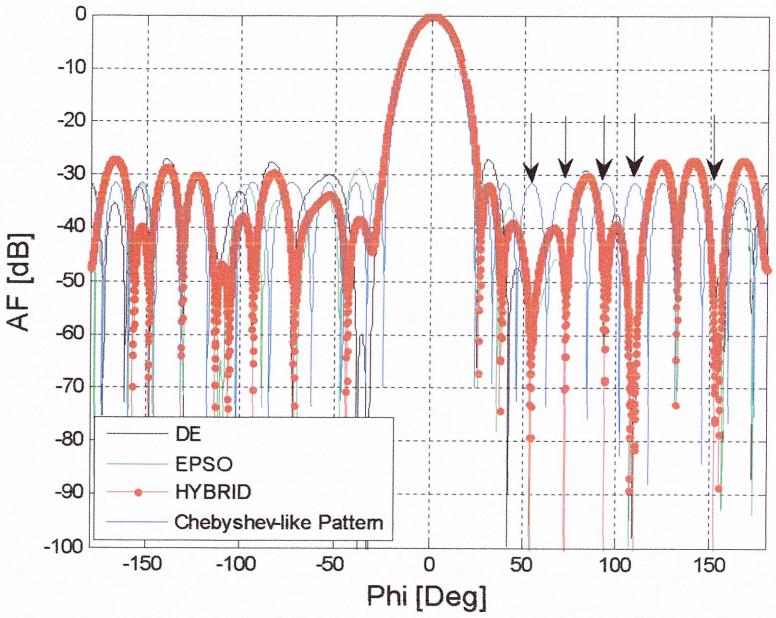


Figure 3.8 The initial and the three algorithms perturbed pattern for circular array with imposed nulls at 54°, 73°, 94°, 110° and 152°.

Table 3.6 Values of the position vector for arbitrary perturbation of circular array using hybrid DE/EPSO

Element's Location	Nulls 54°, 110°		Nulls 54°,73°, 94°, 110°, 152°	
	Δr_n (λ)	$\Delta\phi_n$	Δr_n (λ)	$\Delta\phi_n$
1,19	-0.02	0.412	0	0
2,18,20,36	0	0	0	0
3,17,21,35	0.0046	0.272	0.0169	-0.097
4,16,22,34	0	0	0.023	-0.0657
5,15,23,33	0	-0.0495	-0.02	-0.186
6,14,24,32	-0.02	-0.042	-0.053	-0.2211
7,13,25,31	0	0	-0.025	-0.277
8,12,26,30	0	0	0	0
9,11,27,29	0.007	-0.168	0	0
10,28	0	0	-0.005	0.261

3.3 Conclusion

A novel null steering method depending on position perturbation of selected elements of linear and circular arrays using newly developed Hybrid EPSO/DE optimization algorithm was presented. The new method of null steering succeeded to place deep nulls in the initial pattern, up to five nulls simultaneously with acceptable increase in the MSL and main beamwidth. This null control method is proved to eliminate the elements with less contribution to the null forming. The remaining array elements will be selected to be perturbed to form the desired prescribed nulls. This method was applied successfully with different perturbation directions in axial direction (array line), elevation direction (normal to the array line) or arbitrary directions for the linear array and radial, angular and arbitrary directions for the circular array. To conclude, Hybrid EPSO/DE was found to be an excellent optimization tool for the problem of null steering using selected position perturbed array elements, and the arbitrary case was the most efficient in null forming, with less elements of both linear and circular array to be perturbed.

Chapter 4

Design of Concentric Circular and Concentric Hexagonal Antenna Array Using Hybrid EPSO/DE Algorithm

4.1 Introduction

A very low sidelobe level radiation pattern of a linear array could be synthesized with a high gain main lobe and narrow beam width in any given direction for the elevation plane, but it does not work equally well in the azimuth plane. The two dimensional antenna arrays have the capability to transmit and receive data in elevation and azimuth angles as well, thus two dimensional antenna arrays configurations have been widely used in the field of *3D* beamforming.

One of the best configuration of two dimensional antenna arrays is the circular antenna array, since its main lobe could be steered an all azimuth angles without changing its beam width [36-38], Nevertheless, a circular array is a high sidelobe geometry. If the inter-element distance is decreased to minimize the sidelobes level, the mutual coupling effect becomes more severe. For reducing the high sidelobe levels, concentric arrays could be used which have some other advantages like smaller array size compared to the circular array. Furthermore, the hexagonal array could overcome the problem of high sidelobes [38-39]. It is proved that the hexagonal array has better steerability and higher gain properties than circular array for both hexagonal and concentric hexagonal arrays [40]. The circular array has a high sidelobe level pattern so the inter-element distance of array antenna should be small to minimize the SLL [38]. But the small distance between elements increase the mutual coupling effect. To overcome this, the multi-ring

antenna arrays with adequate inter-element distance are utilized in synthesizing radiation pattern with low SLL in the azimuth plane.

4.2 The objective and organization of chapter 4

In this chapter it will be focused on studying and designing the circular, concentric circular, hexagonal and concentric hexagonal arrays, with same number of elements (36 elements) in each case to minimize the SLL in the azimuth plane, while preserving the main lobe beamwidth. The minimum distance between adjacent elements is intended to be not less than 0.5λ for the concentric configurations, to mitigate the effect of mutual coupling between elements.

After designing these arrays, the outer ring(s) in the case of multi-ring arrays will be rotated to get the low sidelobe level SLL. Furthermore, the complex weights excitations (amplitude and phase) will be optimized to get the lowest SLL and will be compared to a reference pattern utilized circular array. Also the effect of including central element in the array will be studied in the case of concentric arrays.

The rest of this chapter will be organized as follow:

Section 4.3 describes the design of circular array CA; **section 4.4** presents design of hexagonal array HA. In **section 4.5** a design example of 36 isotopic elements uniform CA and HA is presented and **section 4.6** introduces the design of concentric circular and concentric hexagonal array. **Section 4.7** illustrates a design example of 36 isotropic elements uniform amplitude concentric circular array UCCA and uniform concentric hexagonal array UCHA.

The first optimization problem in this chapter is in **section 4.8** by rotating the outer ring(s) of the UCCA and UCHA. The second optimization problem is found in **section 4.9** by optimizing the complex weights of CA, HA, then two-ring, three-ring and four-ring of CCA and CHA, the effect of adding the central element to the configurations is illustrated in this section. Finally this chapter is concluded in **section 4.10**.

4.3 Design of Circular Array

Consider a circular array (CA) as shown in Fig.4.1. The array consists of *2N* isotropic elements equally spaced by d_0 around the circumference of a circle of radius *r* on the $x-y$ plane. So the radiation pattern of this array can be described by its array factor which is given by [34] as:

$$AF(\theta,\phi)=\sum_{n=1}^{2N} I_n \, e^{j(k\,r\,\sin\theta\cos(\phi-\phi_n)+\alpha_n)} \tag{4.1}$$

$$r=\frac{2Nd_0}{2\pi} \tag{4.2}$$

Where I_n is Amplitude excitation of n^{th} element, *r* is the radius of the circular array in λ, *k* is the wave number, α_n is the phase excitation of n^{th} element and ϕ_n is the angular position of the n^{th} element on the *x-y* plane and given by:

$$\phi_n=2\pi\left(\frac{n-1}{2N}\right) \quad \text{for } n=1,2,\ldots,2N \tag{4.3}$$

To direct the peak of the main beam in a certain direction ϕ_0, the phase excitation of the n^{th} element can be chosen to be [34]:

$$\alpha_n=-kr\cos(\phi_0-\phi_n) \tag{4.4}$$

Since the circular array has even number of elements 2N with equal spacing between elements, which means:

$$\phi_{n+N}=\phi_n+\pi \tag{4.5}$$

Then equation (4.1) can be rewritten as for the uniform amplitude excitation:

$$AF\ (\phi)=2\sum_{n=1}^{N}\cos\ \{kr[\cos(\phi-\phi_n)-\cos(\phi_0-\phi_n)]\} \tag{4.6}$$

4.4 Design of Hexagonal Array

The hexagonal array (HA) as depicted in Fig. 4.2 is considered a multi-ring array, since its elements placed with different distances (radii) from the center of array. The radii of adjacent elements either the same or have slight difference. To form a hexagonal geometry, the number of elements in it should be six or its multiples. The array factor of the hexagonal array will be:

$$AF(\phi) = \sum_{m=1}^{M} \sum_{n=1}^{N_m} I_{mn} \exp\{kr_m \cos(\phi - \phi_{mn}) + \alpha_{mn}\} \quad (4.7)$$

Where M is the total number of rings in the hexagonal array, N_m is the total number of elements in the m^{th} ring, ϕ_{mn} is the predetermined angular position, I_{mn} and α_{mn} are the amplitude and phase excitation of mn^{th} element and r_m is the radius of the m^{th} ring.

Similarly to [40], the radii and the angular positions of hexagonal elements in this chapter will be calculated according to the number of elements and inter-element distance in the geometry. The maximum radius (r_1) in the hexagonal ring which measured from the array center to the vertices will be used to define the geometry size.

4.5 Design example: 36 elements, uniform amplitude, equally spaced CA and HA

It is assumed here for comparison purpose, a uniform amplitude (i.e. I_n = 1) equally spaced circular array (UCA) and uniform amplitude equally spaced hexagonal array (UHA) with 36 isotropic elements for each. The elements spaced with d_0 = 0.25λ, therefore the radius r will be 1.43λ for the circular and 1.5λ as maximum radius r_1 for the hexagonal array.

The radiation pattern of both geometries in the x-y azimuth plane (θ=90°) is depicted in Fig. 4.3. From this figure it is clear that both patterns almost have the same beam width, with slight reduction in SLL for the hexagonal array by -0.25 dB. The values of beamwidths and SLL for the hexagonal and circular array are summarized in table 4.1

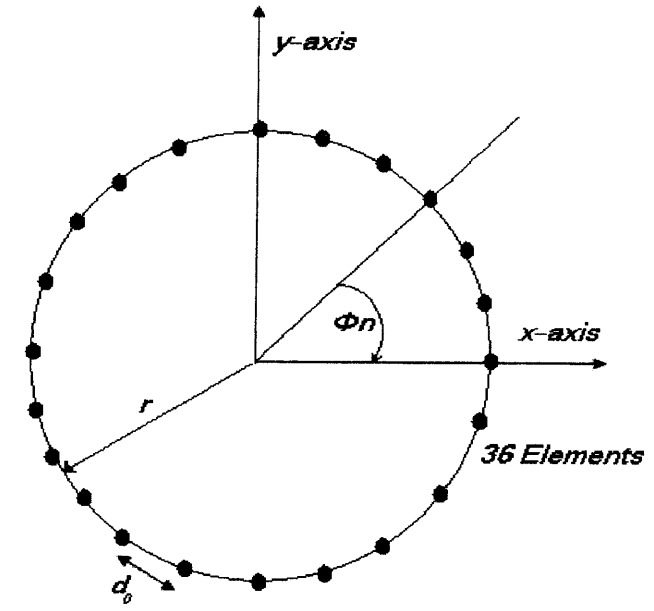


Fig 4.1 Geometry of Circular Array with 36 elements.

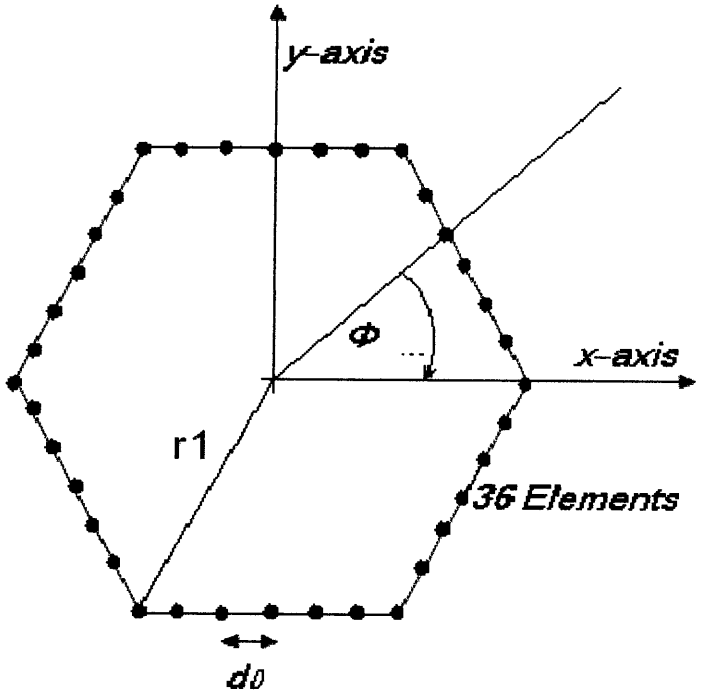


Fig 4.2 Geometry of Hexagonal Array with 36 elements.

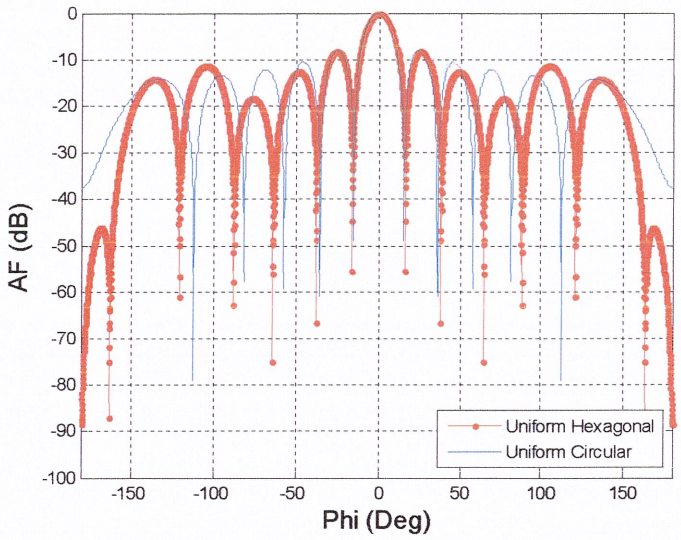


Fig. 4.3 Radiation pattern of uniform Hexagonal and Circular Arrays with 36 elements and 0.25λ inter-element spacing at θ=90°.

Table 4.1 The SLL and Beam width for both 36 elements Geometries.

Configuration	**Beamwidth [Deg]**	**SLL [dB]**
Hexagonal Array	32	-8.15
Circular Array	31	-7.9

4.6 Design of concentric circular and concentric hexagonal antenna array

If several ring arrays sharing the same center point but with different radii, then the formed configuration is a concentric circular/hexagonal array. Recently, the antenna designers have been exerted a lot time in enhancing the performance of mobile and wireless communication systems through increasing channel capacity, customizing antenna beams and increasing coverage area as possible. However, the unstudied well array synthesis could result in many problems like the appearance of undesired radiations which interfere with other communication systems, beside wastage of the radiated power, which consider a distressing problem for power-limited battery-driven wireless devices [41].

Among different types of planar antenna arrays concentric circular array (CCA) was studied in [42-52] gained more popularity in mobile and wireless communications. These arrays have various advantages like steerablity, high gain and their compact size compared to the circular arrays. The array factor for the CCA will be as in the hexagonal array in equation (4.7), but with angular position ϕ_{mn} as follow:

$$\phi_{mn} = 2\pi\left(\frac{n-1}{N_m}\right) \qquad \text{m=1,2,...,M} \quad \text{n=1,2, ..., } N_m \qquad (4.8)$$

If the amplitude excitation are taken to be $I_{mn} = I_{mn+Nm/2}$ then,

$$AF(\phi) = 2\sum_{m=1}^{M}\sum_{n=1}^{N_m/2} I_{mn}\cos\{kr_m\cos(\phi-\phi_{mn})+\alpha_{mn}\} \qquad (4.9)$$

To direct the peak of the main beam in the ϕ_0 direction, the phase excitation of the mn^{th} element can be chosen to be:

$$\alpha_{mn} = -\alpha_{mn+N_m} = -kr_m\cos(\phi_0-\phi_{mn}) \qquad (4.10)$$

The array factor for the concentric hexagonal array (CHA) will be the same as in equation (4.9). Similarly to [40], the radii and the angular positions of the CHA elements will be calculated according to the assumed geometry.

4.7 Design Examples: 36 Isotropic Elements, Uniform Amplitude Concentric Circular and Concentric Hexagonal Antenna Array

CA and HA arrays obtained SLL=-8.15dB as low result in previous section with 36 element equally spaced with 0.25λ. This section presents a comparative study of different types of multi-rings arrays. The uniform concentric circular arrays (UCCA), and uniform concentric hexagonal arrays (UCHA), are designed with fixed number of elements (36 elements). The UCCAs and UCHAs are designed with uniform inter-element distance 0.5λ at least in the same ring. The resulted radiation pattern of each case will be compared to the other, from the aspects of sidelobe level SLL and main lobe beam width BW.

Starting with 36 isotopic elements that are needed to be arranged in two-rings, three-rings and four-rings, many configurations can be assumed according to the number of elements in each ring. One ring at least should have 0.5λ inter-element spacing in the array. This depends on the configuration and the number of ring's elements N_m. Two cases in each configuration for UCCA and UCHA are chosen.

Table 4.2 depicted the definition of these configurations. The table also shows the number of elements N_m, the inter-element distance d_{0m} and the radius of circular ring or the maximum radius r_m of hexagonal ring. Fig. 4.4 shows the geometries of UCCA and UCHA with different configurations for the two, three and four rings arrays.

Table 4.2 The configurations details: number of elements and the dimensions of each ring for UCCA and UCHA.

Configuration		1st Ring [λ]		2nd Ring [λ]		3rd Ring [λ]		4th Ring [λ]	
		r_1	d_{01}	r_2	d_{02}	r_3	d_{03}	r_4	d_{04}
Config.2.1 {18, 18}	UCCA	1.43	0.5	1.91	0.67	-	-	-	-
	UCHA	1.5	0.5	2	0.67	-	-	-	-
Config.2.2 {12, 24}	UCHA	0.95	0.5	1.91	0.5	-	-	-	-
	UCHA	1.0	0.5	2	0.5	-	-	-	-
Config.3.1 {6, 6, 24}	UCHA	0.48	0.5	0.95	1	1.91	0.5	-	-
	UCHA	0.5	0.5	1	1	2	0.5	-	-
Config.3.2 {6, 12, 18}	UCHA	0.48	0.5	0.95	0.5	1.43	0.5	-	-
	UCHA	0.5	0.5	1	0.5	1.5	0.5	-	-
Config.4.1 {6,6,12,12}	UCHA	0.48	0.5	0.95	1	1.43	0.75	1.91	1
	UCHA	0.5	0.5	1	1	1.5	0.75	2	1
Config.4.2 {6, 6, 6, 18}	UCHA	0.48	0.5	0.95	1	1.43	1.5	1.91	0.67
	UCHA	0.5	0.5	1	1	1.5	1.5	2	0.67

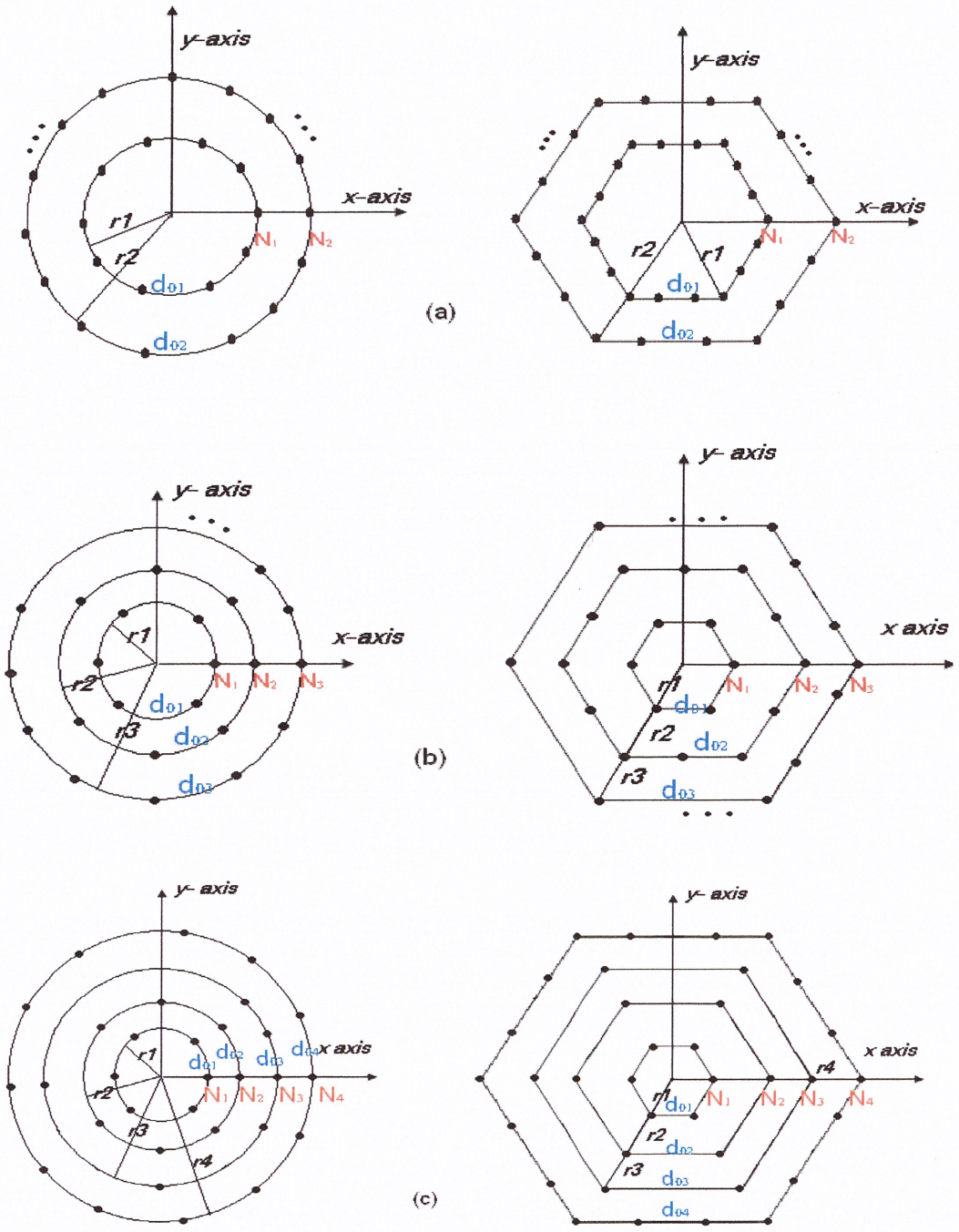


Fig.4.4 Geometries of UCCA and UCHA for different configurations: (a) two-rings, (b) three-rings, and (c) four-rings.

The radiation pattern's characteristics of the designed configurations are shown in table 4.3. It is obvious that the beamwidths of these configurations are close to the beamwidths of the uniform circular and hexagonal array illustrated in table 4.1 earlier. The SLL of most configurations are better than the SLL of the uniform circular and hexagonal array, except the case of config.4.1 {6, 6, 12, 12} UCHA which gave -7 dB.

The best case was for config.3.2 {6, 12, 18} UCHA with SLL= -14.3 dB, by a reduction of -6.15 dB than the uniform hexagonal array with 4° degrees wider beamwidth. It can be seen that the UCHA configurations are better in SLL than the UCCA configurations according to these results on the mentioned table.

It could be said that, for the same number of elements (36 elements) with 0.5λ at least as inter-element distance, many configurations UCCA and UCHA have lower SLL than the uniform circular and hexagonal array with 0.25λ inter-element distance and almost have the same beamwidth. The 0.5λ have been chosen to be the minimum distance between any two adjacent elements in the UCCA and UCHA , to mitigate the effects of the mutual coupling between elements, which will be severe in the case of 0.25λ inter-element distance in the uniform circular and hexagonal array.

Fig. 4.5 illustrates the radiation pattern of Config.3.2 {6, 12, 18} UCHA and UCCA in the azimuth plane at θ=90°.

Table 4.3 The Beam Width and SLL of different configurations of UCCA and UCHA.

Configuration		Beam Width [Deg]	SLL [dB]
Config.2.1 {18, 18}	UCCA	27	-8.5
	UCHA	28	-10.1
Config.2.2 {12, 24}	UCCA	29	-10
	UCHA	30	-9.5
Config.3.1 {6, 6, 24}	UCCA	31	-11.5
	UCHA	32	-9.5
Config.3.2 {6, 12, 18}	UCCA	35	-11.8
	UCHA	36	-14.3
Config.4.1 {6,6,12,12}	UCCA	31	-10.9
	UCHA	32	-7
Config.4.2 {6, 6, 6, 18}	UCCA	30	-7.9
	UCHA	30	-9.3

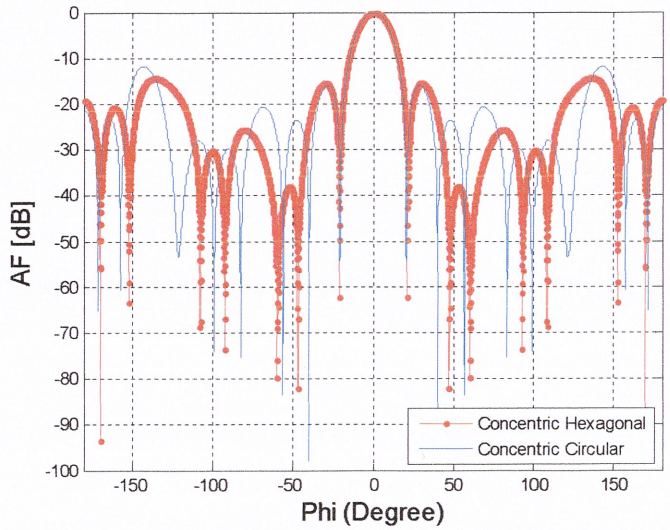


Fig.4.5 The radiation pattern of Config.3.2 {6, 12, 18} UCHA and UCCA at θ=90°.

4.8 First optimization problem: Rotating the Outer Ring(s) of UCCA and UCHA

It is found in (Mahmoud et al [40]) that the rotation of outer ring of UCCA had improved the gain and the null depth. In this section, it is desired to rotate the outer ring(s) in UCCA and UCHA configurations to minimize SLL, without any change in the beamwidth. To achieve this, the inner ring should be fixed, and the angle between the outer ring(s) and the x-axis of the inner ring, should be optimized using the three optimization algorithms EPSO, DE and Hybrid EPSO/DE to get lower SLL.

Fig. 4.6 (a, b) illustrate the rotated angles of the outer rings with respect to the inner ring x-axis, for the UCCA and UCHA respectively.

4.8.1 Objective Function Formulation of the Design Problem.

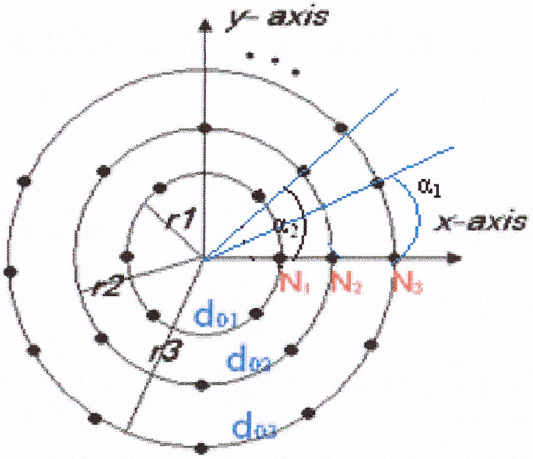
To minimize the SLL by rotating the outer ring(s) of the UCCA and UCHA, it is required to define the objective function of the problem to solve the minimax of the optimization problem under one constrain.
The problem can be defined as follow:

$$\min_{\alpha_m} \in c\left\{\max_{\phi \notin \Delta\phi_{BW}} |AF(\phi,\alpha_m)|\right\} \qquad \textit{Subjected to } \delta BW=0 \qquad (4.11)$$

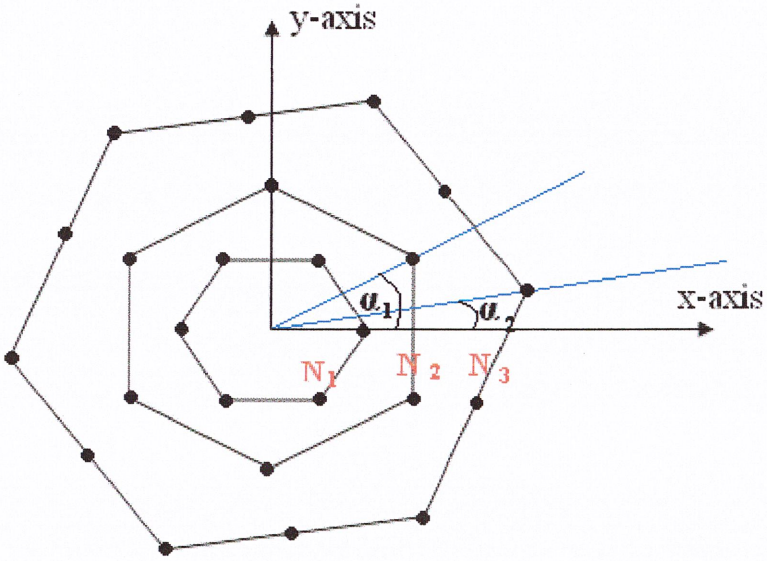
The angular positions ϕ_{mn} of the outer rings will be as follow:

$$\phi_{mn} = 2\pi\left(\frac{n-1}{N_m}\right)+\alpha_m \qquad \text{m=2,3...,M} \quad \text{n=1,2, ..., } N_m \qquad (4.12)$$

Where AF (ϕ, α_m) is the array factor of the multi-ring array. α_m is the optimized angle which will shift all elements in the m^{th} ring. M is the total number of rings in the array, C is the set of all vectors, $\Delta\phi_{BW}$ and δBW are main lobe beamwidth and the change in the main beamwidth respectively.



(a)



(b)

Fig. 4.6 The geometries with rotated outer rings with respect to the inner ring x-axis, for the: (a)UCCA and (b)UCHA.

This problem is optimized using the three algorithms EPSO, DE and the Hybrid EPSO/DE techniques according to the following fitness function:

$$f = \sum_{\phi=-180^{\circ}}^{\phi=180^{\circ}} \left| w_{BW}(\phi).AF(\phi) \right| \tag{4.13}$$

Where,

$$w_{BW}(\phi) = \begin{cases} 0 & if\ \phi \in \Delta\phi_{\mathrm{BW}} \\ 1 & otherwise. \end{cases} \tag{4.14}$$

4.8.2 Analysis and numerical results

The goal of this optimization problem is to minimize SLL of the designed configurations in table 4.3. This optimization will be performed by rotating the outer ring(s) of the arrays with certain angle(s), without affecting the main lobe beamwidths i.e. $\delta BW=0$. These angles are optimized using the three algorithms. The boundary of the optimized parameter will be {0 – 60} degrees. Table 4.4 illustrates the values of the optimized rotating angles of the outer rings of the arrays, and the resulting SLL. In this table, it is clear that the three-ring and four-ring case are better than the two-ring case in the SLL. So it will be focused on the three-ring and four-ring configurations in the analysis.

In the case of config.4.1 {6,6,12,12} UCHA which is the best, the SLL dropped from -7 dB to -15.8 dB after rotating the outer rings with the values mentioned in the table. This reduction in SLL is considerable, since the SLL is more than the double of its original value before the rotation. The second best rotated configuration is config.3.2 {6, 12, 18} UCHA with SLL= -15.4 dB, and -1.1 dB drop of its original SLL. Figure 4.7 and figure 4.8 illustrate the radiation pattern of the rotated geometries of config.4.1 {6, 6, 12, 12} UCHA and config.3.2 {6, 12, 18} UCHA respectively, using the three algorithms versus the radiation pattern of the unrotated geometries.

4.8.3 Conclusion of Rotating the Outer Ring(s) of UCCA and UCHA

A successful method to suppress the SLL without affecting the beam width, by rotating the outer ring(s) of the UCCA and UCHA has been presented. The three algorithms DE, EPSO and Hybrid EPSO/DE showed the same results in this optimization problem. To conclude, redesigning arrays by rotating the outer ring(s), the UCHA arrays has been proved to give better SLL of the radiation pattern than the UCCA arrays of the designed configurations earlier.

Table 4.4 The values of rotated angles in each ring and SLL of all configurations of UCCA and UCHA without affecting the main lobe beam width.

Configuration		Rotated Angle(s) [Deg.]			SLL [dB]
		α_1	α_2	α_3	
Config.2.1 {18, 18}	UCCA	10	-	-	-9.3
	UCHA	0	-	-	-10.1
Config.2.2 {12, 24}	UCCA	16.7	-	-	-10.2
	UCHA	30	-	-	-10.3
Config.3.1 {6, 6, 24}	UCCA	56.4	12.8	-	-11.7
	UCHA	58.1	5.5	-	-11.7
Config.3.2 {6, 12, 18}	UCCA	13.4	10.7	-	-13
	UCHA	30	0	-	-15.4
Config.4.1 {6,6,12,12}	UCCA	15.9	12.5	13.7	-14.5
	UCHA	42	16.6	57.3	-15.8
Config.4.2 {6, 6, 6, 18}	UCCA	34.3	11.5	13.2	-14.2
	UCHA	43	15	37	-14.2

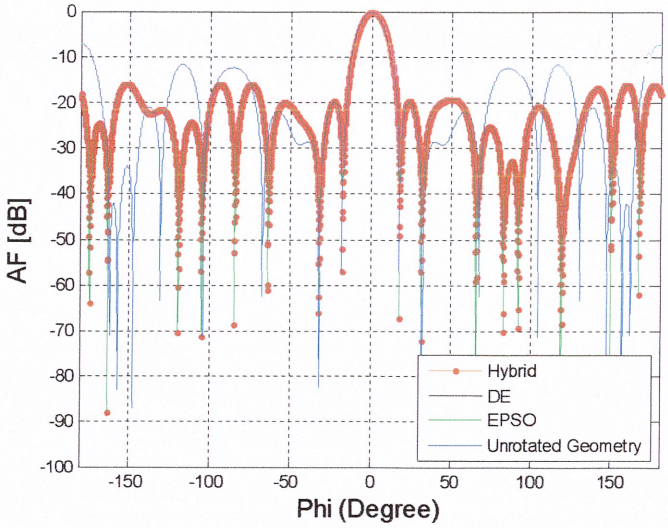


Fig.4.7 The radiation pattern of rotated Config.4.1 {6, 6, 12, 12} UCHA using the three optimization algorithms, versus unrotated geometry pattern at θ=90°.

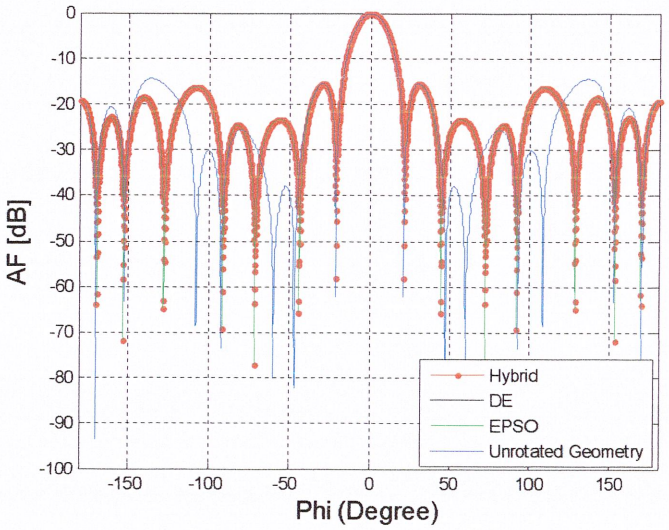


Fig.4.8 The radiation pattern of Rotated Config.3.2 {6, 12, 18} UCHA using the three optimization algorithms, versus unrotated geometry pattern at θ=90°.

4.9 Second optimization problem: Optimizing Complex weights in hexagonal, Concentric Circular and Concentric Hexagonal Antenna Arrays

A low sidelobes radiation pattern can be synthesized in the azimuth angles by modeling the concentric ring array for invariant ring spacing as a Fourier-Bessel series and optimizing the weights for each ring using a suitable low sidelobe synthesis method [51]. Another method describes a circular Taylor amplitude taper projected onto a line in the azimuth angles to the element distribution in the concentric configuration [52]. In [41 ,45] the authors used the evolutionary algorithm PSO to achieve the maximum SLL reduction in the azimuth plane, by optimizing the excitation amplitude of the elements with and without central feeding in various designs of three-ring concentric circular antenna array CCAA.

In this section the complex weights (Amplitude and Phase) of the elements in the hexagonal, concentric circular antenna array (CCAA) and concentric hexagonal antenna array (CHAA) will be optimized. For the case of CCAA and CHAA, the effect of adding a central feeding element to the array will be studied. At the same time we will compare the resulted radiation patterns with chebyshev-like radiation pattern of a circular array [35], which used the same number (36 elements) of the isotropic elements, from aspects of the SLL, beam width and directivity.

The configurations to be optimized are Config.2.2 {12, 24}, Config.3.2 {6, 12, 18} and Config.4.1 {6,6,12,12}, since they achieved the lowest SLL in the two-ring, three-ring and four-ring of rotated CCAA and CHAA configurations as in table 4.5. In this section the excitation amplitude of the array's elements will not be uniform any more, as well as the excitation phase of the elements. This complex weight of the array's elements will be optimized with three algorithms DE, EPSO and Hybrid EPSO/DE, to get the lowest SLL with acceptable change in main lobe beam width compared to the reference pattern in [35], which use the same number of elements with 0.25λ inter-element distance.

4.9.1 Objective Function Formulation of the Design Problem.

To optimize the complex weights of the array's elements, the optimized parameters will be the Amplitude I_{mn} and the Phase α_{mn} of the array's elements. It is needed to solve the mini-max of the optimization problem under one constraint, according to the following objective function of the problem:

$$\min_{I_{mn},\alpha_{mn}} \in \; c\left\{\max_{\phi \notin \Delta\phi_{BW}} \left|AF(\phi, I_{mn}, \alpha_{mn})\right|\right\} \quad \textit{Subject to } \delta BW \leq \varepsilon. \tag{4.15}$$

Where AF (Φ, I_{mn}, α_{mn}) is the array factor of the multi-ring array. I_{mn}, α_{mn} are the excitation amplitude and phase of the mn^{th} element, C is the set of all vectors, $\Delta\Phi_{BW}$ and δBW are main lobe beam width and the change in the main lobe beam width respectively. Finally ε is the maximum allowable change in the main lobe beam width.

This problem is optimized using the three algorithms EPSO, DE and the Hybrid EPSO/DE techniques according to the following fitness function:

$$f = \sum_{\phi=-180^{\circ}}^{\phi=180^{\circ}} w_1 . \left| w_{BW}(\phi).AF(\phi) \right| + w_2 . \mu(\phi_0) \tag{4.16}$$

Where

$$\mu(\phi_0) = \left| AF(\phi_0) - \max\{AF(\phi)\} \right|^2 \tag{4.17}$$

w_1, w_2 are weighting factors in the fitness function, w_{BW} will be the same as in equation 4.14. The directivity will be calculated according to following equation [34]:

$$D = \frac{\left|E\ (\theta_0, \phi_0)\right|^2}{\frac{1}{4\pi} \int_0^{2\pi} \int_0^{\pi} \left|E(\theta,\phi)\right|^2 . \sin\theta . d\theta . d\phi} \tag{4.18}$$

4.9.2 Analysis and numerical results.

It is desired to optimize the complex weights of the arrays with different configurations, to suppress the sidelobe of the radiation pattern according to the previous fitness function. First the hexagonal array as in figure 4.1 will be optimized using the three algorithms, and compare it to an optimized circular array [35], from aspects of SLL, beam width (BW) and directivity. It is found by trial and error concept, that the best value of w_1=0.1and w_2=1. The boundaries of the optimized parameters are: the amplitude I_{mn} = {0.1–1}, for the phase α_{mn}= {-π – π}, and ε =7.

4.9.2.1 CA and HA case

Table 4.5 illustrates a comparison between the hexagonal and circular array, with 0.25λ inter-element distance for both of them, using the three algorithms. This table shows that the hexagonal array optimized by Hybrid EPSO/DE with SLL=-32.1dB is better than the reference circular pattern by -0.7dB. Also the directivity of the hexagonal array using the hybrid algorithm is better as well by 2 dBi, but with beam width wider by 6° than the reference pattern of the circular array. Both of hexagonal and circular array has the same dynamic range ratio I_{max}/I_{min}=2. The radiation pattern of the hexagonal array optimized using the three algorithms, versus the reference pattern for the circular array are depicted in figure 4.9, while the optimized amplitude and phase values of hexagonal array elements using Hybrid EPSO/DE algorithm are illustrated in figure 4.10.

4.9.2.2 Two-ring case

Second for the two-ring arrays, configuration Config.2.2 {12, 24} CCAA and CHAA are chosen to be optimized using the three algorithms. This configuration will be optimized with and without additional central element, to study the effect of this central element on the radiation pattern features like SLL, BW and I_{max}/I_{min}. From table 4.6, it is clear that neither SLL of config.2.2 {12, 24} CCAA nor CHAA are close to the SLL of the reference pattern, since the best SLL was -19.4 dB for the CCAA case using the Hybrid algorithm, this case for the arrays without central element. While for the case of adding central element, the CCAA array has SLL= -28.2 dB using Hybrid algorithm, which is close to the SLL=-31.4 dB of the reference pattern. The directivity of

this case was 9.7 dBi with increase of 1.8 dBi compared to the reference pattern's directivity. The increase of the beam width for this case was 1.8° and the dynamic range ratio I_{max}/I_{min}=4 which consider a low ratio. Table 4.6 illustrates a comparison between Config.2.2 {12, 24} CCAA and CHAA with and without central element in SLL, BW, directivity and I_{max}/I_{min}.

Table 4.5 Comparison between optimized Hexagonal array and optimized circular array Ref. [35] in SLL, BW and directivity.

Geometry	Algorithm	SLL [dB]	δBW [Deg.]	Directivity [dBi]	I_{max}/I_{min}
Chebyshev-like Ref. [35]		-31.4	0	7.9	2
Hexagonal Array	**DE**	-28.7	7	9.1	2
	EPSO	-25	-1	12.8	2
	HYBRID	-32.1	6	9.9	2

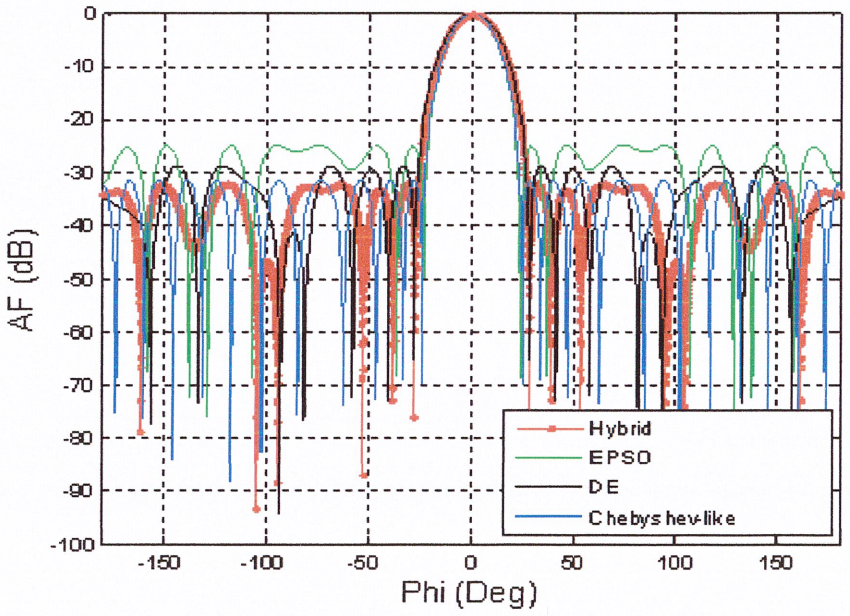


Fig. 4.9 The radiation pattern of the hexagonal array optimized using the three algorithms, versus the reference pattern of the circular array.

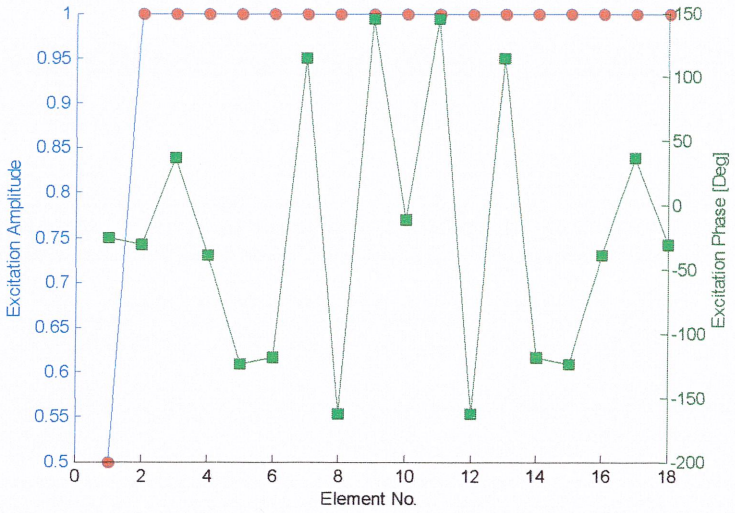


Fig.4.10 Optimized amplitude and phase values of hexagonal array elements using Hybrid EPSO/DE algorithm.

Table 4.6 Comparison between Config.2-2 {12, 24} CCAA and CHAA with and w/o central element in SLL, δBW , directivity and I_{max}/I_{min}.

Config.2-2 {12, 24}	Algorithm	SLL [dB]	δBW [Deg.]	Directivity [dBi]	I_{max}/I_{min}
Chebyshev-like [35]		-31.4	0	7.9	2
CCAA without central element	DE	-15.6	-12.8	10.8	8
	EPSO	-17.5	-11.9	10.8	8
	HYBRID	-19.4	-4.4	10.5	7.4
CCAA with central element	DE	-18.5	-7.8	10.4	2.8
	EPSO	-22.8	-3	10.5	5
	HYBRID	-28.2	1.8	9.7	4
CHAA without central element	DE	-15.7	-13.4	10.9	5.1
	EPSO	-16.8	-9	10.3	7
	HYBRID	-17.6	-8.2	10.3	7.3
CHAA with central element	DE	-18.7	-7.5	10.7	4.6
	EPSO	-19.2	-7	10.4	5
	HYBRID	-22	-3.5	9.7	3.9

Figures 4.11 and 4.12 illustrate the radiation pattern of optimized Config.2.2 {12, 24} CCAA using the 3 optimization algorithms compared to Chebyshev-like pattern, without and with central element respectively, while figures 4.13 and 4.14 depict the values of the complex weights of the array elements using the hybrid algorithm, for the same configuration without and with central element respectively.

4.9.2.3 Three-ring case

Third for the three-ring arrays, config.3.2 {6, 12, 18} CCAA and CHAA are chosen to be optimized using the three algorithms. As in two-ring arrays, an additional central element will be added to this configuration to study its effect on the radiation pattern. Table 4.7 illustrates a comparison between config.3.2 {6, 12, 18} CCAA and CHAA with and without central element in SLL, BW, directivity and I_{max}/I_{min}. According to the result in this table, the CCAA arrays couldn't reach the SLL of the reference pattern. While the CHAA array without central element using Hybrid algorithm, succeeded to have lower SLL= -35 dB than the reference pattern SLL=-31.4 dB. This low SLL was achieved with slight change (1.8°) in the beam width. The obtained directivity = 8.85 dBi, with an increase of 0.95 dBi compared to the reference pattern's directivity. These required a little high dynamic range ratio I_{max}/I_{min}=8.2. Figure 4.15 depict the radiation pattern of optimized config.3.2 {6, 12, 18} CHAA without additional central element, using the three optimization algorithms versus chebyshev-like pattern. While figure 4.17 shows the values of the complex weights of the array elements, using the hybrid algorithm, for this configuration.

For the CHAA with central element feeding, the achieved SLL =-37 dB, was better than all other configurations. The beam width of this configuration's pattern increased by 1.4° only, with respect to the reference beam width. Also it has high directivity =10 dBi, and low range ratio I_{max}/I_{min}=4.4, compared to the same array without central element. Figure 4.16 depict the radiation pattern of optimized config.3.2 {6, 12, 18} CHAA with additional central element, using the three optimization algorithms versus chebyshev-like pattern. Figure 4.18 shows the values of the complex weights of the array elements, using the hybrid algorithm, for this configuration.

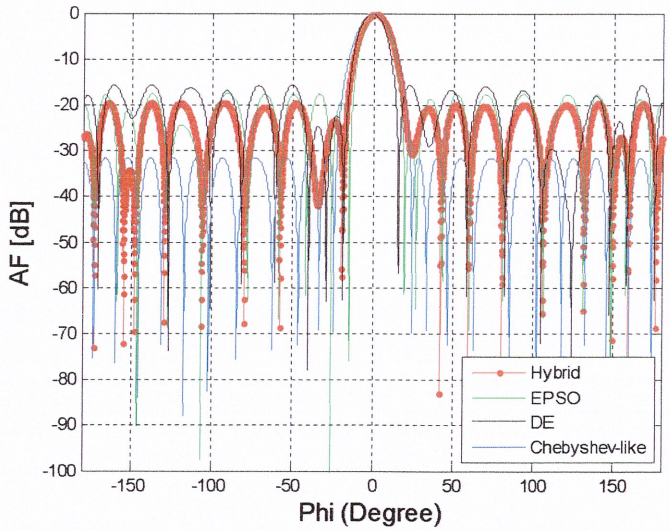


Fig4.11 The radiation pattern of optimized Config.2.2{12, 24} CCAA without central element using the 3 optimization algorithms compared to chebyshev-like pattern.

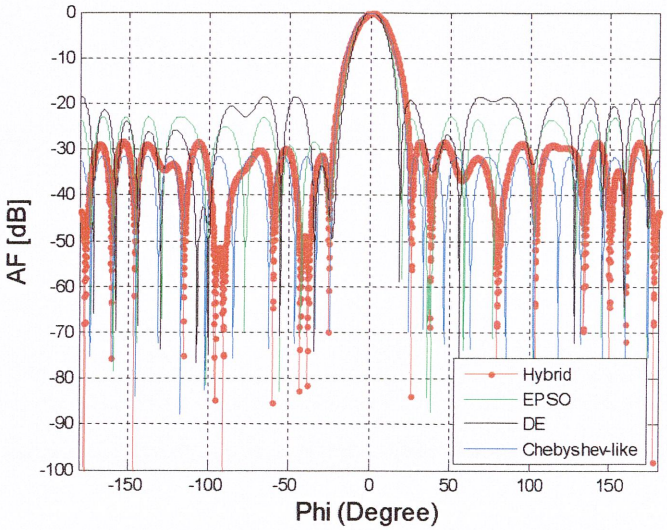


Fig4.12 The radiation pattern of optimized Config.2.2 {12, 24} CCAA with central element using the 3 optimization algorithms compared to chebyshev-like pattern.

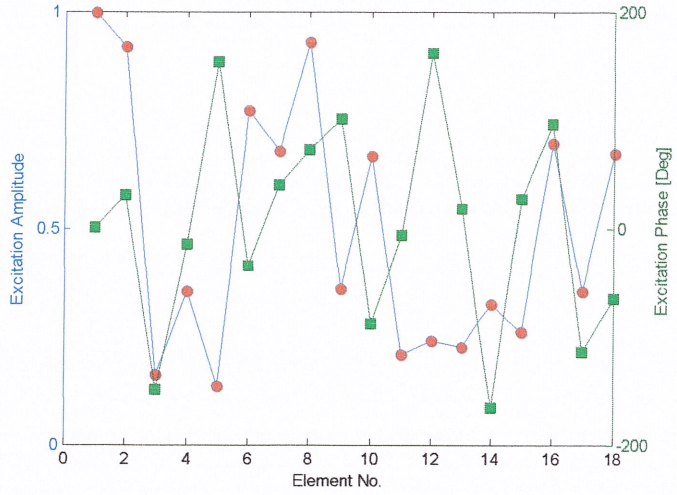


Fig.4.13 Optimized Amplitude and Phase of Config.2.2 {12, 24} CCAA elements, without central element using Hybrid EPSO/DE algorithm.

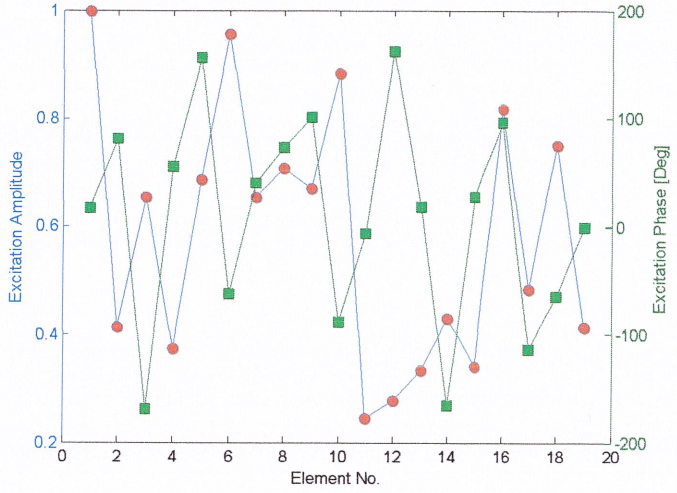


Fig.4.14 Optimized Amplitude and Phase of Config.2.2 {12, 24} CCAA elements, with central element using Hybrid EPSO/DE algorithm.

Table 4.7 Comparison between Config.3.2 {6,12 ,18} CCAA and CHAA with and without central element in SLL, BW and Directivity.

Config.3.2 {6,12 ,18}	Algorithm	SLL [dB]	δBW [Deg.]	Directivity [dBi]	I_{max}/I_{min}
Chebyshev-like [35]		-31.4	0	7.9	2
CCAA without central element	**DE**	-22.2	2	7.47	5
	EPSO	-24.2	5.8	7.22	6.2
	HYBRID	-25.4	6	8.03	8.4
CCAA with central element	**DE**	-18	0	8.19	3
	EPSO	-23.5	4.3	9.02	4.5
	HYBRID	-26.8	6.7	9.29	4.2
CHAA without central element	**DE**	-15.2	-2.2	6.67	5.4
	EPSO	-23.1	-4.4	8.9	6.3
	HYBRID	-35	1.8	8.85	8.2
CHAA with central element	**DE**	-12.7	-3.4	9.66	4.9
	EPSO	-27.1	-3.6	8.2	5.2
	HYBRID	-37	1.4	10.06	4.4

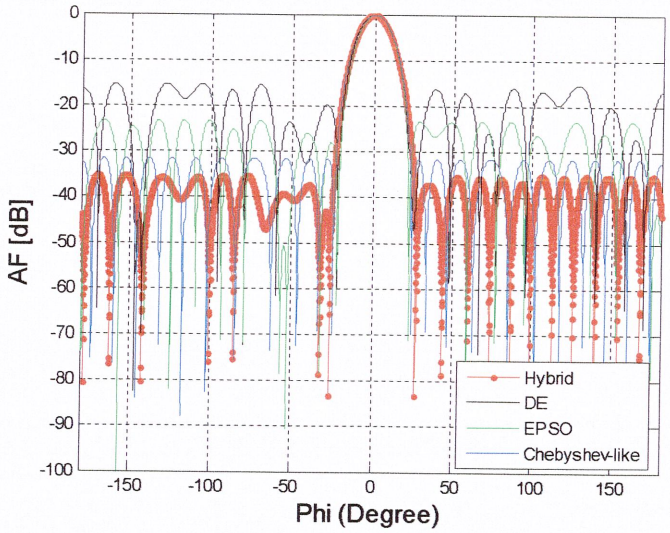


Fig4.15 The radiation pattern of optimized Config.3.2 {6, 12, 18} CHAA without central element using the 3 optimization algorithms compared to chebyshev-like pattern.

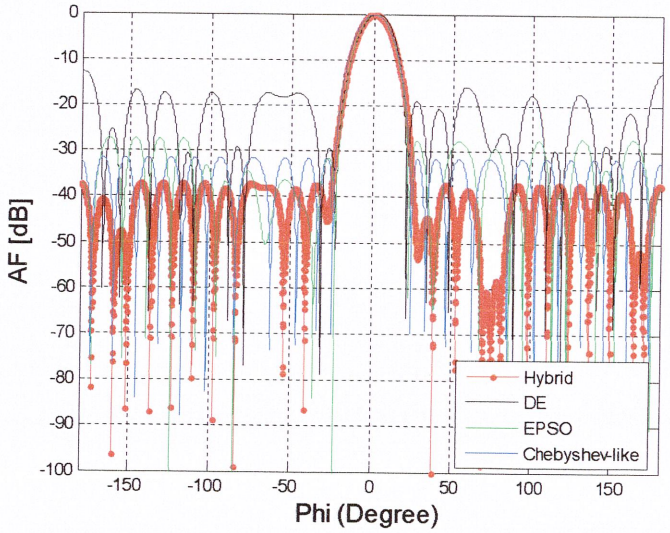


Fig4.16 The radiation pattern of optimized Config.3.2 {6, 12, 18} CHAA with central element using the 3 optimization algorithms compared to chebyshev-like pattern.

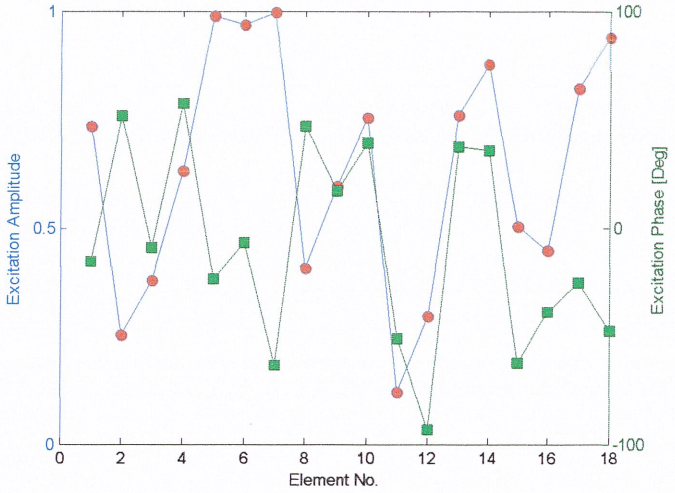


Fig.4.17 Optimized Amplitude and Phase of Config.3.2 {6, 12, 18} CHAA elements without central element using Hybrid EPSO/DE algorithm

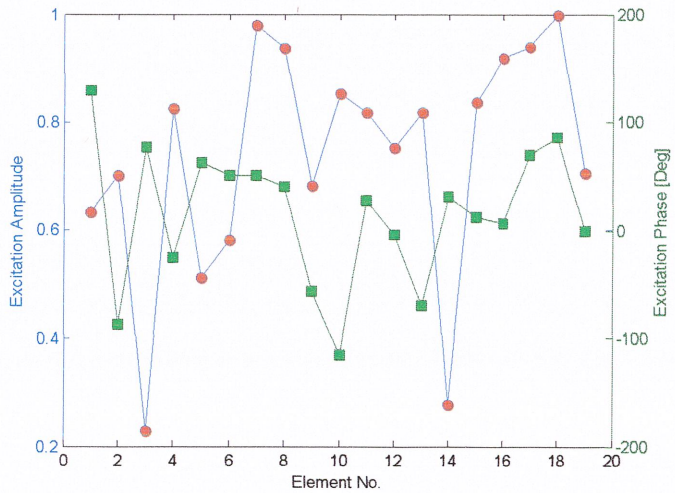


Fig.4.18 Optimized Amplitude and Phase of Config.3.2 {6, 12, 18} CHAA elements with central element using Hybrid EPSO/DE algorithm.

4.9.2.4 Four-ring case

Finally for the four-ring arrays, config.4.1 {6, 6, 12, 12} CCAA and CHAA are chosen to be optimized using the three algorithms. Table 4.8 summarized the results of optimizing these configurations with and without central element. Similar to the CCAA configurations of two-ring and three-ring, the CCAA in the four-ring array couldn't reach the SLL of the reference pattern. However, it was the closer to it with SLL= -29.9 dB, optimized with the Hybrid algorithm in the case of adding central element.

For the case of config.4.1 {6, 6, 12, 12} CHAA, the obtained SLL = -33.4 dB optimized with the Hybrid algorithm. This low SLL achieved with a little increase in the BW with δBW= 1.6° compared to the reference BW. Obviously the directivity = 10.2 dBi is high with respect to the reference's directivity. Figure 4.19 depict the radiation pattern of optimized config.4.1 {6, 6, 12, 12} CHAA without additional central element, using the three optimization algorithms versus the reference pattern. While figure 4.21 shows the values of the complex weights of the array elements, using the hybrid algorithm, for this configuration.

Config.4.1 {6, 6, 12, 12} CHAA with central element, obtained SLL= -34 dB in the case of using the Hybrid algorithm. With decrease of -2.6 dB compared to the reference pattern and directivity =9.8 dBi. The dynamic range ratio I_{max}/I_{min}=6, is lower than the ratio of the same configuration without central element. Figure 4.20 illustrate the radiation pattern of optimized config.4.1 {6, 6, 12, 12} CHAA with central element, using the three optimization algorithms versus the reference pattern. While figure 4.22 depict the values of the complex weights of the array elements, using the hybrid algorithm, for this configuration

4.9.3 Conclusion of Optimizing Complex weights in hexagonal, Concentric Circular and Concentric Hexagonal Antenna Arrays

It can be conclude that, for certain radiation pattern synthesized by a circular array with certain number of elements, spaced with uniform 0.25λ inter-element distance, this radiation pattern could be synthesized with better features using reconfigurable arrays. These different configuration arrays utilized the same number of elements with 0.5λ inter-element distance at

least, to mitigate the effect of mutual coupling between elements. The presented concentric hexagonal antenna array CHAA for the three-ring and four-ring succeeded to synthesize lower SLL pattern, than the circular reference pattern. The synthesized patterns have higher directivity up to 10.2 dBi with minor change in the BW. With adding a central element to the previous configurations, lower SLL and lower I_{max}/I_{min} ratio are achieved compared to the original configuration. The Hybrid algorithm in this optimization gave the best result in the SLL of the radiation pattern.

Table 4.8 Comparison between Config.4.1 {6, 6, 12, 12} CCAA and CHAA with and without central element in SLL, BW and Directivity.

Config.4.1 {6, 6, 12, 12}	Algorithm	SLL [dB]	δBW [Deg.]	Directivity [dBi]	I_{max}/I_{min}
Chebyshev-like [35]		-31.4	0	7.9	2
CCAA without central element	DE	-19.2	-12.2	10.95	3.3
	EPSO	-23.5	-4.2	10.77	6.6
	HYBRID	-27.8	-2.4	10.48	7.9
CCAA with central element	DE	-22.2	-3.7	10.7	4.9
	EPSO	-25.8	-2.8	10.52	5
	HYBRID	-29.9	2	10.34	4.4
CHAA without central element	DE	-22	-9.1	10.87	3
	EPSO	-27.4	-1.2	10.38	7.8
	HYBRID	-33.4	1.6	10.2	6.5
CHAA with central element	DE	-21.3	-2	10.12	8.4
	EPSO	-28.3	-4.5	10.59	9.4
	HYBRID	-34	3.3	9.81	6

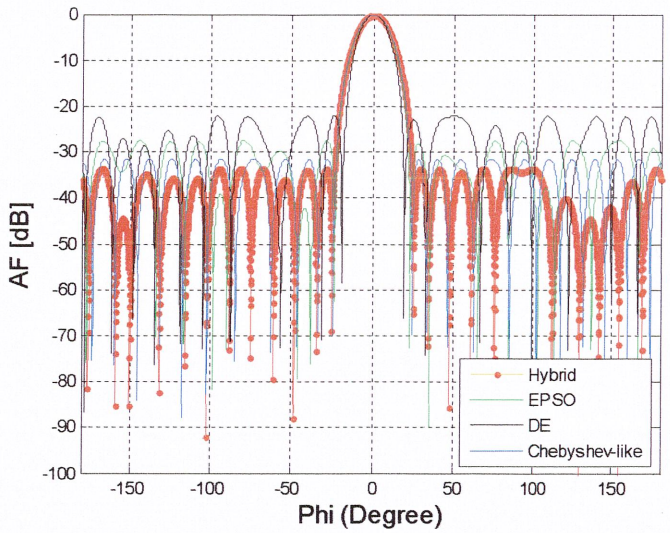


Fig.4.19 The radiation pattern of Config.4.1 {6, 6, 12, 12} CHAA without central element using the 3 optimization algorithms compared to chebyshev-like pattern.

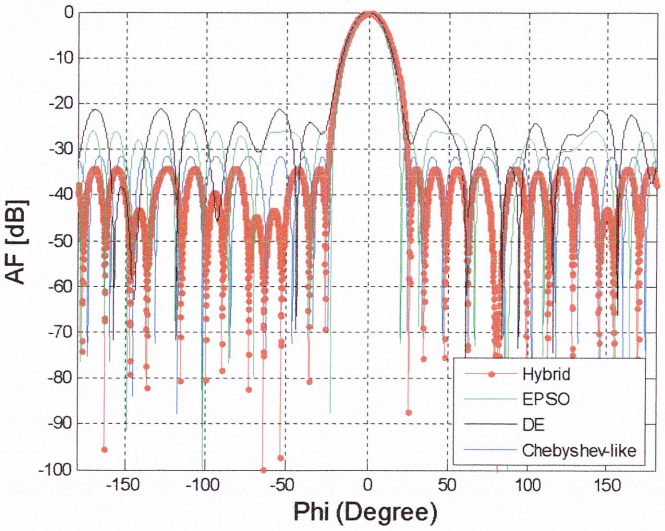


Fig.4.20 The radiation pattern of optimized Config.4.1 {6, 6, 12, 12} CHAA with central element using the 3 optimization algorithms compared to chebyshev-like pattern.

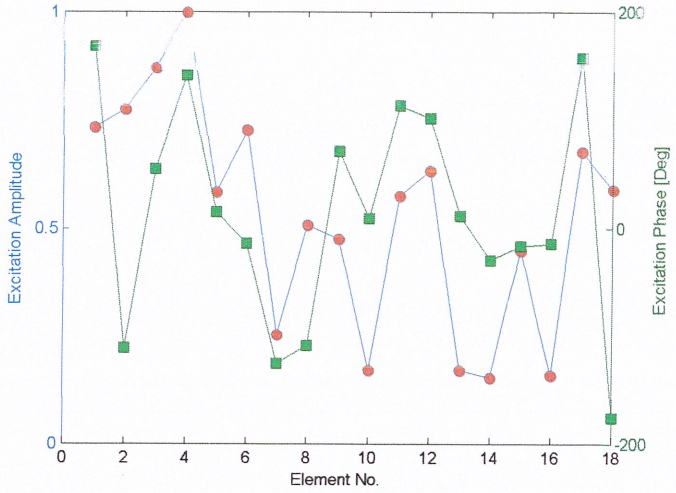


Fig.4.21 Optimized Amplitude and Phase of Config.4.1 CHAA elements w/o central element using Hybrid EPSO/DE algorithm.

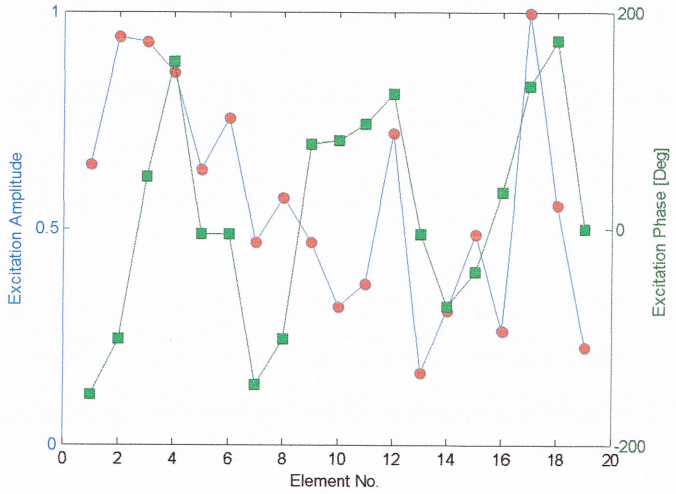


Fig.4.22 Optimized Amplitude and Phase of Config.4.1 CHAA elements with central element using Hybrid EPSO/DE algorithm.

4.10 Conclusion

A study compares between different configurations of antenna arrays utilizing the same number of elements were presented. The patterns of circular and hexagonal arrays with 36 elements spaced with 0.25λ, versus the concentric circular and concentric hexagonal arrays with 36 elements spaced with 0.5λ. The 0.5λ was chosen to be the minimum distance between any two adjacent elements, to mitigate the effect of mutual coupling between elements.

The uniform concentric hexagonal arrays UCHA proved to give lower SLL in the azimuth plane, than the uniform concentric circular arrays UCCA, the circular and the hexagonal arrays after rotating the outer ring(s) of the arrays. After optimizing the complex weights of these concentric arrays, a pattern with SLL= -35 dB and directivity =8.85 dBi was achieved with slight change in BW compared to a circular reference pattern [35] used the same number of elements arranged in circular array.

This study was extended to explore the effects of adding a central element to these configurations. Lower SLL (-37dB) and lower I_{max}/I_{min} ratio =4.4, compared to the SLL and I_{max}/I_{min} of the original configuration are the advantages of the additional central element. It could be concluded, that the concentric hexagonal arrays with 0.5λ inter-element distance is a promising alternative to the circular array with 0.25λ inter-element distance in synthesizing low SLL radiation pattern for the same number of elements in the azimuth plane. The Hybrid ESPO/DE technique is expected to be very promising evolutionary optimization technique for the global optimization of any antenna array problem.

Chapter 5

Sidelobe Suppression in Time Modulated Unequally Element Spaced Linear and Planar Arrays Using Hybrid DE/EPSO

5.1 Introduction

Phased array antennas with low/ultra-low side lobe level radiation pattern are widely used in high performance electronic systems, especially those operating in high electromagnetic pollution environment. Theoretically, low/ultra-low side lobes can be achieved by tapering the excitation amplitude of array elements. Several analytical and numerical techniques, such as the well-known Chebyshev and Taylor distributions [53] have been utilized to locate the appropriate weighting factors of the array element. However, for low/ultra-low side lobes, very high dynamic-range ratios for the amplitude excitation are needed, which could result in random errors, and eventually restricting the side lobe performance in practical arrays [54].

This motivates the antenna designers to realize low/ultra-low side lobes by other approaches. One of the practical approaches is to present the time as the fourth degree of freedom in the design [55-56]. Antenna arrays with the time parameter can be named as time modulated arrays TMAs. The amplitude excitations of TMAs elements only need a low dynamic range ratios or a uniform distribution for low/ultra-low sidelobe patterns, which result in more flexible hardware realization.

The time modulation can be implemented by simple "on-off" switching of antenna elements in a preset sequence. By filtering the antenna output, the pattern side lobes were minimized. Compared to conventional antenna arrays, the realization of time modulated antenna arrays increase the overall cost by adding RF switches or IF filters. However, these components are also

required in radar systems. Thus, the time modulated antenna arrays are very convenient for radar systems.

Time modulation is presented to minimize the influences of mechanical tolerances which lead to degrade side-lobe levels from their desired values. The time-modulated arrays are very flexible in controlling the array excitation since the time factor could be adjusted very easily using high-speed RF switches. The RF power requires only two discrete states, on and off, instead of the static amplitude control required in traditional arrays [57]. The collateral disadvantage of time modulated arrays is that there are many harmonics separated at multiples of the modulation frequency, which means that portion of the radiated or received power is moved to the sidebands. These harmonics –sidebands– considered as a power wastage that affect the directivity and gain of the antenna array at the center frequency. In this chapter we will demonstrate the time modulated arrays TMAs linear and planar, to achieve low/ultra-low side-lobe level SLL, while suppressing the sidebands level SBL using the hybrid EPSO/DE algorithm.

5.2 Sidelobe Suppression in Unequally Spaced Linear Arrays through Time Modulation

The inherent drawback of the time modulation technique in antenna array design is the undesired appearance of harmonics whose levels has direct relation to the Fourier coefficients used when expanding the element array excitations. In previous works [58-59], the sideband radiation is minimized through the use of the differential evolution DE algorithm applied to a linear array. In [60] the suitable use of the simulated annealing SA algorithm is applied to determine the time sequences that control the antenna pattern radiated by a uniformly amplitude excited linear array of equally spaced elements, while suppressing the sideband radiation. The approach in [61] applied an optimization process of the time sequence of each array element using the well-known genetic algorithm to minimize the sidelobe level at center frequency and the sideband levels of uniformly amplitude excited time modulated linear array (TMLA). In [62] the authors studied and analyzed the performance of the radiation pattern and used the particle swarm optimization PSO algorithm to optimize the switch-on instants of each array element used for the synthesis of time-modulated linear arrays TMLAs to reduce the SBLs, while in [63] the authors used PSO to optimize switch-on instants to minimize the power losses in TMLAs.

In this section we will optimize the switch-on instants and the values of inter-element distances of the linear array to suppress the side-lobe level SLL, while suppressing the sideband levels SBLs to the minimum as possible, and minimize the beam-width BW simultaneously, using hybrid EPSO/DE algorithm. The comparison between numerical results of this section and results in [3] which used position-phase synthesis, demonstrates the effectiveness of the proposed approach on the SLL and SBL suppression.

5.2.1 Objective Function Formulation of the Design Problem

Consider a linear array with $2N$ isotropic and symmetrically placed along x-axis, each element is connected with a high-speed RF switch that controls excitation time, as shown in Figure 5.1. It is required to minimize the SLL and SBL of the TMLA through optimizing the switch-on times τ_n and the element positions x_n. If a plane wave of frequency f_0 is incident at an angle θ with respect to the axis of the array, the array factor AF can be written by:

$$AF(\theta,t) = e^{j2\pi f_0 t} \sum_{n=-N}^{N} I_n U_n(t) e^{jx_n u} \qquad (5.1)$$

Where I_n is the n^{th} static amplitude excitation, x_n is the n^{th} element position from array's center, $u=k\cos(\theta)$ and $k=2\pi/\lambda$ is the wave-number.

The time switching function $U_n(t)$ in a time modulation period T_p is given by [57]:

$$U_n(t) = \begin{cases} 1 & 0 \le t \le \tau_n \\ 0 & Otherwise \end{cases} \qquad (5.2)$$

Where τ_n is the pulse width of the n^{th} element of the linear array as in Figure 5.2.

Due to the periodicity of $U_n(t)$, the space and frequency responses of equation (5.1) can be achieved by expanding it into Fourier series, and each frequency component has a frequency of m/Tp ($m = 0, \pm1, \ldots, \pm\infty$).

The m^{th} order Fourier component can be written as:

$$AF_m(\theta,t) = e^{j2\pi(f_0+mf_p)t} \sum_{n=-N}^{N} a_{mn}.e^{jx_n u} \tag{5.3}$$

where $f_p = 1/T_p$ and a_{mn} is the complex amplitude and is given by:

$$a_{mn} = \frac{I_n \tau_n}{T_p}.\frac{\sin(\pi\, m\, f_p \tau_n)}{\pi\, m\, f_p \tau_n}.e^{-j\pi\, m\, f_p \tau_n} \tag{5.4}$$

Since we consider a uniform amplitude excitation i.e. I_n=1, then, at the center frequency f_0, equation (5.3) becomes as follow:

$$AF_0(\theta,t) = e^{j2\pi f_0 t} \sum_{n=-N}^{N} \frac{\tau_n}{T_p}.e^{jx_n u} \tag{5.5}$$

This equation represents the array factor AF of time modulated linear array (TMLA) at the center frequency f_0 which model the side-lobe level SLL, equation (5.3) will be used in minimizing the sideband levels SBLs of undesired harmonics.

The Hybrid EPSO/DE algorithm is used to find out the optimum values of the switch-on times and elements positions to reduce the SLL and the SBL, and minimize the beam-width BW to maximize the directivity and gain of the TMLA comparing to the results in [3].
To facilitate the optimization process, it will be focused to optimize the inter-element distance d_n instead of x_n where:

$$x_n = \sum_{i=1}^{n} d_i \tag{5.6}$$

The optimization vector in this section is $v = \{\tau_n, d_n\}$, and the cost function to get the targeted pattern is:

$$f(v) = w_1.SLL_{\max}(v)\Big|_{f_0} + w_2.\Omega^{SBL}(v) + w_3.\theta_{BW}(v)\Big|_{f_0} \tag{5.7}$$

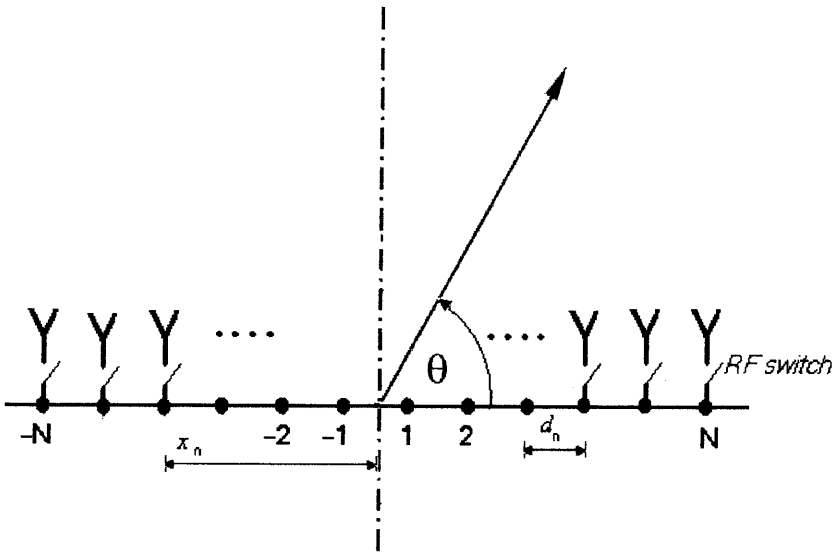


Figure 5.1 Geometry of the Time Modulated Linear Array TMLA.

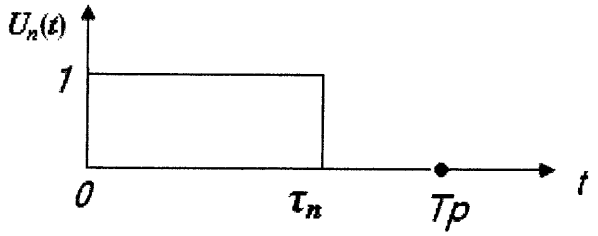


Figure 5.2. Scheme of the time switching function.

Where

$$\Omega^{SBL}(v) = \max(SBL^{(1)}(v)\Big|_{f_0+f_p}, SBL^{(2)}(v)\Big|_{f_0+2f_p}) \qquad (5.8)$$

SLL_{max} is the optimized maximum SLL at the center frequency, , $SBL^{(1)}$, $SBL^{(2)}$ are the maximum SBL at the first sideband and the second sideband respectively, θ_{BW} is the beam width of the main lobe at the center frequency. w_1, w_2, and w_3 are the corresponding weighting factors of each term in the cost function.

Similar to time-modulated linear arrays in [64], to calculate the directivity and gain of TMLA, the total radiated power should include the center frequency and all the sideband components. Therefore, the directivity is given by

$$D_{TM} = \frac{|E_0(\theta_0,\phi_0)|^2}{\frac{1}{4\pi}\sum_{m=-\infty}^{\infty}\int_0^{2\pi}\int_0^{\pi}|E_m(\theta,\phi)|^2 \sin\theta d\theta d\phi.} \qquad (5.9)$$

In this chapter the numerical integration to calculate the directivity will be used. For time-modulated linear arrays, the feed-network efficiency η_f is given by :

$$\eta_f = \frac{\sum_{n=-N}^{N}|I_n|^2.\frac{\tau_n}{T_p}}{\sum_{n=-N}^{N}|I_n|^2} \qquad (5.10)$$

The gain of the time-modulated linear array TMLA is obtained by:

$$G_{TM} = D_{TM}.\eta_f \qquad (5.11)$$

5.2.2 Analysis and numerical results

For comparing purposes, it has been chosen unequally spaced 32 elements linear array with position-phase case in [3] to be compared with position-time modulation in our case. The search ranges for the normalized switch-on times $\tau_n/T_p = \{0, 1\}$, and the values of inter-element $d_n = \{0.5\ \lambda, 1\ \lambda\}$. The proper values of w_1, w_2, and w_3 were found by trial and error concept to be 1, 0.1 and 1 respectively.

Table 5.1 shows different results of radiation pattern features of 32-elements with position-time modulation using the three algorithms versus the position-phase result in [3]. It can be noticed that the lowest SLL (-36 dB) is the position-time modulation using hybrid algorithm with first $SBL^{(1)}$= -20dB and $SBL^{(2)}$= -27.2dB, while the reference pattern (position-phase case) has SLL=-23.3dB. The DE and EPSO algorithm showed better SLL than the reference pattern in [3]. It is clear that the sidebands radiation affected the directivity since it was 18.8dBi and dropped to 15.5dBi in the best cases. Figure 5.3 depicts the radiation pattern at center frequency and the first and second side bands optimized with Hybrid EPSO/DE algorithm, while figure 5.4 illustrates the related switch-on times sequence for the radiation pattern.

Figure 5.5 shows the element's location in λ of 32-elements TMLA synthesized using hybrid EPSO/DE algorithm. Figure 5.6 demonstrates the three-dimensional (3D) space and frequency response of the optimized array with time modulation if we consider the f_p=1MHz. It is seen that the radiated or received power is highly concentrated within the main beam at f_0.

Table 5.1 A comparison of 32-Elements TMLA features SLL, BW, Directivity and SBLs, using the three algorithms versus the results in reference [3].

Algorithm	SLL[dB]	BW [Deg]	Directivity [dBi]	SBL(1) [dB]	SBL(2) [dB]
Reference [3]	-23.34	6.5	18.8	–	–
DE	-31.18	7.9	15.39	-21.12	-26.27
EPSO	-35.58	8.2	15.34	-20.0	-25.94
Hybrid EPSO/DE	-36.06	8.2	15.53	-20.0	-27.26

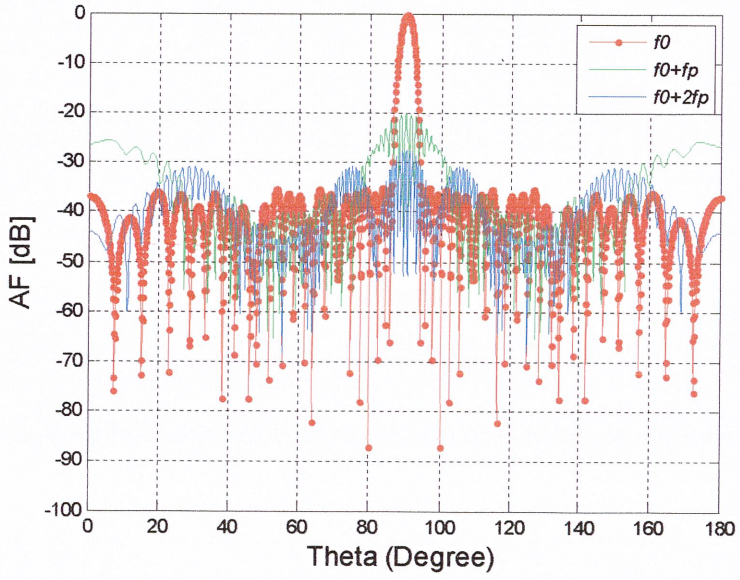


Fig.5.3 Normalized power patterns at the carrier frequency f_0 and the related to the sideband radiations (f_0+f_p, f_0+2f_p) optimized with hybrid EPSO/DE algorithms.

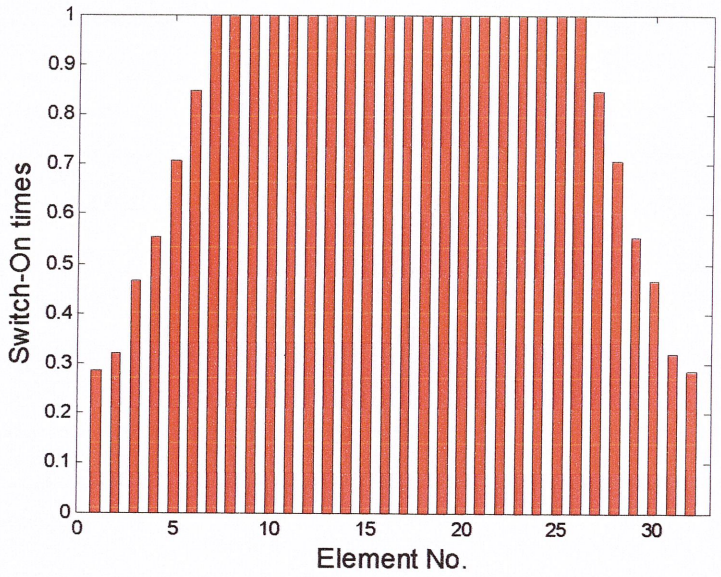


Fig.5.4 Switch-on time's sequence of 32-Elements TMLA synthesized using hybrid EPSO/DE algorithms for Fig. 5.3.

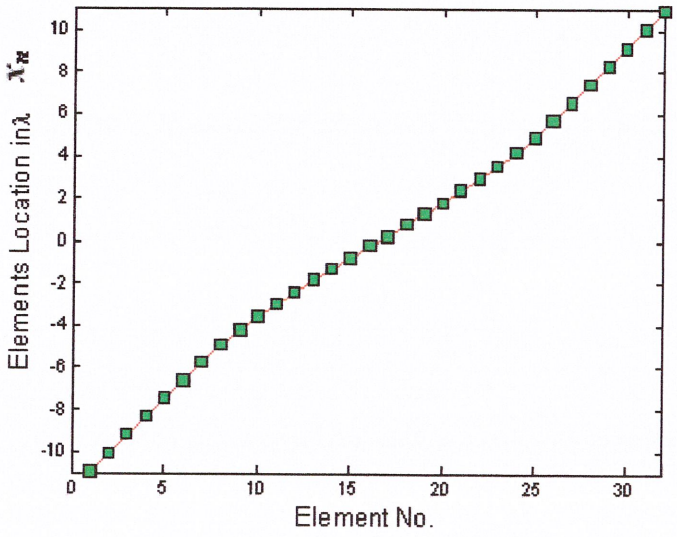


Fig.5.5 Element's location in λ of 32-Elements TMLA synthesized using hybrid EPSO/DE algorithms.

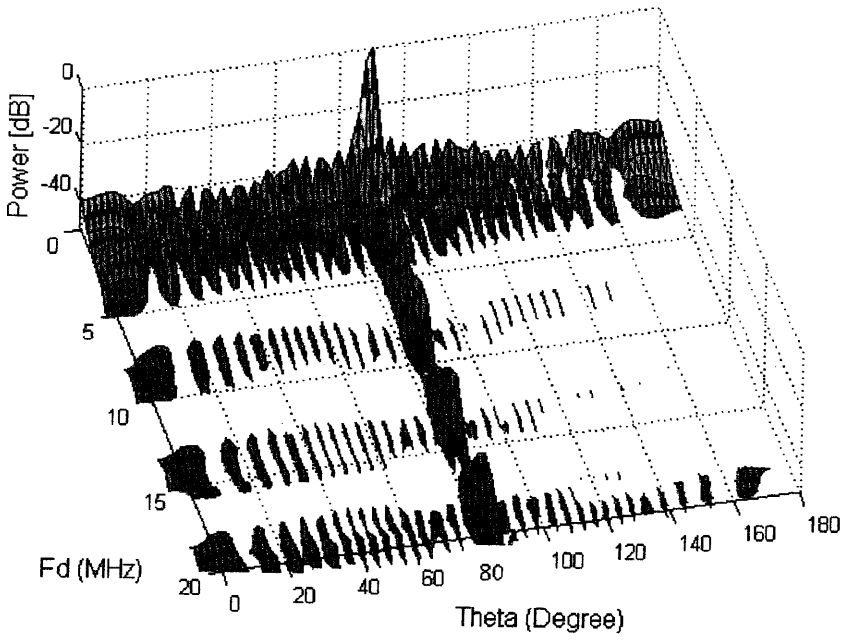


Fig. 5.6 The 3-D space and frequency response of the time modulated linear array in correspondence with the pulse sequence and element's location in Fig.5.4 and Fig.5.5 respectively.

5.2.3 Conclusion of unequally spaced TMLA

It can be concluded that the position-time modulation could obtain a low SLL radiation pattern with low SBL, compared to the position-phase technique for the same linear array. A draw back of the position-time modulation technique could be noted in the decreasing of the directivity, due to the power losses of sidebands. The novel hybrid EPSO/DE algorithm proved itself to be a promising optimization tool.

5.3 Sidelobe Suppression in Planar Arrays through Time Modulation and Complex Weights Optimization

As it is known from [54], that for synthesizing low/ultra-low side lobes, very high excitation dynamic-range ratios are more likely required, which may result in random errors, and eventually restricting the side lobe level in realizing the arrays. These very high excitation dynamic-range ratios will complicate the realization of the arrays configuration. In chapter 4 earlier a low side-

lobe levels SLL up to -35 dB was achieved in the azimuth plane by optimizing the complex weights of the 36-elements with different configurations. To obtain ultra-low SLL in the azimuth plane, the dynamic-range ratio of the amplitude excitation of the array's elements should be increased, which will be difficult on the practical implementation of the arrays.

The challenge now is to synthesize a pattern with ultra-low SLL in the azimuth plane and low dynamic-range ratio of the amplitude excitation for the same 36-elements configurations. Because of that we will use the time modulation technique besides controlling the complex weights – similar to the approach in [59] – to synthesize the ultra-low SLL in the azimuth plane. Of course this will complicate building the array structure since it needs three controls: phase shifters, attenuators and RF switches at the same time, but this will synthesize ultra-low SLL to enhance the performance of the array and suppress the power losses in the sidebands.

The ultra-low SLL in the azimuth plane synthesis and the sidebands suppression are the goal to be fulfilled simultaneously using the Hybrid EPSO/DE algorithm. From chapter 4, we have chosen the best optimized CCAA configuration on the SLL which is Config.4-1 CCAA with I_{max}/I_{min}=7.9, and the best optimized CHAA configuration on the SLL is Config.3-2 CHAA with I_{max}/I_{min}=8.2. It can be noticed that both of these dynamic-range ratios are high, and the use of the time-modulation intend to mitigate them.

In this section it is aimed to optimize the switch-on instants and the complex weights of the 36-elements of the Concentric Hexagonal Antenna Array CHAA and Concentric Circular Antenna Array CCAA to suppress the side-lobe level SLL and the sideband levels SBLs to the minimum as possible, and minimize the main-lobe beam-width BW at center frequency f_0 simultaneously using Hybrid EPSO/DE algorithm. A comparison between numerical results of this section and results in [65] which used a 36-elements Circular array with 0.25λ spacing between elements. The reference pattern in [65] used the time modulation besides the phase excitation optimization with fixed amplitude excitation – not uniform – to suppress the SLL and SBLs.

5.3.1 Objective Function Formulation of the Design Problem.

Consider Config.3.2 {6,12 ,18} CHAA and Config.4.1{6, 6, 12, 12} CCAA from chapter 4 with the same dimensions for the rings diameter and the isotropic elements spacing that mentioned in chapter 4 earlier, and each element is connected to a high-speed RF switch then the array factor is given by

$$AF(\theta,\phi,t) = e^{j2\pi f_0 t}\sum_{h=1}^{H}\sum_{n=1}^{N_h} I_{hn}U_{hn}(t).e^{j[kr_h \sin\theta\cos(\phi-\phi_{hn})+\alpha_{hn}]} \tag{5.12}$$

$$\phi_{hn} = 2\pi\left(\frac{n-1}{N_h}\right) \tag{5.13}$$

Where H is the total number of rings in the array, N_h is the total number of elements in the h^{th} ring, I_{hn} is the amplitude excitation, r_h is the radius of the h^{th} ring. α_{hn} is the phase excitation.

The time switching function $U_{hn}(t)$ in a time modulation period T_p is defined by equation 5.2 earlier.

Similar to TMLA and Due to the periodicity of $U_{hn}(t)$, the array far-field pattern in equation (5.12) can be expanded into a Fourier series, and given by

$$AF(\theta,\phi,t) = \sum_{m=-\infty}^{\infty}\left\{\sum_{h=1}^{H}\sum_{n=1}^{N_h} a_{hnm}(t).e^{j[kr_h \sin\theta\cos(\phi-\phi_{hn})+\alpha_{hn}]}\right\}.e^{j2\pi(f_0+mf_p)t} \tag{5.14}$$

At the center frequency (m=0), the dynamic amplitude of the Fourier component a_{hn0} can be simplified as

$$a_{hn0} = i_{hn}.\tau_{hn}/T_p \tag{5.15}$$

To facilitate the optimization process it will be divided into two-step fitness function using the Hybrid EPSO/DE algorithm, this idea was proposed in [66] for TMLA and it will be used

here in time modulated concentric circular array TMCCA and time modulated concentric hexagonal array TMCHA. In the first step of the fitness function, it is aimed to find the desired fundamental radiation having a prescribed main-lobe beam-width and the lowest SLL, and in the second step of the fitness function, the SBL is tried to be suppressed as low as possible in according with the results of the first step. In the first step of the optimization, a single optimization vector $v_1 = \{a_{hn0}, \alpha_{hn}\}$ is used, and the so-called dynamic amplitude a_{hn0} here is treated as one variable according to the following fitness function:

$$f_1(v_1) = w_1 . SLL_{\max}(v_1)\Big|_{f_0} + w_2 . \phi_{BW}(v_1)\Big|_{f_0} \tag{5.16}$$

SLL_{max} is the optimized maximum SLL at the center frequency, Φ_{BW} is the beam-width of the main-lobe at the center frequency, w_1 and w_2 are the corresponding weighting factors of each term in the cost function.

For the second step of the optimization, the related vector will be $v_2 = \{\tau_{hn}/T_p\}$, where τ_{hn}/T_p is the normalized switch-on time for each element to be optimized to suppress the different SBLs of the TMCCA and TMCHA, according to the following fitness function:

$$f_2(v_2) = \max\left\{ SBL^{(1)}(v_2)\Big|_{f_{0+}f_p}, SBL^{(2)}(v_2)\Big|_{f_{0+}2f_p}, SBL^{(3)}(v_2)\Big|_{f_{0+}3f_p} \right\} \tag{5.17}$$

$SBL^{(1)}$, $SBL^{(2)}$ and $SBL^{(3)}$ are the maximum SBL at the first sideband, the second sideband and the third sideband respectively.

5.3.2 Analysis and Numerical Results

The search ranges for the first vector will be: the dynamic amplitude $a_{hn0} = \{0.1, 2\}$, and the excitation phase $\alpha_{hn} = \{-\pi, \pi\}$. The proper values of w_1 and w_2 were found by trial and error to be 1 and 2 respectively. For the second vector the normalized switch-on times range will be $\tau_{hn}/T_p = \{0, 1\}$.

It is obvious from Table 5.2 that the time modulation technique in the case of TMCHA using Hybrid EPSO/DE succeeded to achieve ultra-low SLL up to -43.1 dB in the azimuth plane, with a

considerable gain up to 9 dBi compared to the pattern in reference [65] which has lower SLL =-45 dB, but low gain = 6.2 dBi and high sideband level SBLs reached -20 dB in the first sideband level, while in the case of TMCHA the highest SBL was -39.7 dB as shown in Fig.5.7. The first null beamwidth FNBW=56.4 degrees, which is thinner than the beamwidth of the reference pattern FNBW=60 degrees and with acceptable dynamic-range ratio I_{max}/I_{min}=5.55. For the case of TMCCA the SLL couldn't exceed the -40dB with the use of time modulation technique, this proved the role of the geometry in synthesizing the radiation pattern for the same number of elements in the antenna array. The complex weights of the element arrays of TMCHA and the corresponding switch-on times, optimized using the Hybrid EPSO/DE algorithm are depicted in Fig.5.8 and Fig.5.9 respectively. Fig.5.10 illustrates the 3-D space and frequency response of TMCHA using Hybrid EPSO/DE algorithm, while Fig. 5.11 shows the radiation pattern of optimized TMCHA at f_0, f_0+f_p, f_0+2f_p and f_0+3f_p on polar coordinates.

Table 5.2 A comparison of 36-elements TMCHA and TMCCA features SLL, SBL, BW, Gain and I_{max}/I_{min} using the three algorithms with the results in reference [65].

Configuration	Algorithm	SLL [dB]	BW [Deg]	SBL(1) [dB]	SBL(2) [dB]	Gain [dBi]	I_{max}/I_{min}
Circular Ref. [65]	DE	-45	60	-20	-23.5	6.2	2
Config.3-2 TMCHA	DE	-33.2	50.7	-26.4	-27.2	9.6	4.2
	EPSO	-39.83	55.4	-29.7	-32.8	9.0	4.9
	Hybrid EPSO/DE	-43.1	56.4	-39.7	-45	9.0	5.55
Config.4-1 TMCCA	DE	-30.3	50.2	-31.0	-27.8	13	3.2
	EPSO	-34.6	51.4	-32.4	-32.8	12.2	3.35
	Hybrid EPSO/DE	-35.6	51.6	-33.2	-39.6	11.59	4.15

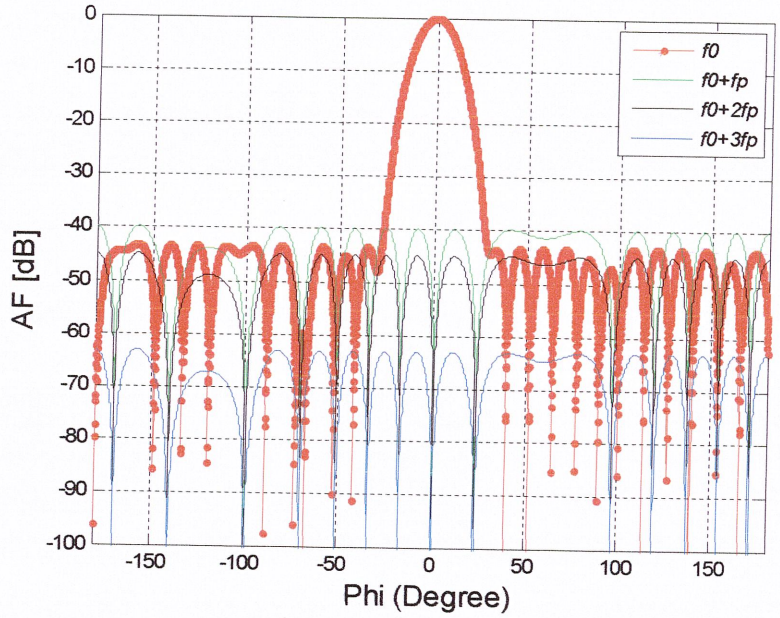


Fig. 5.7 shows the radiation pattern of optimized TMCHA at f_0, f_0+f_p, f_0+2f_p and f_0+3f_p using hybrid EPSO/DE algorithm.

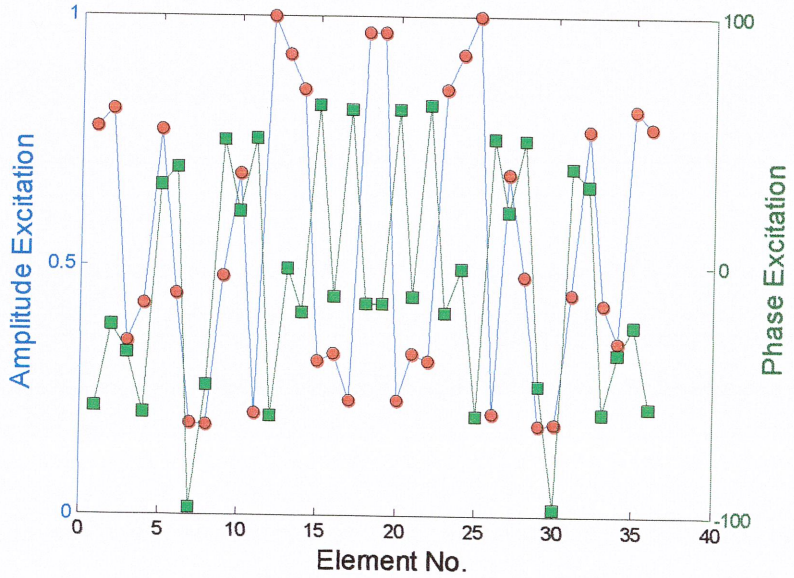


Fig.5.8 The optimized Amplitude and Phase of TMCHA elements using hybrid EPSO/DE algorithm of Fig.5.7.

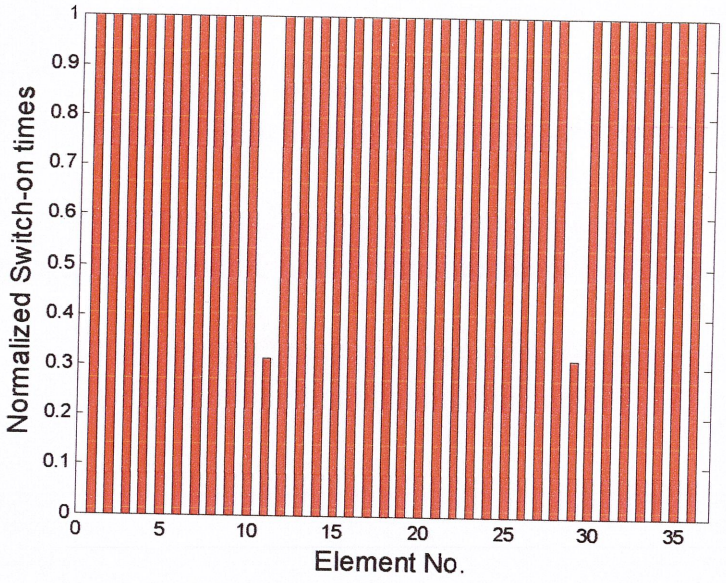


Fig.5.9 The optimized Switch-on times sequence of TMCHA elements using hybrid EPSO/DE algorithm of Fig.5.7.

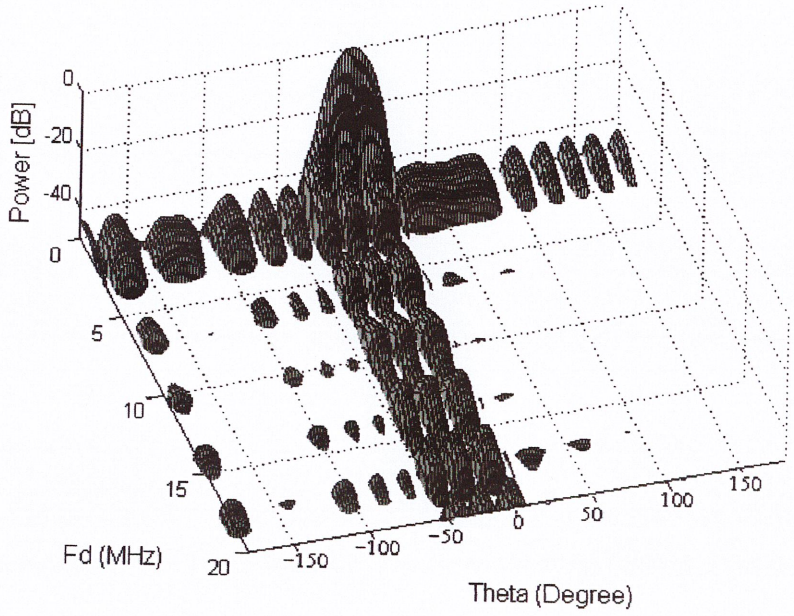


Fig. 5.10 The 3-D space and frequency response of TMCHA using hybrid EPSO/DE algorithm.

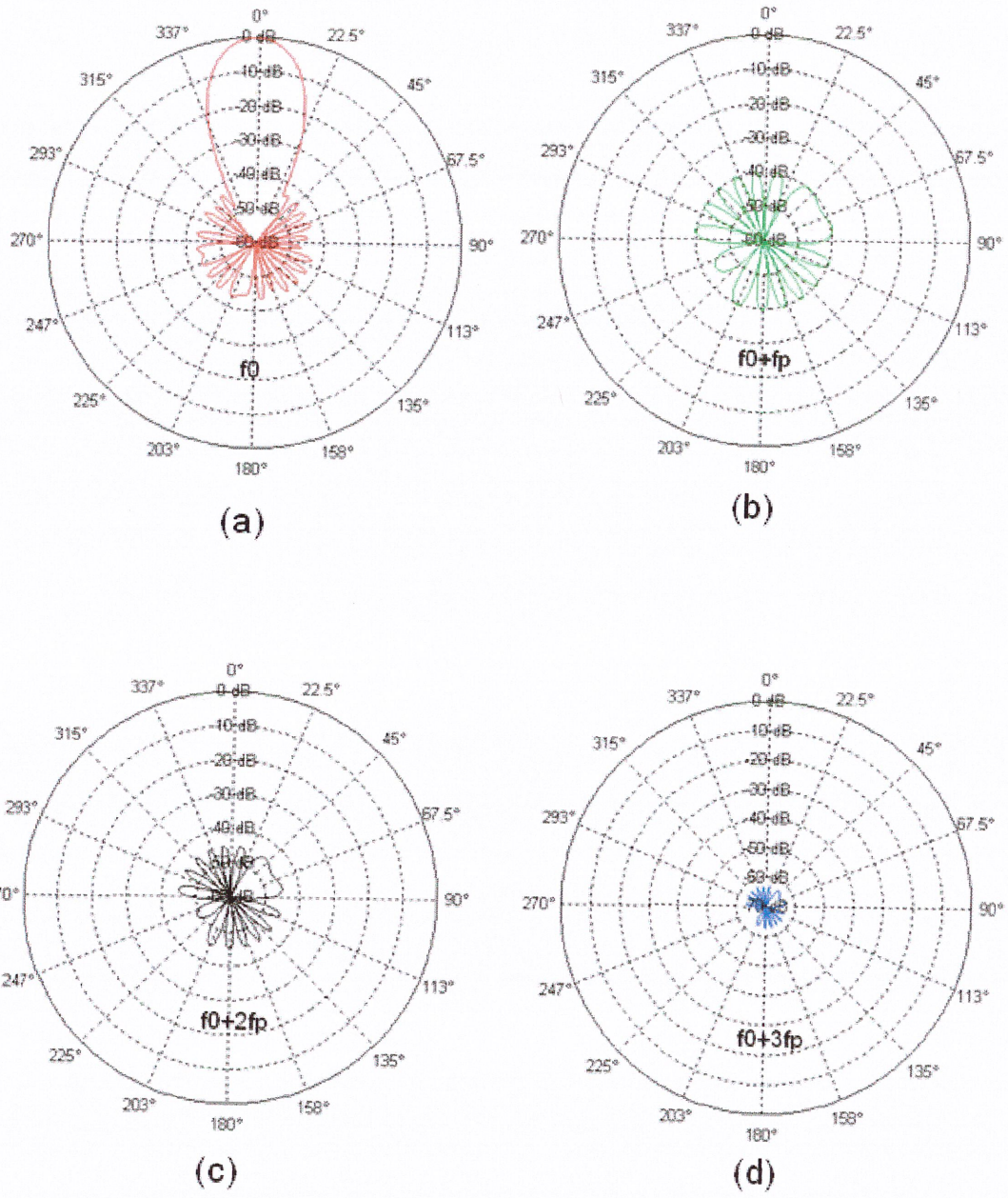


Fig. 5.11 shows the radiation pattern of optimized TMCHA in polar coordinates at (a) f_0, (b)f_0+f_p, (c)f_0+2f_p and (d) f_0+3f_p using hybrid EPSO/DE algorithm at $\theta=0°$.

5.3.3 Conclusion of TMCCA and TMCHA

An ultra low SLL pattern could be synthesized using time modulation in parallel with complex weights optimization of planar antenna array. The TMCHA has pattern features SLL, SBL BW and Gain better than the TMCCA and TMCA in reference [65], beside less mutual coupling effect of the later geometry due to close distance between elements.

5.4 Conclusion

In this chapter, innovative approaches for the synthesis of time-modulated arrays have been proposed for linear and planar array as well. This time modulation technique solved the problem of the high dynamic-range ratio that required to synthesize low SLL pattern as discussed earlier in unequally spaced TMLA with uniform amplitude excitation and SLL=-36 dB with excellent gain up to 15.5 dBi. In the case of planar array the time modulation had been applied to TMCCA and TMCHA in parallel with the complex weights optimization, and it achieved ultra-low SLL reached -43.1 dB with excellent gain up to 9 dBi using the Hybrid EPSO/DE algorithm.

Moreover, the SBL can be suppressed to be less than −20dB for linear array and less than -39.7 dB for planar array which means that the electromagnetic energy shifted to sidebands are relatively small. The study presented in this chapter shows that the unequally spaced TMLA is a promising approach which can be used to synthesize low side-lobe patterns with excellent gain and can be easily applied to the synthesis other desired beams as well. Also this study proves the applicability of synthesizing ultra-low SLL in the azimuth plane using TMCHA with excellent gain and very low dynamic-range ratio compared to other works, which ease the practical implementation.

Chapter 6

Conclusions and Future work

This thesis examined design of phased antenna array using new optimization algorithms; hybrid DE/EPSO. It is been focused in this thesis to cover many topics in the phased antenna array design like; multiple null steering, SLL minimization and time modulation, applied into different array geometries like linear, circular, concentric circular and concentric hexagonal array.

6.1 Conclusions

This research investigated a novel hybrid global optimization algorithm DE/EPSO combining differential evolution (DE) and enhanced particle swarm optimization (EPSO). The hybridization purpose is to include the essence and merits of both techniques. Hybrid DE/EPSO procedure gave a fairly accurate optimum solution by increasing the solution space. This technique proved to be efficient tool to decrease the chance of trapping in local minima if it compared to each algorithm individually.

Numerical results show that the hybrid DE/EPSO outperforms the classical DE and EPSO in obtaining the desired pattern. It can be concluded that the hybrid DE/EPSO is an effective algorithm with improved accuracy, and it could be a promising tool to be applied for the design of reconfigurable antenna arrays.

In this thesis, a novel null steering method depending on position perturbation of selected elements of linear and circular arrays using newly developed hybrid EPSO/DE optimization algorithm was presented. The new method of null steering succeeded to place deep nulls (less than -200dB) in the initial pattern, up to five nulls simultaneously with acceptable increase in the MSL and main beamwidth. This null control method is proved to eliminate the elements with less contribution to the null forming. The remaining array elements will be selected to be perturbed to form the desired prescribed nulls. This method was applied successfully with different perturbation directions in axial direction (array line), elevation direction (normal to the array line) or arbitrary directions for the linear array and radial, angular and arbitrary directions for the circular array. To conclude, the arbitrary case of both linear and circular array was the most efficient case in null steering using selected position perturbed array elements, with fewer elements to be perturbed

Also in this thesis, a study compares between different configurations of antenna arrays utilizing the same number of elements were presented. The patterns of circular and hexagonal arrays with 36 elements spaced with 0.25λ, versus the concentric circular and concentric hexagonal arrays with 36 elements spaced with 0.5λ. The 0.5λ was chosen to be the minimum distance between any two adjacent elements, to mitigate the effect of mutual coupling between elements.

The uniform concentric hexagonal arrays UCHA proved to give lower SLL in the azimuth plane, than the uniform concentric circular arrays UCCA after rotating the outer ring(s) of the arrays. After optimizing the complex weights of these concentric arrays, a pattern with SLL= -35 dB and directivity =8.85 dBi was achieved with slight change in beamwidth compared to a circular reference pattern [35] has SLL=-31.4dB and directivity =7.9 dBi used the same number of elements.

This study was extended to explore the effects of adding a central element to these configurations. Lower SLL (-37dB) and lower I_{max}/I_{min} ratio =4.4, compared to the SLL and I_{max}/I_{min} of the original configuration are the advantages of the additional central element. It could be concluded, for the same number of elements, the geometry redesign could obtain better feature of radiation pattern than original design. The concentric hexagonal array with 0.5λ inter-element

distance is a promising alternative to the circular array with 0.25λ inter-element distance in synthesizing low SLL radiation pattern for the same number of elements in the azimuth plane.

In this thesis, innovative approaches for the synthesis of time-modulated arrays have been proposed for linear and planar array as well. This time modulation technique solved the problem of the high dynamic-range ratio that required to synthesize low SLL pattern. By this method, an unequally spaced TMLA with uniform amplitude excitation obtained low SLL =-36 dB with excellent gain up to 15.5 dBi. These results were compared to a linear array has the same number of elements utilized the phase-position technique. By comparing the results it can be concluded that the position-time modulation method, proved to be better than the position-phase method in SLL minimization for the unequally spaced linear array

In the case of planar array the time modulation had been applied to concentric circular array CCA and concentric hexagonal array CHA, in parallel with the complex weights optimization. Using the time modulation, a pattern with ultra-low SLL reached -43.1 dB and excellent gain up to 9 dBi was achieved.

Moreover, the sideband level SBL can be suppressed to be less than −20dB for linear array and less than -39.7 dB for planar array which means that the electromagnetic energy shifted to sidebands are relatively small. The unequally spaced TMLA is a promising approach which can be used to synthesize low side-lobe patterns with excellent gain and can be easily applied to the synthesis other desired beams as well. Also this study proves the applicability of synthesizing ultra-low SLL in the azimuth plane using TMCHA with excellent gain and very low dynamic-range ratio compared to other works, which ease the practical implementation.

6.2 Future work

The following topics could be taken in consideration in phased antenna design using optimization algorithms for the future work:

1- It may be useful to hybridize different algorithms together instead of EPSO and DE. The researchers could chose different pair of algorithms like: Ant colony, Simulated annealing, Bees algorithms, Genetic algorithm and Firefly algorithm and compare between their performances and application in the phased antenna arrays design.

2- It is desirable to study the effect of mutual coupling between array's elements in the concentric circular and concentric hexagonal array, when calculating the nulls and SLL of the radiation pattern.

3- In the time modulation, the switch on times for all elements started at the same instant time, it may be possible to trigger the switch on times with different instant times t_{0n} (to be optimized) i.e. with delays between elements excitation. The switch-on times τ_n and their related instants t_{0n} will be the optimization parameters and new $U_n(t)$ will be:

$$U_n(t) = \begin{cases} 1 & t_{0n} \leq t \leq t_{0n} + \tau_n \\ 0 & Otherwise \end{cases} \qquad (6.1)$$

4- In the time modulation also, it has been focused in minimizing the SBL to reduce the wasted power. For the future work, the sideband radiation power could be added to the cost function to be minimized. This idea may take more time in the optimization process, but it will give more accurate result in reducing power wastage.

References

[1] Soni, RA, Buehrer, R. M., & Benning, R. D. "Intelligent antenna system for cdma2000". *IEEE Signal Processing Magazine*, 19, pp. 54-67, 2002.

[2] Godara, L. C. *Handbook of Antennas in Wireless Communications*. CRC Press 2002.

[3] Kurup, D., Himdi, M., & Rydberg, A. "Synthesis of uniform amplitude unequally spaced antenna arrays using the differential algorithm," *IEEE Transactions on Antennas and Propagation*, 51, pp. 2210-2217, 2003.

[4] Michielssen, E., Sajer, J.-M., Ranjithan, S., and Mittra, R., "Design of lightweight, broad band microwave absorbers using genetic Algorithms," *IEEE Transactions on Microwave Theory and Techniques*, Vol. 41, pp. 1024–1031, July 1993.

[5] Haupt, R. L., "An introduction to genetic algorithms for electromagnetics," IEEE Antennas and Propagation Magazine, Vol. 37, pp. 7–15 April 1995.

[6] A. Hoorfar, "Evolutionary programming in electromagnetic optimization: a review" *IEEE Trans. Antennas Propagat.*, Vol. 55, No.3, pp. 523 -537, March 2007.

[7] Haupt, R. "Thinned arrays using genetic algorithms". *IEEE Transactions on Antennas and Propagation*, Vol. 42, 993-999, 1994.

[8] Zhiqiang L.,. Minli Y, Xiaowei S. "Sidelobe reduction of the low profile phased array antenna for satellite communication on-the-move" *3rd international conference on Advanced Computer Theory and Engineering ICACATE 2010*, Vol. 4, pp 120-122, Sep 2010.

[9] Murino, V., Trucco, A., & Regazzoni, C. S. "Synthesis of unequally spaced arrays by simulated annealing," *IEEE Transactions on Signal Processing*, 44, 119–123, 1996.

[10] Singh, U., Rattan, M.; Singh, N. "Optimization of gain and impedance of Yagi-Uda antenna using simulated annealing" *19th international conference on applied electromagnetic and communication ICECom 2007*, pp 1-4, 2007.

[11] Shihab, M., Najjar, Y., Dib, N., Khodier, M. , "Design of nonuniform circular antenna arrays using particle swarm optimization," *Journal of Electrical Engineering*, vol. 59(4), pp. 216-220, 2008.

[12] Mandal D., S.P. Ghoshal, A. K. Bhattacharjee "Optimized radii and current excitations for low sidelobed concentric circular antenna array using Particle Swarm Optimization," *IEEE Symposium on Industrial Electronic and Application ISIEA*, pp.629-633, 2010.

[13] J. Guo and J. Li "Pattern Synthesis of Conformal Array Antenna in the Presence of Platform Using Differential Evolution Algorithm" *IEEE Trans. Antennas Propag.*, vol. 57, No. 9, pp. 2615–2621, 2009.

[14] Chowdhury, A. Giri, R. Ghosh, A. Das, S. Abraham, A. Snasel, V. "Linear antenna array synthesis using fitness-adaptive differential evolution algorithm" 2010 Congress on Evolutionary Computation (CEC), pp. 1-8, 2010.

[15] M. A. Panduro, C. A. Brizuela, "A comparative analysis of the performance of GA, PSO and DE for circular antenna arrays," *Antennas and Propagation Society International Symposium*, 2009. APSURSI '09. IEEE , vol., no., pp.1-4, 1-5 June 2009

[16] M. A.-A. Mangoud and H. M. Elragal "Antenna Array Pattern Synthesis and Wide Null Control Using Enhanced Particle Swarm Optimization," *Progress In Electromagnetics Research B*, PIERB 17, 1-14, 2009.

[17] Donelli, M., S. Caorsi, F. De Natale, M. Pastorina, and A. Massa, "Linear antenna synthesis with a hybrid genetic algorithm,"*Progress In Electromagnetics Research*, PIER 49, 1–22, 2004.

[18] S. Zhang, S.-X. Gong, Y. Guan, P.-F. Zhang, and Q. Gong, "A novel IGA-EDSPSO hybrid algorithm for the synthesis of sparse arrays," *Progress In Electromagnetics Research*, PIER 89, 121–134, 2009

[19] Rody P.S. Oldenhuis, "Trajectory Optimization of a Mission to the Solar Bow Shock and Minor Planets," *Thesis Report, Delft University of Technology*, 2010.

[20] Vink´o T., Izzo D., and Bombardelli C., " Benchmarking different global optimisation techniques for preliminary space trajectory design," *58th International Astronautical Congress, Hyderabad, India*, 2007.

[21] S. Khamsawang, P. Wannakarn, and S. Jiriwibhakorn, " Hybrid PSO-DE for Solving the Economic Dispatch Problem with Generator Constraints," *The 2nd International Conference on Computer and Automation Engineering (ICCAE)*, 2010

[22] Musrrat Ali, Millie Pant, and Ajith Abraham, "Inserting Information Sharing Mechanism of PSO to Improve the Convergence of DE," *VIII International Conference on Computer Information Systems and Industrial Management (CISIM 2009)*, December 08-11, Coimbatore, India, 2009.

[23] R. Storn, K. Price, "Differential evolution-A simple and efficient heuristic for global optimization over continuous spaces," *Journal of Global Optimization*, Vol. 11, No. 4, pp. 341–359, 1997.

[24]. Feoktistov, "Differential Evolution: In Search of Solutions (Springer Optimization and Its Applications)", Springer-Verlag New York Inc., 2006.

[25] Kennedy J. and Eberhart R. "Particle swarm optimization". In *Proceedings of the IEEE International Conference on Neural Networks*, pages 1942–1948, Piscataway, NJ, 1995.

[26] Robinson, J. Rahmat-Samii, Y.. "Particle swarm optimization in electromagnetic", *IEEE Transactions on Antennas and Propagation* 52 No. 2 (February 2004), 397-407

[27] Wysota, M., Jagodzinska, K. and Walkowiak, M., "Sidelobe suppression in unequally spaced antenna arrays". In *Proceedings of the 2008 1st International Conference on Information Technology*, pages 1-4, Poland, 2008.

[28] H. Steyskal, R.A. Shore and R.L. Haupt, "Methods for Null Control and Their Effects on the Radiation Pattern," *IEEE Trans. Ant. and Propagation*, Vol. AP-34, pp. 404-409, 1986.

[29] J. A. Hejres, "Null Steering in Phased Arrays by Controlling the Positions of Selected Elements, " *IEEE Trans. Antennas and Propagation*, Vol. 52, NO. 11, Nov 2004.

[30] S. Yang, Y. B. Gan, A. Qing, "Antenna-array pattern nulling using a differential evolution algorithm," *Int. J RF and Microwave CAE*, Vol. 14, No. 1, pp. 57–63, 2004.

[31] A. Alphones, V. Passoupathi, "Null Steering In Phased Array By Positional Perturbation: A Genetic Algorithm Approach," *Proc. IEEE Phased Arrays*, pp. 203-207, 1996.

[32] Steyskal, H., "Simple method for pattern nulling by phase perturbation," *IEEE Trans. on Antennas and Propagation*, Vol. 31, 163–166, 1983.

[33] K. Güney, M. Onay, "Amplitude-only pattern nulling of linear antenna arrays with use of bees algorithm," *Progress in Electromagnetic Research*, vol. 70, pp. 21- 36, 2007.

[34] Balanis, C.: Antenna Theory-Analysis and Design. 3rd Edition New York: Wiley, 2005.

[35] N Goto and Y. Tsunoda " Side lobe Reduction of Circular Array with a constant Excitation Amplitude," *IEEE Trans. Antennas Propag.*, vol. 25, No. 6, pp. 896–898, Nov. 1977.

[36] Ioannides, P. and C. A. Balanis, "Uniform circular arrays for smart antennas," *IEEE Antennas and Propagation Magazine*, Vol. 47,No. 4, 192–206, August 2005.

[37] Ioannides, P. and C. A. Balanis, "Uniform circular and rectangular arrays for adaptive beamforming applications" *IEEE Antennas and Propagation Magazine*, Vol. 4, 351–354,2005.

[38] Gozasht, F., G. R. Dadashzadeh, and S. Nikmehr, "A comprehensive performance study of circular and hexagonal array geometries in the LMS algorithm for smart antenna applications," *Progress In Electromagnetics Research*, PIER 68, 281–296, 2007.

[39] Kretly, L. C., A. S. Cerqueira Jr., and A. A. S. Tavora, "A hexagonal adaptive antenna array concept for wireless communication applications," *The 13th IEEE International Symposium on Personal, Indoor and Mobile Radio Communications*, Vol. 1, 247–249, Sept. 2002.

[40] Mahmoud K. R.,M. El-Adawy,and S. M. M. Ibrahem,"A comparison between circular and hexagonal geometries for smart antenna systems using particle swarm optimization algorithm," *Progress In Electromagnetics Research, PIER* 72, 75–90, 2007.

[41] Mandal D., S.P. Ghoshal, A. K. Bhattacharjee "Concentric Circular Antenna Array Synthesis Using Particle Swarm Optimization with Constriction Factor Approach," *A workshop on advanced antenna technology, 2010 Indian antenna week* pp. 1-4, June 2010.

[42] Haupt R. L., "Optimized element spacing for low sidelobe concentric ring arrays," *IEEE Trans. Antennas Propag.*, vol. 56(1), pp. 266-268, Jan. 2008.

[43] Dessouky M., H. Sharshar and Y. Albagory, "Efficient sidelobe reduction technique for small-sized concentric circular arrays," *Progress in Electromagnetics Research, PIER* 65, pp. 187–200, 2006.

[44] Chan S. C., and H. H. Chen "Uniform Concentric Circular Arrays With Frequency-Invariant Characteristics—Theory,Design, Adaptive Beamforming and DOA Estimation," *IEEE Trans. on signal processing*, vol. 55, No.1, pp. 165-177, Jan. 2007.

[45] Mandal D., S.P. Ghoshal, A. K. Bhattacharjee "A Novel Particle Swarm Optimization Based Optimal Design of Three-Ring Concentric Circular Antenna Array," *International Conference on Advances in Computing, Control, and Telecommunication Technologies*, pp.385-389, Dec. 2009.

[46] G.K., T.K. Sinhamahapatra, A.Ahmed and A.Chakrabarty "Synthesis of Flat-top Beam Pattern with a Multiple Concentric Circular Ring Array Antenna," *IEEE region 10 and the third International conference on Industrial and Information Systems*, pp.1-4, Dec.2008.

[47] Li Y., K.C. Ho and C. Kwan "Beampattern synthesis for concentric circular ring array using MMSE design," *Proceeding of the 2004 International Symposium on circuits and systems*, vol. 3, pp.329-332, May 2004.

[48] Gunasekaran T., D. Kumar "Modified concentric circular microstrip array configurations for WiMax base stations," *Journal of Theoretical and Applied Information Technology*, vol.12 No.1,pp. 8-12, 2010.

[49] Lozano M., F. Ares-Pena, and E. Moreno "Pencil-Beam pattern synthesis with a uniformly excited Multi-Ring planar antenna," *IEEE Antenna and Propagation Magazine*, vol.42, No.6, pp. 70-74, Dec. 2000.

[50] Chatterjee A., G.K. Mahanti and A. Chakrabarty "Synthesis of Pencil Beam Pattern with a Multiple Concentric Circular Ring Array Antenna with Minimum Side Lobe Level and Fixed First Null Beamwidth, " *2010 International conference on electronic computer Technology ICECT*, pp.71-74, May 2010.

[51] Stearns C. and A. Stewart, "An investigation of concentric ring antennas with low sidelobes," *IEEE Trans. Antennas Propag.*, vol. 13, No. 6, pp. 856–863, Nov. 1965.

[52] Das R., "Concentric ring array," *IEEE Trans. Antennas Propag.*, vol. 14, no. 3, pp. 398–400, May 1966.

[53] Mailloux, R. J., *Phased Array Antenna Handbook,* Artech House, London, 1993.

[54] H. E. Schrank, "Low sidelobe phased array antennas," *IEEE Antennas Propagation Society Newsletter,* Vol. 25, No. 2, 4-9. Apr. 1983.

[55] H. E. Schanks and R.W. Bickmore, "Four-dimensional electromagnetic radiators," *Canad. J. Phys.*, vol. 37, pp. 263-275 March, 1959.

[56] R. W. Bickmore, "Time versus space in antenna theory," in *Microwave Scanning Antennas*, R. C. Hansen, Ed. New York, NY: Academic, 1966, vol. III.

[57] Kummer, W. H., A. T. Villeneuve, T. S. Fong, and F. G. Terrio, "Ultra-low sidelobes from time-modulated arrays," *IEEE Trann. Antennas Propagat,* Vol. 11, No. 5, 633-639, Nov. 1963.

[58] Y. Shiwen, Y. B. Gan, and A. Qing, "Sideband suppression in time-modulated linear arrays by the differential evolution algorithm," *IEEE Antennas Wireless Propagat. Lett.*, vol. 1, pp. 173–175, Dec. 2002.

[59] S. Yang,, Y. Gan, and P. Tan "A New Technique for Power-Pattern Synthesis in Time-Modulated Linear Arrays," *IEEE Antennas Wireless Propagat. Lett.*, vol. 2, pp. 285–287, 2003.

[60] J. Fondevila, J. C. Bregains, F. Ares and E. Moreno, "Optimizing Uniformly Excited Linear Arrays Through Time Modulation," *IEEE Antennas Wireless Propagat. Lett.*, vol. 3, pp. 298–301, 2004.

[61] S. Yang, Y. Gan, A. Qing, and P. Tan "Design of a Uniform Amplitude Time Modulated Linear Array With Optimized Time Sequences," *IEEE Transaction ON Antenna and Propagt.*, VOL. 53, NO. 7, pp.2337-2339, JULY 2005

[62] L. Manica, P. Rocca, L. Poli, and A. Massa "Almost Time-Independent Performance in Time-Modulated Linear Arrays," *IEEE Antennas Wireless Propagat. Lett.*, vol. 8, pp. 843–846, 2009.

[63] L. Poli, P. Rocca, L. Manica, and A. Massa "Handling Sideband Radiations in Time-Modulated Arrays Through Particle Swarm Optimization," *IEEE Antennas Wireless Propagat. Lett.*, vol. 58, No. 4, pp. 1408–1411, April 2010..

[64] S. Yang, Y. B. Gan, and P. K. Tan, "Evaluation of directivity and gain for time-modulated linear antenna arrays," *Microwave and Optical Technology Letters* 42(2), 167–171 (2004)

[65] M. Huang, S. Yang, G. Li and Z. Nie "Synthesis of Low and Equal-Ripple Sidelobe Patterns in Time-Modulated Circular Antenna Arrays," *J Infrared Milli Terahz Waves* vol. 30, pp. 802–812, 2009.

[66] E. Aksoy and E. Afacan "Thinned Nonuniform Amplitude Time-Modulated Linear Arrays," *IEEE Antennas Wireless Propagat. Lett.*, vol. 9, pp. 514–517, 2010.

Publication List

1. Elragal H., Mangoud M., Alsharaa M. "Hybrid differential evolution and enhanced particle swarm optimization technique for design of reconnfigurable phased antenna arrays" IET Microw., Antennas Propag. Vol. 5, Issue 11, p. 1280-1287, Aug. 2011.

2. Mangoud M., Elragal H., Alsharaa M. ; "Hybrid EPSO-DE optimization technique for null steering of circular antenna array by selected position" 2011 IEEE GCC conference and Exhibition. (GCC), Dubai p. 609-612, 19-22 Feb. 2011.

3. Alsharaa M., Mangoud M., Elragal H.; "Null control by position perturbation of selected elements for phase antenna array using hybrid EPSO/DE optimization"2010 IEEE International conference on Comm. Sys. (ICCS), Singapore p. 621-624, 17-19 Nov. 2010.

ملخص الرسالة

"التقنية الهجينة للتطور التفاضلي وسرب الجسيمات المحسن في تصميم الهوائيات الطورية"

تماشيا مع التطور العلمي المتزايد في السنوات الأخيرة، شاع استخدام الخوارزميات التطورية في مجال الأتصالات كتقنية فاعلة في تطوير وتصميم الهوائيات الطورية(Phased Antenna Arrays). هذه الخوارزميات ساعدت في ايجاد هوائيات ذات نمط أشعاعي ذو جودة عالية من ناحية القدرة على مقاومة التشويش وتوجيه الطاقة الاشعاعية للهوائي في أتجاه معين من الأثير ما يؤدي إلى توفير الطاقة التي قد تكون محدودة عند أستخدام البطاريات مثلا كمصدر للطاقة كما هو الحال في الهواتف المحمولة.هناك الكثير من الخوارزميات التطورية المستخدمة في وقتنا الحاضر نذكر منها على سبيل المثال الخوارزمية الجينية (Genetic Algorithm) وخوارزمية (Simulated Annealing) وخوارزمية التطور التفاضلي (Differential Evolution) وخوارزمية سرب الجسيمات (Particle Swarm Optimization).

في هذه الرسالة نستعرض خوارزمية جديدة تم تطويرها لتكون هجين بين خوارزمية التطور التفاضلي (DE) وخوارزمية سرب الجسيمات المحسنة (EPSO). هذه الخوارزمية الهجين تتميز بوصولها لحل المسألة المطروحة ضمن فضاء الحلول بطريقة أفضل من استخدام الخوارزميات المذكورة فيما لو استخدمت كلا على حده. حيث ان كلا الخوارزميتين تتبادلان المعلومات داخل جسم الخوارزمية الهجين للوصول الى افضل الحلول للمسألة (Best Global Solution). ولمعرفة مدى فعالية هذه الخوارزمية تم تطبيق استخدامها في هذه الرسالة أولا لأخماد التشويش المتعدد على النمط الأشعاعي للهوائيات الخطية والدائرية،ثانيا تقليل مستوى الاشعاع الجانبي للهوائي بالنسبة للاشعاع الرئيسي في الهوائيات الدائرية والسداسية متحدة المركز. أخيرا وليس آخرا تم تطبيقها في تقليل مستوى الاشعاع الجانبي (SLL) و مستوى الاشعاع الحزمي الجانبي (SBL) للهوائيات ذات تقنية التضمين الزمني (Time Modulation).

وقد تم تقسيم الرسالة كما يلي:

الباب الأول : مقدمة في الخوارزميات المستخدمة في تصميم الهوائيات الطورية وتفصيل بعض منها.

الباب الثاني: يستعرض في هذا الباب الخوارزمية الهجينة المطروحه في هذه الرسالة معززة بمقارنة توضيحية لفعاليتها مع تجارب ونتائج عملية سابقة.

الباب الثالث: يتم في هذا الباب شرح كيفية أخماد التشويش في اتجاهات متعددة للنمط الاشعاعي بالتحكم المحدود لمواضع عناصر الهوائيات الخطية والدائرية باستخدام الخوارزمية الهجينة.

الباب الرابع: ويختص بتصميم الهوائيات الدائرية والسداسية متحدة المركز والتي تحوي نفس عدد العناصر والموزعة على عدد مختلف من الحلقات للمقارنة بينها بالأضافة إلى طرق تقليل مستوى الاشعاع الجانبي للهوائيات المذكورة بمساعدة الخوارزمية الهجينة.

الباب الخامس: يشرح تقنية التضمين الزمني وقدرتها على تقليل مستوى الاشعاع الجانبي بشكل كبير للنمط الأشعاعي للهوائيات الخطية و الهوائيات متحدة المركز وكيفية تقليل مستوى الأشعاعات التي تظهر على ترددات مختلفة نتيجة لأستخدام هذه التقنية بأستخدام الخوارزمية الهجينة.

الباب السادس: يلخص اهداف الرسالة مع الأقتراحات الجديدة لهذا المجال.